Studies on Chemo- and Site-Selective C−H Amination of Aniline and Phenol Derivatives with Dirhodium Catalysts and Catalytic Asymmetric Synthesis of Inherently Chiral Calixarenes

2020

CHEN Gong

Studies on Chemo- and Site-Selective C−H Amination of Aniline and Phenol Derivatives with Dirhodium Catalysts and Catalytic Asymmetric Synthesis of Inherently Chiral Calixarenes

ロジウム二核錯体によるアニリン及びフェノール誘導体の位置及び化学選択的 C-H アミノ化並びに分子不斉カリックスアレーンの触媒的不斉合成に関する研究

2020

CHEN　Gong

Table of contents

Experimental Section

Abbreviation

Ac	acetyl
aq.	aqueous
Bn	benzyl
^{t}Bu	*tert*-butyl
cat.	catalyst
CDI	carbonyldiimidazole
de	diastereoselective excess
DFT	density functional theory
ee	enantioselective excess
equiv.	equivalent
ESI	electron spray ionization
G	Gibbs free energy
H	enthapy
h	hour
HPLC	high performance liquid chromatography
HRMS	high resolution mass spectrometry
^{i}Pr	isopropyl
^{n}Pr	normalpropyl
IR	infrared
K	equilibrium constant
KIE	kinetic isotope effect
Me	methyl
min	minute
m.p.	melting point
NMR	nuclear magnetic resonance
o	*ortho*-
p	*para*-
Ph	phenyl
r.t.	room temperature
S	entropy
T	temperature
TS	transition state
TIPDS	1,1,3,3-tetraisopropyldisiloxane-1,3-diyl
Troc	2,2,2-trichloroehtoxycarbonyl
THF	tetrahydrofuran
Ts	*p*-toluenesulfonyl

Theoretical Section

Chapter 1 Introduction

Development of new methods to construct C−N bonds is of great significance in current synthetic organic chemistry because C−N bonds are ubiquitously involved in functional materials and bioactive molecules.[1] From this context, the methods for C−N bond construction such as nucleophilic N-substitution, reductive amination and Buchwald-Hartwig coupling reaction were intensively studied and successfully applied to fine chemical synthesis.[2] Although the above methods are now reliable, preparation of functionality prior to the amination is necessary. In recent years, transition metal-catalyzed C−H amination provides a straightforward access to various amines without any pre-functionalization, offering a great opportunity to the quick access to diverse nitrogen-containing molecules with high efficiency.[3]

In general, transition metal-catalyzed C−H amination reactions can be classified into three categories, C−H activation catalysis, C−H insertion catalysis, and single-electron-transfer (SET) catalysis (Scheme 1.1).[3f] In the mechanism of C−H insertion catalysis, a metal nitrene species is proposed to be generated and interact with a substrate in either a concerted or a stepwise manner to result in C−N bond formation. To date, much efforts have been devoted to develop C−H amination reaction via C−H insertion process, by virtue of various transition metals such as Cu, Ru, Rh, Ag, Ir, and Co.[3b,3f]

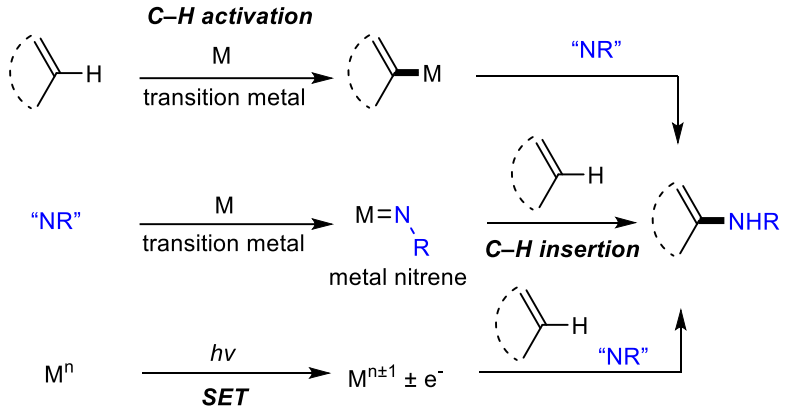

Scheme 1.1 Reaction categories for metal-catalyzed C−H amination.

Dirhodium tetracarboxylates displayed a notable reactivity in the amination of unactivated C(sp^3)−H bonds via formation of dirhodium nitrene complexes and their C−H insertion process.[4] The first example of dirhodium-mediated intramolecular C(sp^3)–H amination was reported by Breslow and Gellman in the early 80s (Scheme 1.2).[4a] After the report, development of efficient reagents and excellent catalysts expanded the utility of dirhodium-catalyzed intramolecular C−H amination and the improved methods have been successfully applied to total synthesis of complex natural products.[5]

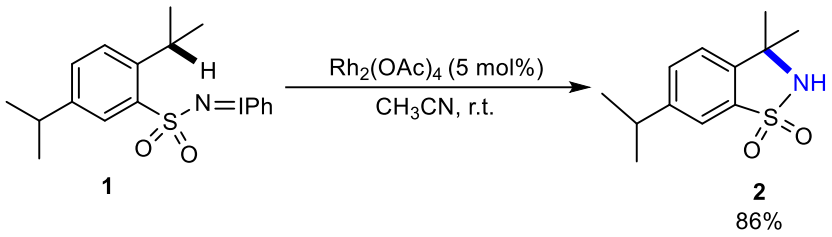

Scheme 1.2 The first example of dirhodium-catalyzed C−H amination.

While the cleavage of C−H bonds is position-limited in intramolecular reactions, control of chemo- and site-selectivity becomes an issue in intermolecular reactions.[6] In 1997, Müller's group reported the first example of intermolecular chemo-selective C(sp^3)–H amination using dirhodium catalysts to reveal that electron rich C(sp^3)–H bonds such as benzylic, allylic, and tertiary C(sp^3)–H bonds and C(sp^3)–H bonds α to oxygen atoms can be selectively converted to C–N bonds (Scheme 1.3).[7] Recently, Ueda, Kawabata and coworkers reported dirhodium-catalyzed site-selective C(sp^3)–H amination of organosilicon compounds directed by *β* effect of the silicon atom (Scheme 1.4).[8]

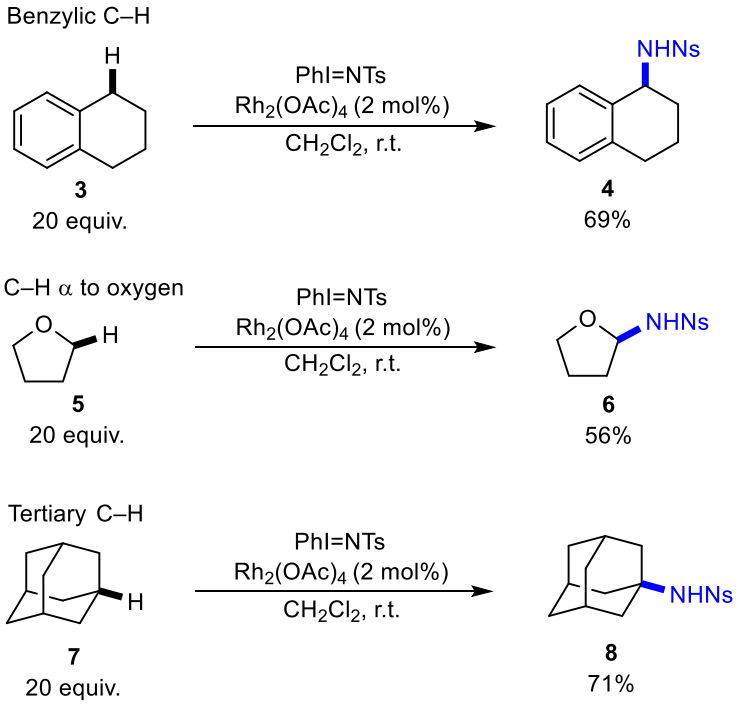

Scheme 1.3 Intermolecular chemoselective C(sp^3)–H amination by dirhodium nitrenes.

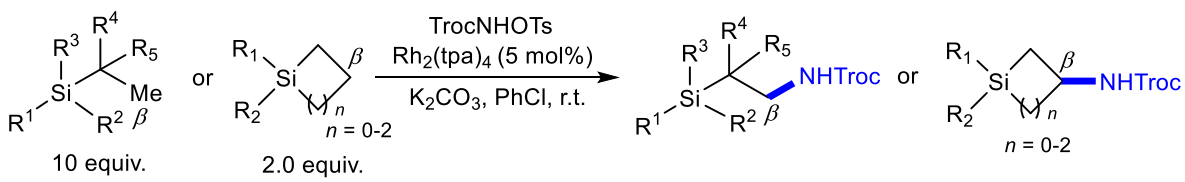

Scheme 1.4 *β*-silicon-effect promoted dirhodium-catalyzed site-selective C(sp^3)–H amination.

Compared to C(sp^3)−H amination, intermolecular C(sp^2)−H amination by dirhodium catalysts was less studied.[9] In 2007, Hashimoto *et al* unexpectedly found that the intermolecular C(sp^2)–H amination took place at *para* position of the silyl ketene acetal moiety of compound **9**, during the study of amination reaction of silyl ketene acetals to provide α-chiral amino acid derivatives (Scheme 1.5).[10] Ten years later, Falck *et al* reported a general method for dirhodium-catalyzed intermolecular C(sp^2)−H amination of various arenes (Scheme 1.6).[11] In this research, it was claimed that nitrenium ion species generated in the acidic medium are the key to the electrophilic aromatic amination.

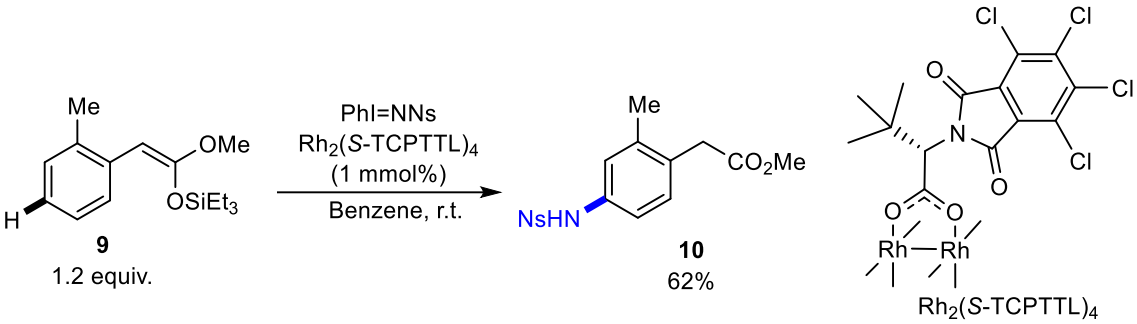

Scheme 1.5 The first example of dirhodium catalyzed intermolecular C(sp^2)−H amination.

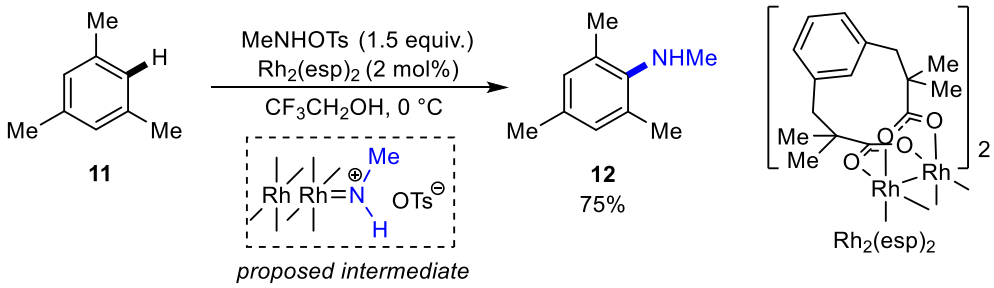

Scheme 1.6 Dirhodium-catalyzed C(sp^2)−H amination via dirhodium nitrenium ions.

In 2018, Ueda and Kawabata *et al* reported dirhodium-catalyzed intermolecular chemo- and site-selective C(sp^2)−H amination of alkoxyarenes (Scheme 1.7a).[12] Under the condition, a neutral dirhodium nitrene complex is assumed to be generated to promote C(sp^2)−H amination via electrophilic aromatic substitution. The aromatic C(sp^2)−H amination took place at the *para* position of the oxygen substituent, even in the presence of otherwise reactive benzylic C(sp^3)–H bonds (Scheme 1.7b).[13]

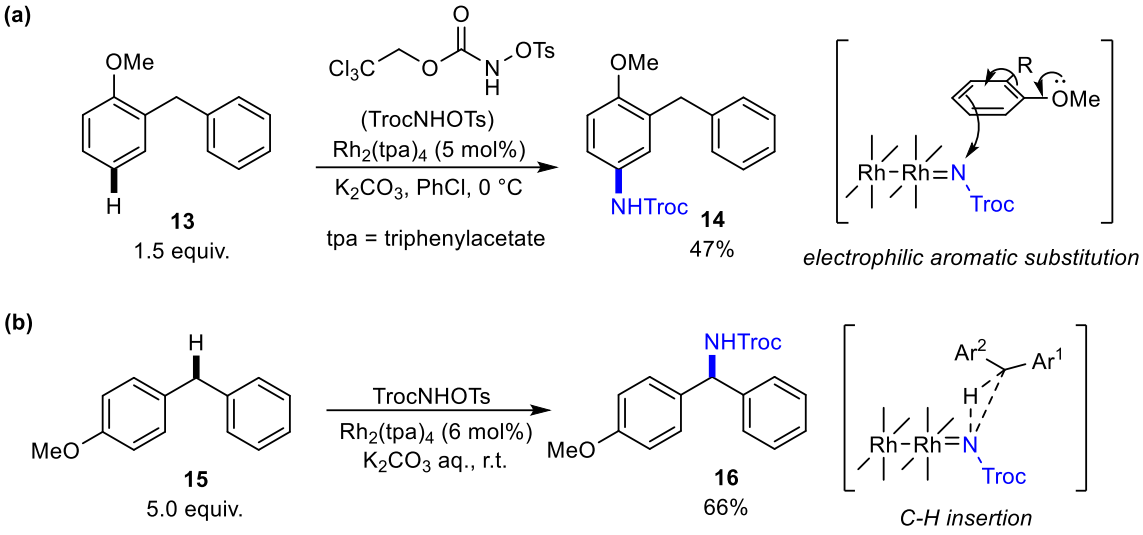

Scheme 1.7 (a) Intermolecular chemo- and site-selective C(sp^2)–H amination via electrophilic aromatic substitution of dirhodium nitrene complex. (b) Intermolecular benzylic C(sp^3)–H amination.

Based on the background, I started investigation for development of other chemo- and site-selective C−H aminations by use of dirhodium catalysts. And also, I tried to apply the method described in Scheme 1.7a to unprecedented enantioselective reactions. The contents of my thesis were outlined below.

In chapter 2, the method for chemo- and site-selective C−H amination of *N*,*N*-dialkylanilines catalyzed by rhodium catalyst was developed. The C−H amination of *N*,*N*-dimethylaniline catalyzed by $Rh_2(oct)_4$ proceeded selectively at C(sp^3)–H bonds α to the nitrogen atom, in the presence of aromatic C(sp^2)–H bonds. C(sp^3)–H amination of the *N*-methyl group of various *N*-alkyl-*N*-methylanilines (alkyl ≠ methyl) was observed exclusively even in the presence of potentially reactive benzylic and tertiary C−H bonds α to the nitrogen atom.[14]

In chapter 3, chemoselectivity in C–H amination of anisole and aniline derivatives was discussed. Experimental and theoretical studies indicated that phenyl rings on the α carbon of the carboxylate ligands of dirhodium complexes strongly affected the efficiency of both C−H amination reactions. In the case of C(sp^3)−H amination of aniline derivatives, the phenyl rings stabilize the coordination state of amine to Rh center to inhibit the reaction strongly. On the other hand, the phenyl rings accelerate the C(sp^2)−H amination of anisole, which suggested that generating δ+ of aromatic ring in the transition state structure would be stabilized by the phenyl rings through cation/π or C–H/π interactions.

In chapter 4, the catalytic asymmetric synthesis of inherently chiral calixarenes (ICCs) was investigated. Use of a chiral dirhodium complex for selective C(sp^2)–H amination of a C_s-symmetric calix[4]arene derivative effectively promoted the chemo-, site- and enantioselective C(sp^2)–H amination to provide the desymmetrized ICC in up to 88% ee. To the best of my knowledge, this is the first efficient example of catalytic asymmetric synthesis of ICCs, using artificial catalysts.

Chapter 2 Development of chemo- and site-selective C−H amination of *N*,*N*-dialkylanilines

2.1 Background

Since arylamine motifs are privileged structural units for the development of functional materials and bioactive molecules,[15] C–H bond functionalization of aniline derivatives have been extensively studied.[16] In the past few decades, considerable achievements have been made in C–H amidation of *N*,*N*-dimethylaniline derivatives *via* cross dehydrogenative coupling between amides and C(sp^3)–H bonds α to a nitrogen atom (Scheme 2.1).[17-20] For example, Fu and co-workers developed Cu-catalyzed C(sp^3) – H amidation of *N*,*N*-dimethylaniline with amides and imides in the presence of *tert*-butyl hydroperoxide as an oxidant.[17a] Fe-catalyzed oxidative protocols as well as transition-metal-free C(sp^3)–H amidation have also been developed.

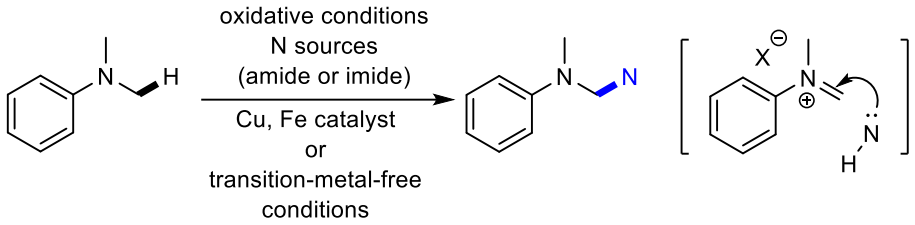

Scheme 2.1 Oxidative C(sp^3)−H amidation of *N*,*N*-dimethylanilines via iminium intermediates.

While various types of C−H amidation reaction of *N*,*N*-dimethylaniline derivatives were reported, control of the site selectivity is still an unsolved problem in C(sp^3)−H amidation of *N*,*N*-dialkylanilines with two different alkyl groups. Fu and coworkers reported that treatment of *N*-benzyl-*N*-methylaniline (**17**) with copper bromide and *tert*-butyl hydroperoxide provided the desired *N*-methyl-amidated product **18** in 28% yield along with the undesired dephenylated product **19** as a major product in 56% yield (Scheme 2.2a).[17a] The possible reaction paths were described in Scheme 2.2b. The primary C−H bond cleavage provided the iminium intermediate **A** and following nucleophilic addition of acetamide to **A** gave **18**. On the other hand, the benzylic C−H bond cleavage provided the favored iminium intermediate **B**. Hydrolysis of **B** and condensation with formaldehyde, derived from hydrolysis of **A**, generated the iminium intermediate **C** to afford undesired **19** by reaction with acetamide.

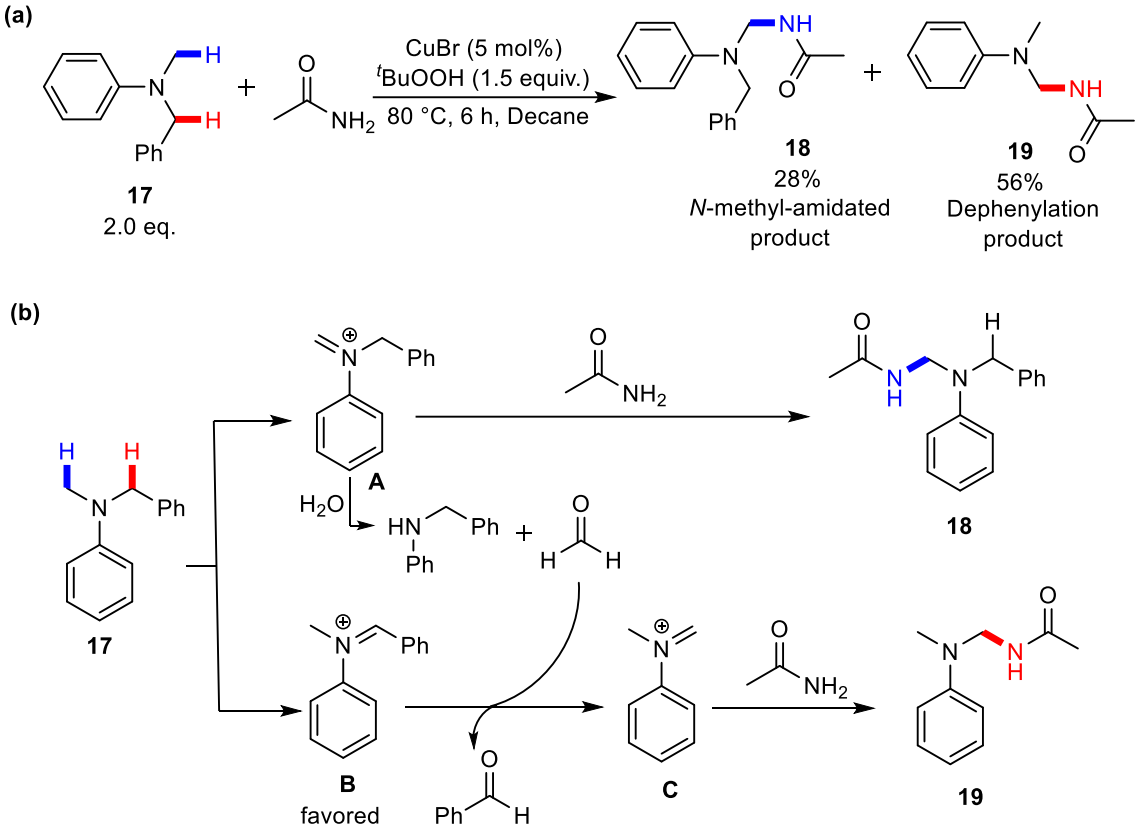

Scheme 2.2 The problem of site-selectivity in copper-catalyzed C(sp^3)–H amidation.

C−H insertion of metal nitrene complexes is considered as an alternative method for C−H amidation reaction to solve the problem about site selectivity, while metal nitrene-mediated C(sp^3)−H amidation α to a nitrogen atom has been relatively unexplored.[21]

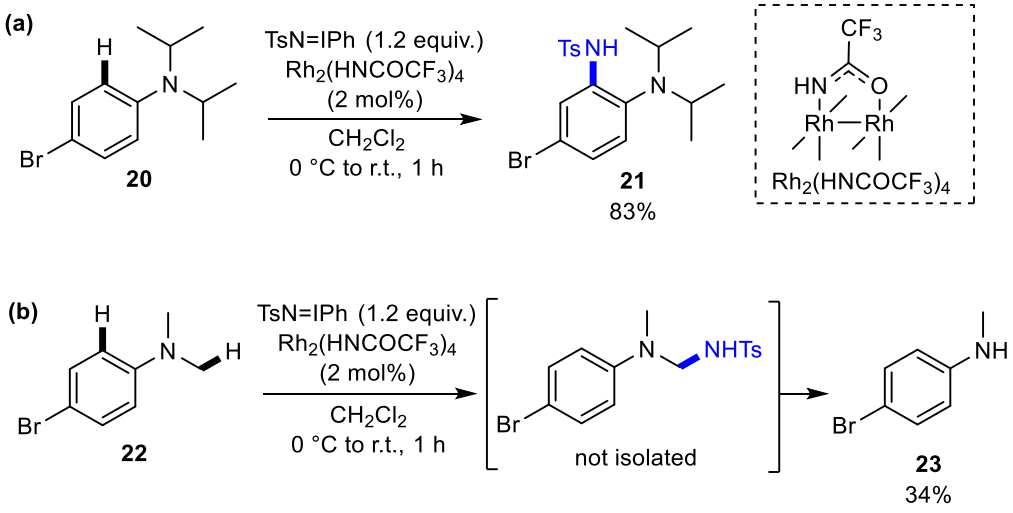

Scheme 2.3 (a) Dirhodium-catalyzed *ortho* C(sp^2)−H amidation of *N*,*N*-diisopropylaniline derivative. (b) Side reaction in the reaction of *N*,*N*-dimethylaniline derivative.

Ito and Sugiyama *et al* reported dirhodium-catalyzed *ortho*-selective C(sp^2)−H amidation of *N*,*N*-diisopropylaniline derivatives **20** (Scheme 2.3a).[22] In this report, when *N*,*N*-dimethylaniline derivative **22** was used as a substrate, demethylated product **23** was obtained as a side product, which indicated that competitive C(sp^3)−H amidation took place and the unstable aminal structure was decomposed during the reaction or purification process (Scheme 2.3b). In addition, the *para* position of the amino group was substituted to inhibit the *para*-C(sp^2)−H amidation.

Based on the background, there is remained uncertainty that which C−H bond of *N*,*N*-dialkylanilines is the most reactive in dirhodium-nitrene-mediated C−H amination reaction. To check the reactivity, I started examination of the previously reported condition to C−H amination of *N*,*N*-dimethylanilines and *N*-alkyl-*N*-methylanilines (alkyl ≠ methyl) (Scheme 2.4).

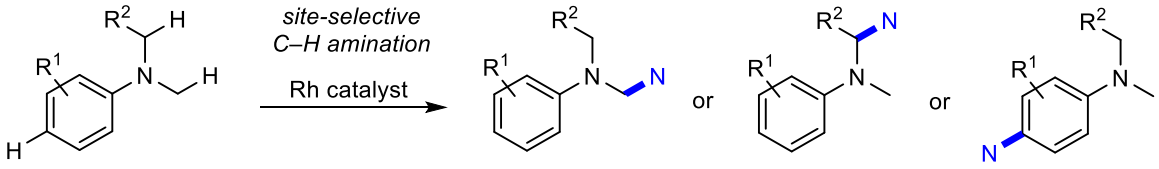

Scheme 2.4 Rhodium catalyzed chemo- and site-selective C−H amination of aniline derivatives.

2.2 Catalyst screening

The study was commenced with C−H amination of *N*,*N*-dimethylaniline (**24**) as a substrate in the presence of various dirhodium catalysts (Table 2.1). According to the previously optimized conditions for C−H amination of anisole derivatives[12] and organosilanes[8], 1.5 equiv. of **24** were treated with *N*-trichloroethoxycarbonyl-*O*-tosylhydroxylamine (TrocNHOTs) in the presence of $Rh_2(tpa)_4$ and K_2CO_3 in chlorobenzene at r.t., which gave no C−H aminated products. Instead, in the presence of $Rh_2(esp)_2$, amination of C(sp^3)−H α to the nitrogen atom selectively took place to give **25** in 39% yield as a single regioisomer. Screening of catalysts demonstrated that $Rh_2(oct)_4$ promoted the C(sp^3)−H amidation most effectively to provide **25** in 46% yield. In all cases, C(sp^2)−H aminated product was not obtained at all.

Table 2.1 Catalyst screening for C−H amination of *N*,*N*-dimethylaniline.

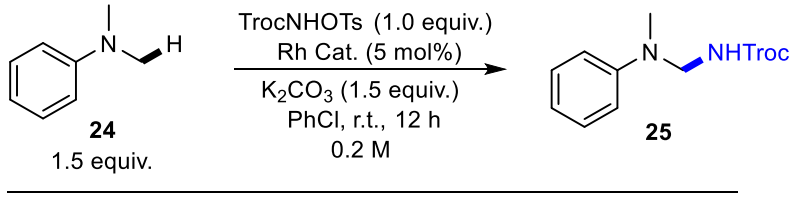

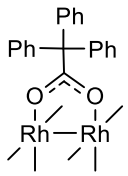	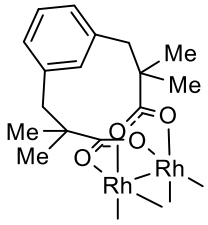	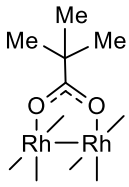
$Rh_2(tpa)_4$ 0% yield[a]	$Rh_2(esp)_2$ 39% yield[a]	$Rh_2(piv)_4$ 40% yield[a]
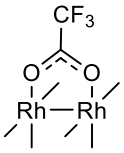	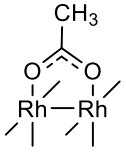	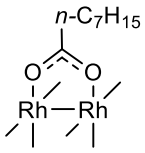
$Rh_2(tfa)_4$ 36% yield[a]	$Rh_2(OAc)_4$ 42% yield[a]	$Rh_2(oct)_4$ 46% yield[a]

[a] Determined by crude ^{1}H NMR, using 1,3-dinitrobenzene as an internal standard.

2.3 Optimization of reaction condition

With $Rh_2(oct)_4$ as a catalyst, the effects of aminating reagents were investigated (Table 2.2). Use of the trifluoroethoxy analogue and the tribromoethoxy analogue of TrocNHOTs provided C(sp^3)−H aminated product **26** and **27** in the comparable yields. Treatment of **24** with *N*-*tert*-butoxycarbonyl-*O*-tosylhydroxylamine and $TrocN_3$ gave only trace amount of the C−H aminated product. *N*-Methyl-*O*-tosylhydroxylamine[23] did not provide any C−H aminated product.

Table 2.2 Aminating agents screening in the amination of *N*,*N*-dimethylaniline.

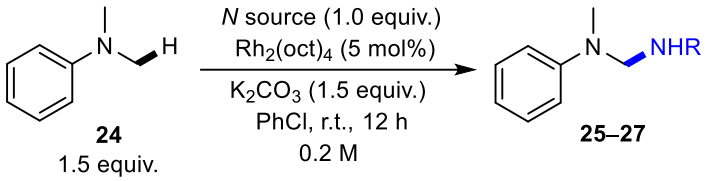

Aminating agent	Product[a]	Aminating agent	Product[a]
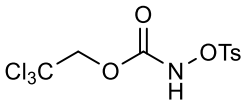	**25** (R = Troc) 46% yield	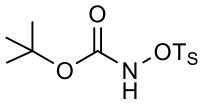	Trace
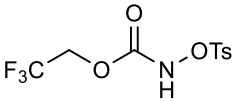	**26** (R = $CO_2CH_2CF_3$) 39% yield	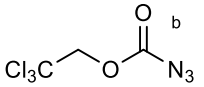	Trace
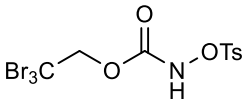	**27** (R = $CO_2CH_2CBr_3$) 43% yield	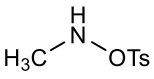	Trace

[a] Determined by crude ^{1}H NMR analysis, using 1,3-dinitrobenzene as an internal standard.
[b] Without base.

Then, the effects of solvents and bases were investigated (Table 2.3). Although the solvent did not affect the efficiency of the reaction, CH_2Cl_2 and toluene were found most suitable for the present purpose (entries 1–7). It is worth noting that the primary benzylic C(sp^3)−H bonds of toluene were totally intact for amination reaction, even when toluene was used as a solvent (entry 7). The use of Li_2CO_3, Na_2CO_3, Cs_2CO_3, Rb_2CO_3, or KOAc instead of K_2CO_3 did not improve the yield of the aminated product **25** (entry 7 vs 8–12). Finally, the yield of **25** was improved by use of 10 equiv. of the substrate **24** to afford **25** in 79% yield (entry 13).

Table 2.3 Effects of solvents and bases.

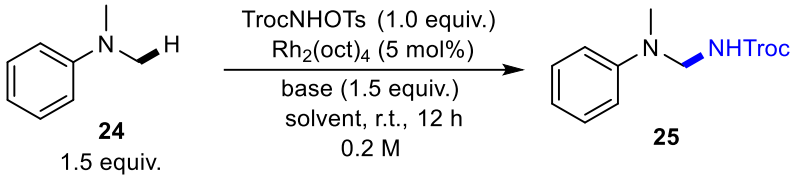

Entry	Solvent	Base	Yield (%)[a]
1	EtOAc	K_2CO_3	40
2	CH_2Cl_2	K_2CO_3	60
3	$CHCl_3$	K_2CO_3	49
4	PhH	K_2CO_3	51
5	PhF	K_2CO_3	52
6	$PhCF_3$	K_2CO_3	48
7	PhMe	K_2CO_3	60
8	PhMe	Li_2CO_3	44
9	PhMe	Na_2CO_3	30
10	PhMe	Cs_2CO_3	41
11	PhMe	Rb_2CO_3	54
12	PhMe	KOAc	40
13[b]	PhMe	K_2CO_3	79(70)[c]

[a] Determined by crude ^{1}H NMR analysis, using 1,3-dinitrobenzene as an internal standard. [b] 10 equiv. of **24** was used. [c] Isolated yield in parentheses.

2.4 Investigation for substrate scope

Substrate scope was then investigated with various *N*,*N*-dimethylarylamines under the optimized conditions for the C−H amination reaction (Table 2.4). Substrates with chloro, bromo, and iodo groups, respectively at C(4) successfully gave the corresponding aminated products **28**, **29**, and **30** in high yields. Treatment of 4,*N*,*N*-trimethylaniline with the present protocol gave **31** as a single product, while the primary benzylic C(sp^3)−H bonds amination was not observed. Either an electron-withdrawing or electron-donating group at C(4) did not affect the efficiency of the C(sp^3)−H amination reaction (**32**−**34**). The present procedure was found applicable to aniline derivatives with various substituents at the C(2), which can be seen in products **35**–**39**. The compound containing fluorescent dansyl group was found also to undergo selective amination of the C(sp^3)−H bond α to the nitrogen atom to give the product **41**. With all substrates examined here, highly chemoselective C(sp^3)−H amination was observed in the presence of aromatic C(sp^2)−H bonds. In all cases, TrocNHOTs was almost completely consumed and the formation of $TrocNH_2$ was observed, which indicated partial decomposition of the aminating reagent under the reaction conditions.[13, 24-26] When slight excess amounts (1.5 equiv.) of the substrates were employed, moderate yields of the desired products were observed in some cases (**28**, **30**, **32**, and **33**).

Site-selectivity of the C−H amination was investigated using several *N*-alkyl-*N*-methylanilines (alkyl ≠ methyl) (Table 2.5). Treatment of *N*-ethyl-*N*-methylaniline by the present protocol provided the *N*-methyl-aminated product **42** as a single regioisomer. Potential reactivity of the *N*-ethyl group toward the C−H amination might be missed because of the instability of the aminal structure of the product generated at the *N*-ethyl group if any. However, *N*-methylaniline, assumed to be generated from the decomposition of the aminal structure,[22] was not obtained under the condition. This result clearly showed that amination of *N*-ethyl-*N*-methylaniline took place site-selectively at the primary C(sp^3)−H bond adjacent to the nitrogen atom. Similarly, C(sp^3)−H amidation of substrates with an *n*-butyl and an *n*-octyl group provided *N*-methyl-amidated products **43** and **44**, respectively, as the single regioisomers. Notably, substrates with tertiary and benzylic C(sp^3)−H bonds α to the nitrogen atom underwent amination at the primary C(sp^3)−H bond selectively, to give **45** and **46**, respectively. The present method was also applicable to *N*-methyl-selective C−H amination of indoline derivative with an electronically reactive tertiary C(sp^3)−H bond adjacent to a nitrogen atom (**47**).

Although amination of some trialkylamines such as *N*,*N*-dimethylbenzylamine (**48**) under the optimized condition was examined, the desired C(sp^3)−H amination did not proceed to give only recovered starting materials (Scheme 2.5). The present protocol could not be applied for C(sp^3)−H amination of aliphatic trialkylamines.

Table 2.4 Chemoselective C(sp^3)–H amination of *N*,*N*-dimethylarylamine.

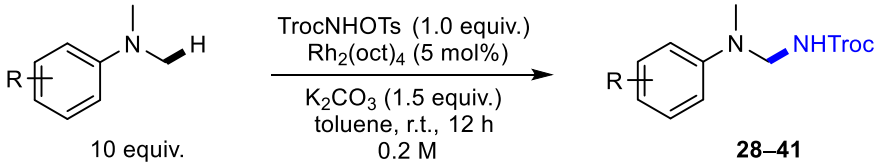

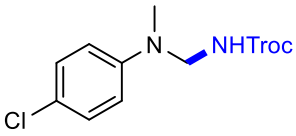

28, 75%[a] (47%)[b]

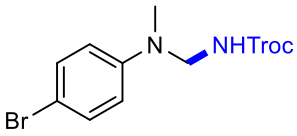

29, 71%[a]

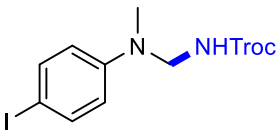

30, 69%[a] (46%)[b]

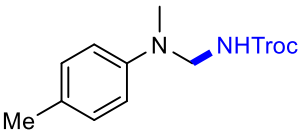

31, 41%[a]

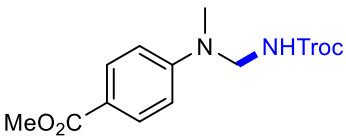

32, 73%[a] (45%)[b]

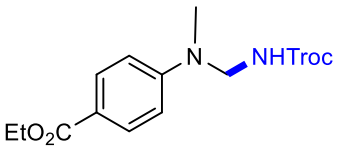

33, 63%[a] (49%)[b]

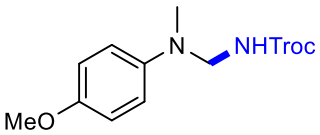

34, 53%[a]

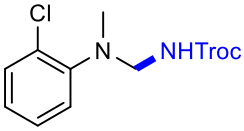

35, 44%[a]

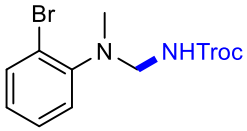

36, 59%[a]

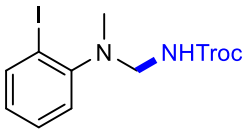

37, 52%[a]

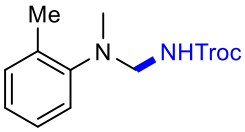

38, 43%[a]

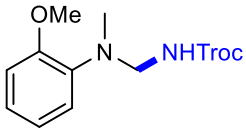

39, 54%[a]

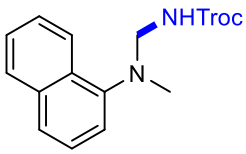

40, 48%[a]

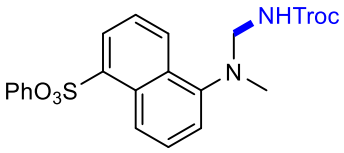

41, 59%[a]

[a] Isolated yields. [b] The number in parentheses is yield with 1.5 equiv. of substrate used, it was determined by crude ^{1}H NMR analysis, using 1,3-dinitrobenzene as an internal standard.

Table 2.5 Site selectivity profiles of C(sp^3)–H amination of *N*-alkyl-*N*-methylaniline derivatives.

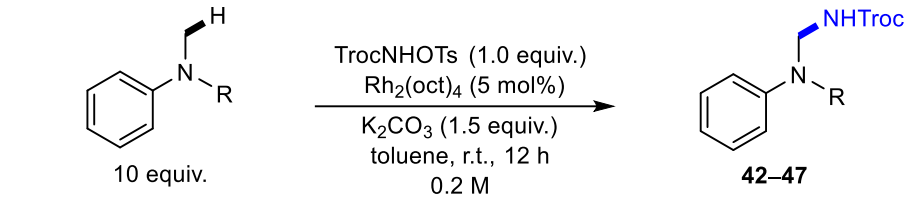

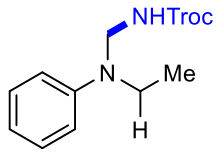

42, 33%[a]

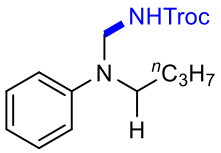

43, 43%[a]

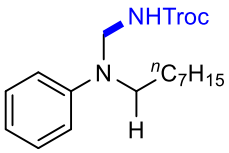

44, 40%[a]

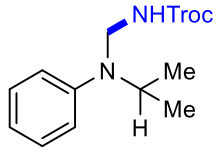

45, 42%[a]

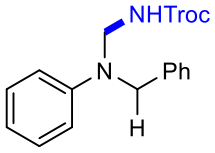

46, 37%[a]

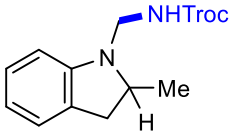

47, 33%[a]

[a] Isolated yields.

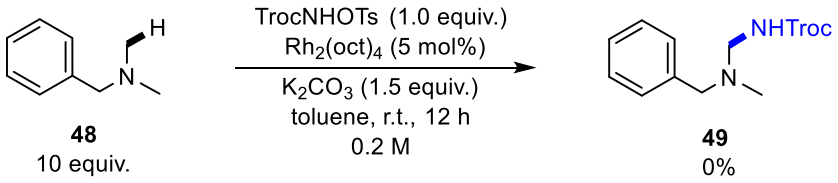

Scheme 2.5 C(sp^3)–H amination of *N*,*N*-dimethylbenzylamine.

2.5 Mechanistic investigation

To get insights into the reaction mechanism, the KIE of the reaction was measured (Scheme 2.6). Under the competitive reaction of a 1:1 mixture of **24** and **24**-d_6, the C−H amination of **24** took place faster than that of **24**-d_6. The KIE value was estimated by the three times experiment of the competitive reaction to be k_H/k_D = 3.7. This result indicated that the C−H bond cleavage is involved in the product-determining step.

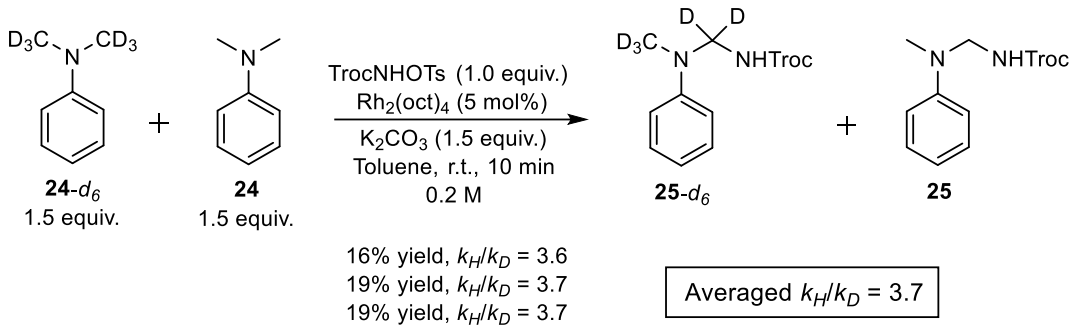

Scheme 2.6 Determination of KIE by competitive reaction between **24** and **24**-d_6.

A possible reaction pathway for the C(sp^3)−H amination is described in Scheme 2.7. The dirhodium nitrene complex is assumed to be generated from $Rh_2(oct)_4$, TrocNHOTs, and K_2CO_3 according to the previous reports for dirhodium-catalyzed C(sp^3)−H amination.[13, 25-26] The C−H insertion of the nitrene species would take place to form the N−H bond and C−N bond in an asynchronous concerted manner, which should be the product-determining step in this reaction according to the KIE experiment. At last, the product was released from the rhodium center and the regenerated $Rh_2(oct)_4$ was participated to the next catalytic cycle.

The reacting C−H bonds were selected at the C−H insertion step. For example, *N*-benzyl-*N*-methylaniline has two possible reaction sites, the primary C(sp^3)−H bonds and the secondary benzylic C(sp^3)−H bonds. Although the secondary benzylic C(sp^3)−H bonds have the less bond dissociation energy, the sterically more accessible primary methyl C(sp^3)−H bonds adjacent to the nitrogen atom was expected to be selectively converted to the C−N bond. Similar site selectivity was observed in *β*-selective C(sp^3)−H amination of organosilicon compounds via C−H insertion of dirhodium nitrene complexes.[8]

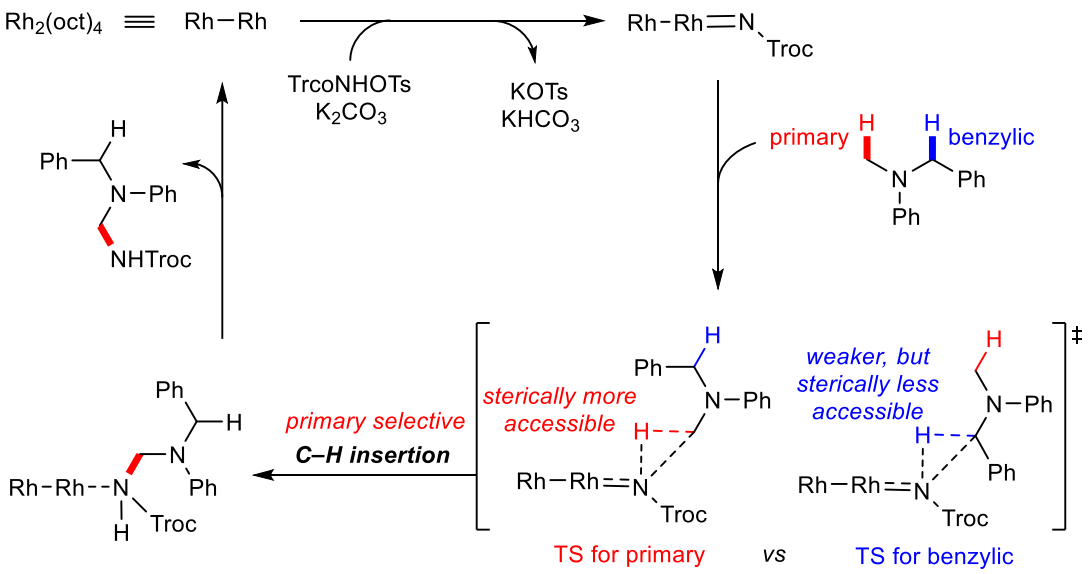

Scheme 2.7 A possible catalytic cycle.

2.6 Application to two-step demethylation

An application to two-step demethylation of the *N*-methyl aniline derivative *N*-methyl-*N*-octylaniline was demonstrated (Scheme 2.8). Treatment of **44,** obtained by C(sp^3)−H amination of *N*-methyl-*N*-octylaniline, with Cs_2CO_3 in toluene under reflux condition afforded the desired N-demethylated product, phenyloctylamine **50**, in 58% isolated yield. Development of N-demethylation reaction under mild condition has great significance because conventional methods for N-demethylation requires relatively harsh conditions.[27] The present method is assumed to be potentially useful for the application to late-stage functionalization of bioactive molecules containing aromatic *N*-methyl group.

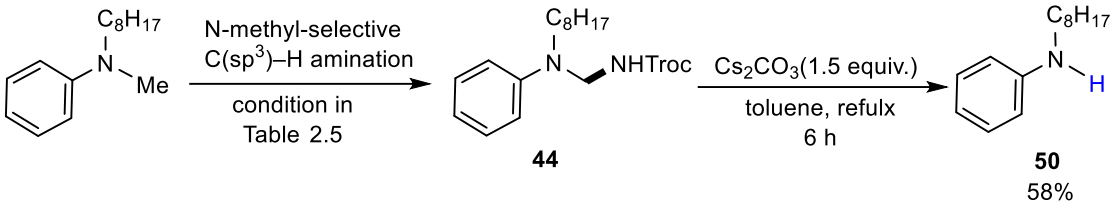

Scheme 2.8 Two-step demethylation of *N*-methyl-*N*-octylaniline.

Chapter 3 Studies on chemoselectivity in C−H amination of anisole and aniline derivatives

3.1 Background

In chapter 2, development of C(sp^3)−H amination of aniline derivatives was described, where $Rh_2(oct)_4$ was an effective catalyst and $Rh_2(tpa)_4$ was totally ineffective (Scheme 3.1a).[14] On the other hand, C−H amination of anisole (**51**) under similar condition took place selectively at *para* postion of the methoxy group, where $Rh_2(oct)_4$ was totally ineffective and $Rh_2(tpa)_4$ was an effective catalyst (Scheme 3.1b).[12] Chemoselectivities in the C−H amination reaction under similar conditions were totally different depending on the substrates. In addition, ligand effects were complementary to each chemoselective reactions. Interested in the reactivity difference and effects of the catalysts, a detailed study, especially about ligand effects on each reaction, was conducted in this chapter to elucidate the origin of the chemoselectivity and reactivity differences (Scheme 3.1c). As described in the introduction of this thesis, engineering chemo- and site selectivity is highly desirable in C−H functionalization reactions. In 2019, Baik, Park, and Chang *et al* reported Ru-catalyzed highly chemoselective C−H amination reaction (Scheme 3.2).[28] Based on the mechanistic investigation, it was proposed that the π-π interaction between the ligand on the catalyst and substrate accelerate the intramolecular benzylic C−H amination selectively rather than tertiary C−H amination. Inspired from the report, I envisaged that elucidation of the origin of the chemoselectivity and the reactivity could lead to improve the reaction efficiency in dirhodium-catalyzed C−H amination and design new catalysts for the purpose.

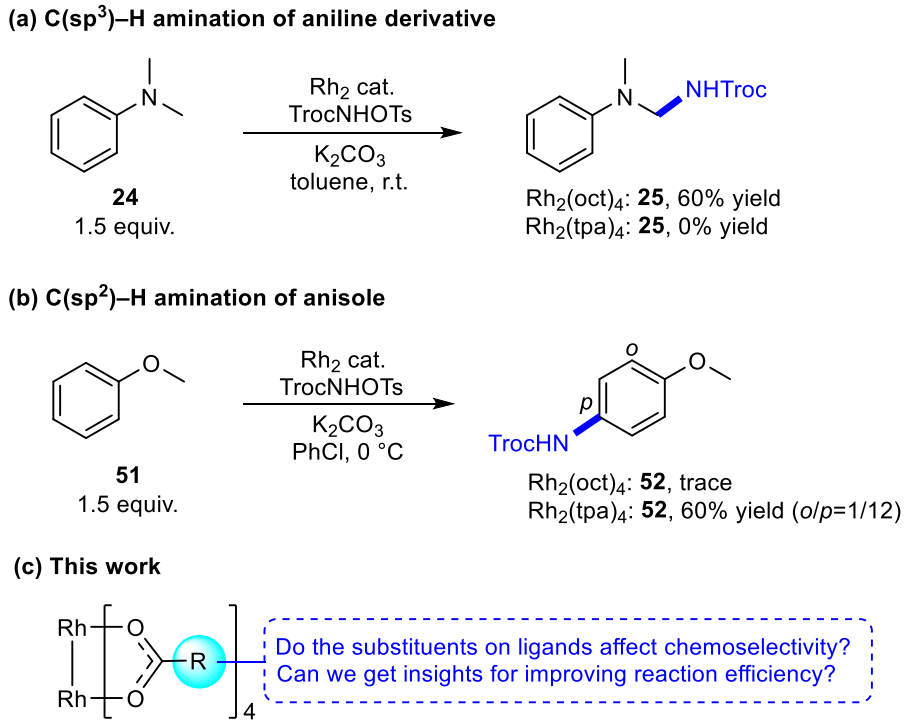

Scheme 3.1 (a) Effects of catalysts in C(sp^3)−H amination of **24**. (b) Effects of catalysts in p*ara*-C(sp^2)−H amination of **51**. (c) The purpose of this chapter.

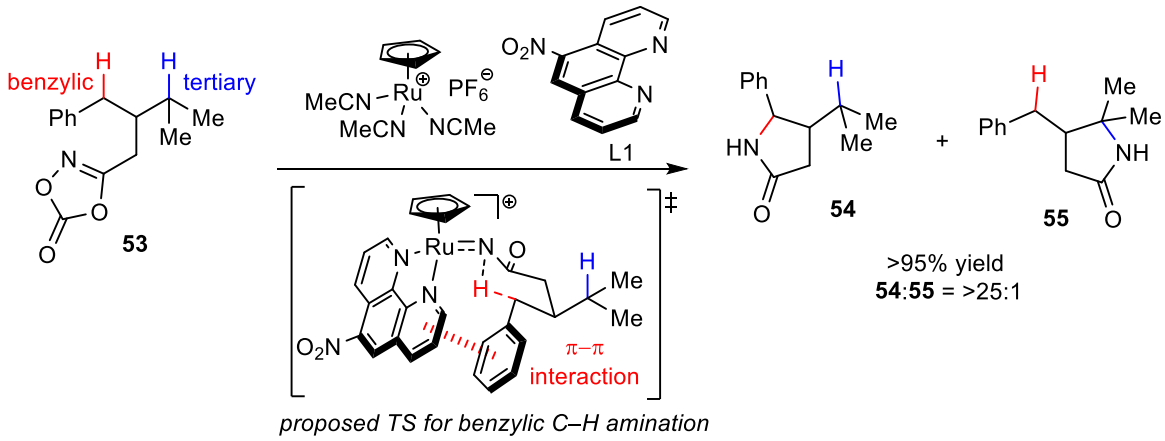

Scheme 3.2 Ru-catalyzed chemoselective C(sp^3)−H amination driven by π-π interaction between the ligand and the substrate.

3.2 Consideration about chemoselectivity

Under the condition described in Scheme 3.1, the reactive intermediate is assumed to be the same species, dirhodium nitrene complexes. Depending on the substrates, the most reactive C−H would be determined and the efficiency should be affected by the structures of the catalysts (Figure 3.1). The dirhodium nitrene species is expected to be inserted into the C(sp^3)−H bond α to the nitrogen atom of **24** in a concerted asynchronous manner (Figure 3.1a). The C−H insertion step includes a hydride transfer process assisted by effective donation of the lone-pair electron of the neighboring nitrogen atom and the following C−N bond formation. On the other hand, C−H amination of **51** took place at the aromatic *para*-C(sp^2)−H bond selectively even in the presence of C(sp^3)−H bonds α to the oxygen atom (Figure 3.1b). The difference in chemoselectivity could be ascribed to the difference in the electronegativity and valence between nitrogen and oxygen. The partial positive charge developed in the transition state of C(sp^3)–H amination of the *N*-methyl group in **24** would be stabilized by the adjacent nitrogen, to provide the *N*-methyl aminated product **25** instead of the C(sp^2)−H amination on the aromatic ring. On the other hand, such stabilization may not be effectively operative in the reaction of **51** because of the relatively stronger negative inductive effect of oxygen, derived from high electronegativity and low valence, than nitrogen. As a result, electrophilic aromatic substitution of the electron-rich aromatic ring of **51** would take place at the *para* position distal from the oxygen atom to selectively provide **52**.

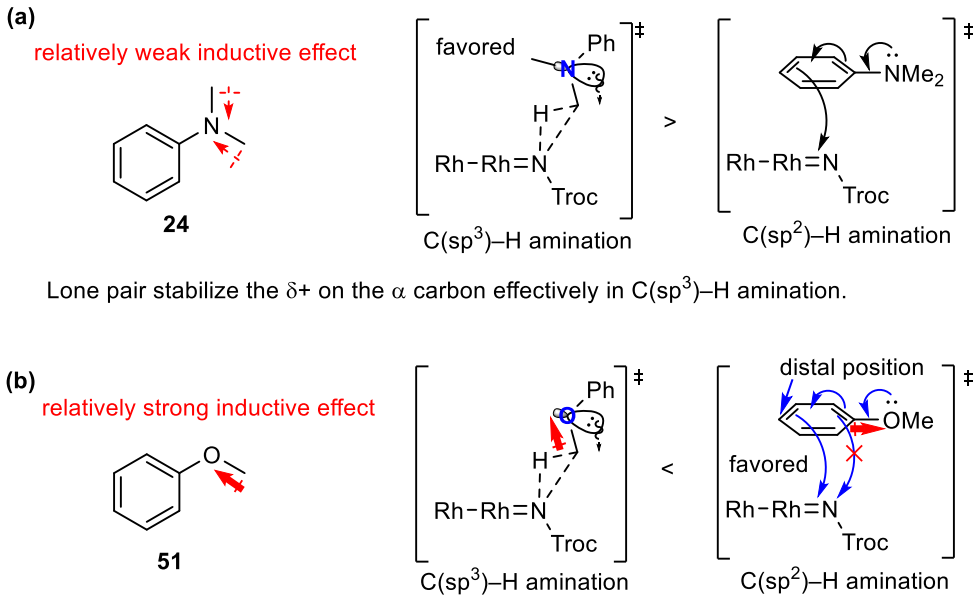

Figure 3.1 Consideration of the reactivity difference between (a) *N*,*N*-dimethylaniline and (b) anisole.

3.3 Ligand effects in C(sp^3)−H amination of *N,N*-dimethylaniline

To check the effects of the ligand structures, the C(sp^3)−H amination of *N,N*-dimethylaniline (**24**) was examined in the presence of dirhodium catalysts with different numbers of phenyl rings on the α carbon of the carboxylate group (Table 3.1). Triphenyl or diphenyl-substituted catalysts were totally ineffective, while the monophenyl-substituted catalyst promoted C(sp^3)−H amination of **24** with less efficiency than $Rh_2(oct)_4$. $Rh(PhCO_2)_4$ accelerated the reaction comparable to $Rh_2(oct)_4$. As the numbers of phenyl substituents on the α carbon to the carboxyl group of the ligands increased, the yield of the aminated product **25** decreased. These results allowed me to hypothesize that the phenyl ring on the α carbon of the carboxylate group inhibit the C(sp^3)−H amination of **24**.

Table 3.1 The effect of the numbers of phenyl rings on the ligand in the C(sp^3)−H amination.

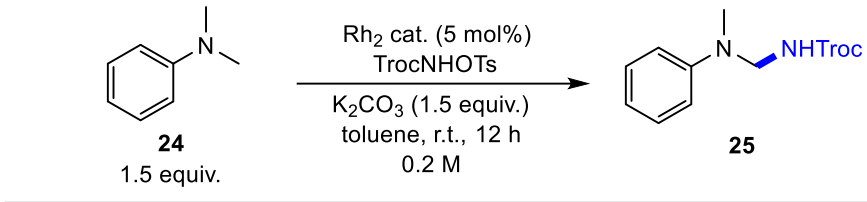

$Rh_2(tpa)_4$	$Rh_2(Ph_2MeCCO_2)_4$	$Rh_2(PhMe_2CCO_2)_4$	$Rh_2(PhCO_2)_4$	$Rh_2(oct)_4$
Trace[a]	Trace[a]	21%[a]	48%[a]	57%[a]

[a] Determined by crude ^{1}H NMR analysis, using 1,3-dinitrobenzene as an internal standard.

3.4 NMR experiments for estimation of association between catalysts and substrates

There seems to be the possibility that coordination of substrate **24** inhibit the catalytic reaction as frequently observed in transition-metal-catalyzed reaction. To estimate the association between substrate and catalyst, ^{1}H NMR spectra of a 1:1 mixture of **24** and dirhodium catalysts were measured and compared to the spectrum of **24** (Figure 3.2). In the ^{1}H NMR of a 1:1 mixture of **24** and $Rh_2(oct)_4$, the chemical shift of Ha was lower field shifted compared to the free state of substrate **24** (Figure 3.2a vs b). The change of the chemical shift of Ha could be ascribed from the coordination of the nitrogen of **24** to the rhodium center of $Rh_2(oct)_4$. On the other hand, in the ^{1}H NMR of a 1:1 mixture of **24** and $Rh_2(tpa)_4$, the chemical shift of Ha was upper field shifted compared to the free state of substrate **24**, contrary to the case of $Rh_2(oct)_4$ (Figure 3.2a vs c). The change of the chemical shift indicated that the Ha protons of **24** were distributed near the phenyl ring on the ligand as a result from coordination of **24** to the rhodium center of $Rh_2(tpa)_4$. The shielding effect of the ring current of the phenyl rings would be responsible for the upper field shift of Ha, which suggested the C−H/π interaction between the substrate and the ligand.

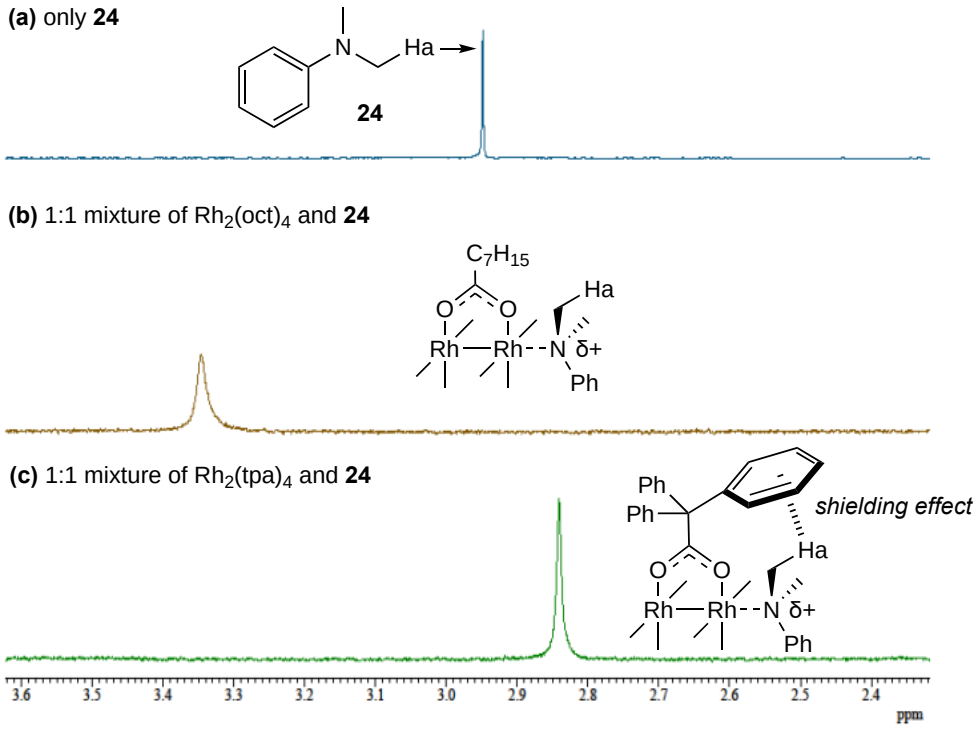

Figure 3.2 ^{1}H NMR spectra ($CDCl_3$, 293 K, 400 M Hz) of (a) **24**, (b) 1:1 mixture of $Rh_2(oct)_4$ and **24**, and (c) 1:1 mixture of $Rh_2(tpa)_4$ and **24**.

The signals of the ligands were also informative for association between **24** and catalysts. ^{1}H NMR spectra of various ratios of mixtures of **24** and $Rh_2(oct)_4$ or $Rh_2(tpa)_4$ were measured and compared to the spectra of only catalysts (Figure 3.3). In the spectra of $Rh_2(oct)_4$, only one signal which can be assigned as the Hb signal was observed in all spectra (Figure 3.3a), which suggested that the association equilibrium was fast and reversible. On the other hand, in the spectra of $Rh_2(tpa)_4$, two different signals which can be assigned as the Hc signal were observed (Figure 3.3b). As the amount of **24** increased, the intensity of the signal in lower field decreased and that in upper field increased. These results indicated that the coordination of **24** to $Rh_2(tpa)_4$ is relatively strong and almost quantitative formation of the complex between **24** and $Rh_2(tpa)_4$. As my expectation, association ability of the catalysts to the substrate **24** was significantly different, depending on the structures of the ligands.

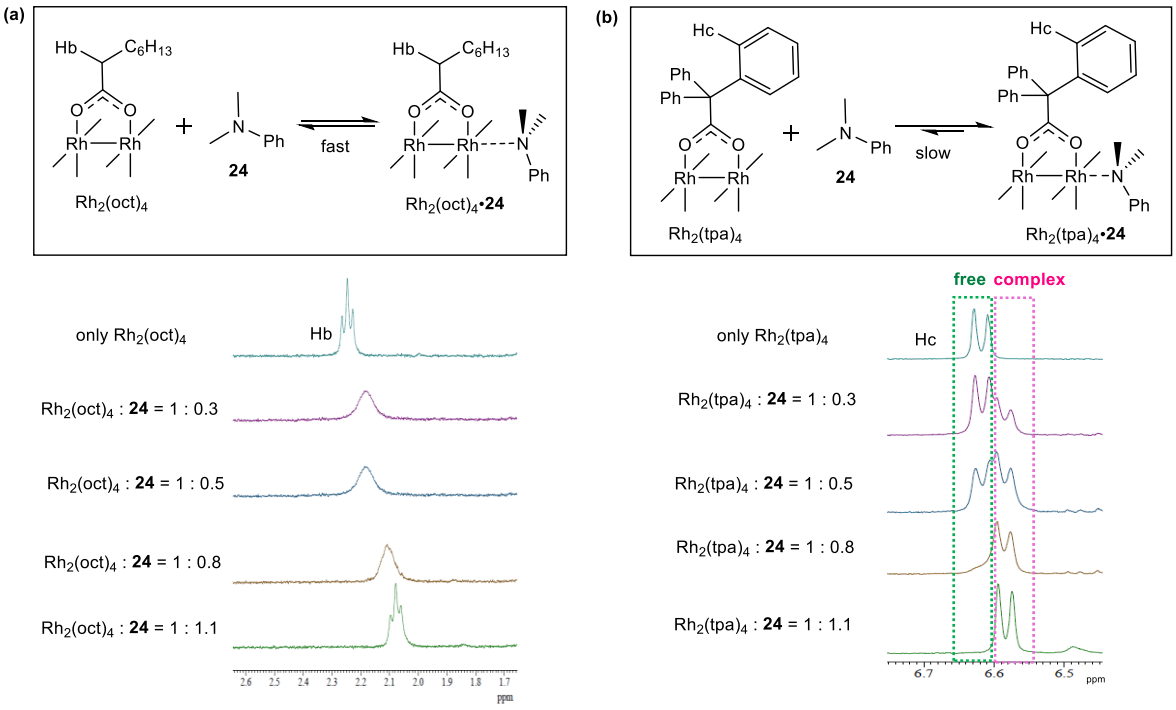

Figure 3.3 (a) ^{1}H NMR spectra ($CDCl_3$, 293 K, 400 MHz) of $Rh_2(oct)_4$ and mixtures with **24**. (b) ^{1}H NMR spectra ($CDCl_3$, 293 K, 400 MHz) of $Rh_2(tpa)_4$ and mixtures with **24**.

3.5 Calculation for effects of ligand structures

To estimate the energy difference in coordination of **24** to the rhodium center, the DFT calculation was performed (Scheme 3.3). Considering existence of huge conformational isomers of $Rh_2(oct)_4$, $Rh_2(OAc)_4$ was used for the model of $Rh_2(oct)_4$ in the calculation. While the stabilization energy by coordination of **24** to $Rh_2(OAc)_4$ was relatively low (ΔG = −2.0 kcal/mol), the complex between **24** and $Rh_2(tpa)_4$ was much more stable than their free state (ΔG = −15.0 kcal/mol). The difference of the stabilization energy depending on the catalysts were in good agreement with the observation in ^{1}H NMR experiment (Figure 3.3).

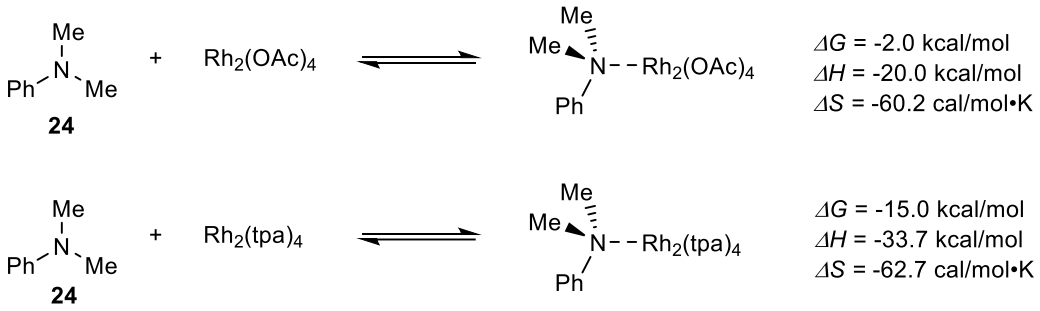

Scheme 3.3 Calculated association energies of **24** with $Rh_2(OAc)_4$ and with $Rh_2(tpa)_4$. Calculation was performed by DFT with M06/LanL2DZ(Rh)/6-31G(d,p) level of theory.

To investigate the origin of the energy difference depending on the catalysts, the obtained 3D structure of the complex between **24** and $Rh_2(tpa)_4$ was shown in Figure 3.4. The structure clearly showed that there are multiple C−H/π interactions between **24** and the phenyl rings on the α carbon of the ligand carboxylates. The calculated structure was consistent with the observation about the upper field shift of the signal of **24** in the ^{1}H NMR spectra shown in Figure 3.2. Based on the results, I concluded that the phenyl rings on the α carbon of the ligand carboxylates stabilized the complex between substrates and catalysts to inhibit smooth catalytic cycle in the C(sp^3)−H amination of aniline derivatives.

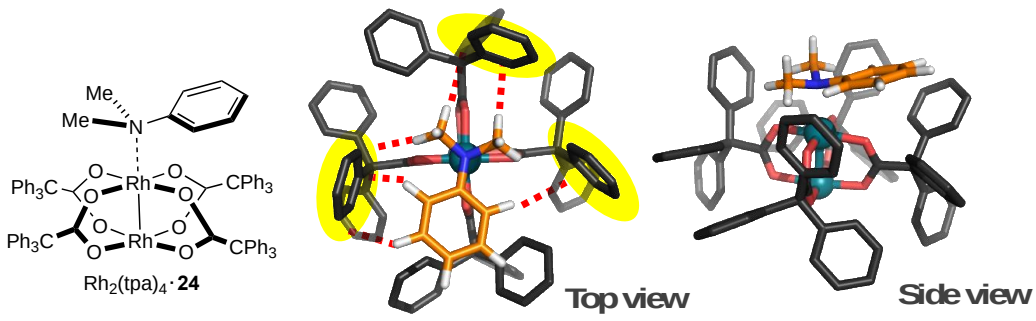

Figure 3.4 Calculated structure of the complex between **24** and $Rh_2(tpa)_4$.

3.6 Interpretation of the effects of catalysts in C(sp^3)–H amination of *N*,*N*-dimethylaniline

Based on the NMR experiments and DFT calculations in the above sections, interpretation of the effects of the catalysts was described in Scheme 3.4. Coordination of substrate **24** to the rhodium center would inhibit the smooth catalytic cycle, where the complex be a resting state in the reaction. In the case of $Rh_2(oct)_4$, coordination of **24** to the catalyst was reversible and coordination of the nitrene source, TrocNHOTs, successfully departed the catalytic cycle including formation of the dirhodium nitrene complex and its C–H insertion (Scheme 3.4a). On the other hand, in the case of $Rh_2(tpa)_4$, coordination of **24** to the catalyst was almost quantitative and the dissociation was very slow because of multiple C–H/π interactions between **24** and the ligands, which was supported by NMR experiments and DFT calculation. Thus, most of $Rh_2(tpa)_4$ form the inactive complex, as a resting state, and almost no coordination-free active catalyst exists in the solution (Scheme 3.4b). As a result, coordination of **24** to $Rh_2(tpa)_4$ could inhibit the catalytic cycle starting from coordination of TrocNHOTs to the rhodium center not to provide any C–H aminated products.

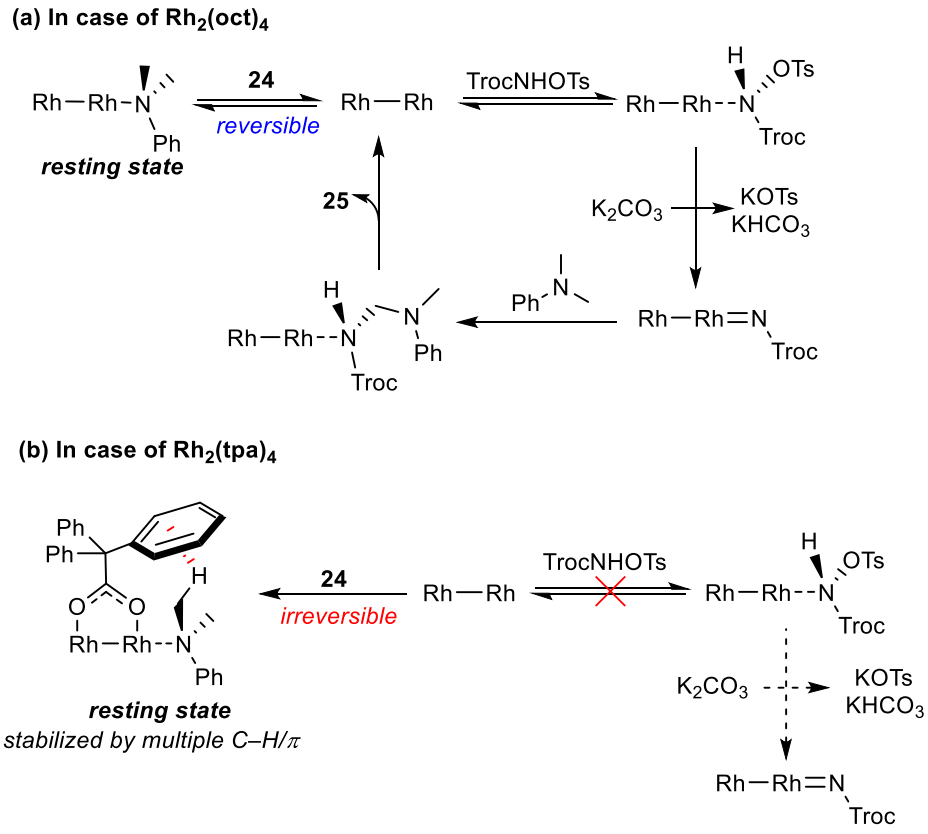

Scheme 3.4 The effects of the catalysts in C(sp^3)–H amination of dimethylaniline **24**.

3.7 Ligand effects in C(sp^2)−H amination of anisole

The ligand effects in C(sp^2)−H amination of anisole (**51**) were also investigated, using dirhodium catalysts with different numbers of phenyl rings on the α carbon of the carboxylate group (Table 3.2). Triphenyl or diphenyl-substituted catalysts accelerated the reaction effectively, while the less substituted catalysts have dramatically reduced activity. On the contrary to the case of C(sp^3)−H amination of aniline derivative, as the numbers of phenyl substituents on the α carbon to the carboxyl group of the ligands increased, the yield of the aminated product **52** increased.

Table 3.2 The effect of the numbers of phenyl rings on the ligand in the C(sp^2)−H amination.

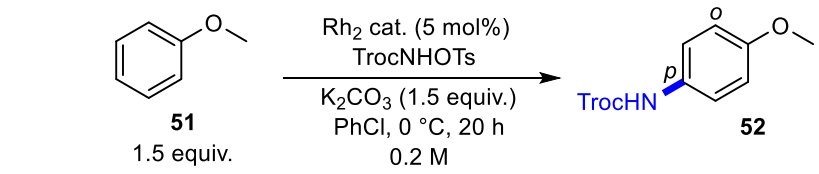

$Rh_2(tpa)_4$	$Rh_2(Ph_2MeCCO_2)_4$	$Rh_2(PhMe_2CCO_2)_4$	$Rh_2(PhCO_2)_4$	$Rh_2(oct)_4$
59%[a]	53%[a]	6%[a]	Trace[a]	Trace[a]
p:*o* = 9/1	*p*:*o* = 9/1	*p*:*o* = 10/1		

[a] Determined by crude ^{1}H NMR analysis, using 1,3-dinitrobenzene as an internal standard.

From the observation of the tendency in Table 3.2 and the effects of the phenyl rings in the C(sp^3)−H amination of aniline derivatives, it was proposed that cation/π or C−H/π interactions between reacting substrate **51** and the phenyl rings on the ligands would stabilize the possible transition state structure for nucleophilic attack of the aromatic ring to the dirhodium nitrene complex (Figure 3.5). Although optimization of the transition state structure using the catalysts with phenyl rings on the α carbon was examined based on the previously calculated structure of the transition state using $Rh_2(OAc)_4$, the desired transition structure was not obtained because the activation electronic energy ($\Delta E^{\ddagger}$) was less than 0 kcal/mol.

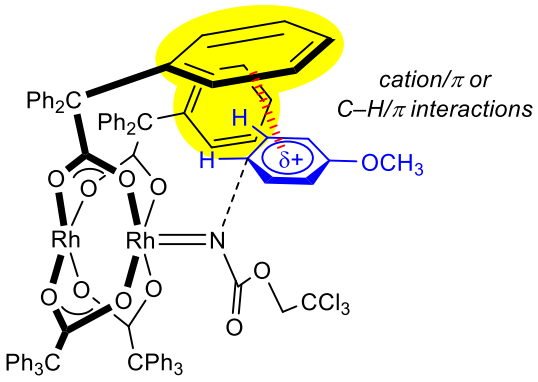

Figure 3.5 Proposed transition state structure.

3.8 Design of a new catalyst for C(sp^2)−H amination and trial

In the former sections, stabilization effect for transition state of C(sp^2)−H amination of anisole by cation/π or C−H/π interactions was proposed according to the results on relationship between ligand structures and catalytic activities. Based on the proposal, a new catalyst **56** was designed for improvement of reaction efficiency in dirhodium-catalyzed C(sp^2)−H amination with the expectation that electron-rich aromatic rings on the ligands of **56** can stabilize the proposed transition state more effectively than $Rh_2(tpa)_4$ (Figure 3.6a). The carboxylic acid **57** was easily prepared from benzoylformic acid and anisole according to the reported procedure[29] and ligand exchange using $Rh_2(OAc)_4$ and the synthesized carboxylic acid **57** provided the catalyst **56** in good yield (Figure 3.6b).

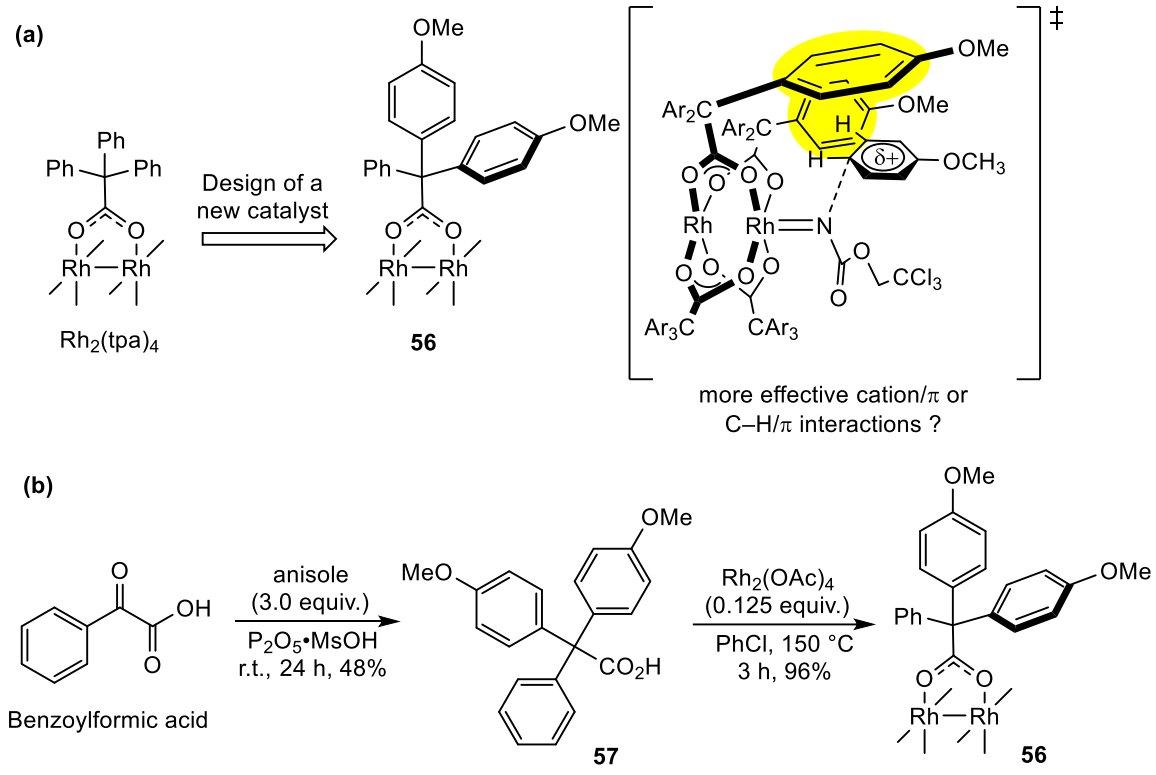

Figure 3.6 Design and synthesis of a new catalyst **56** for C(sp^2)−H amination.

The synthesized catalyst **56** was employed in C(sp^2)−H amination of anisole **51** (Scheme 3.5a). In the presence of **56**, treatment of **51** with TrocNHOTs and K_2CO_3 in chlorobenzene at 0 °C for 20 h gave the *para*-C(sp^2)−H aminated product **52** in 46% yield. The product yield was comparable with $Rh_2(tpa)_4$-catalyzed reaction and the expected improvement in reaction efficiency was not observed. Then, the C(sp^2)−H amination of triphenylamine **58** was investigated with some Rh_2 catalysts (Scheme 3.5b). Although the experimental results and discussions in sections 3.3 to 3.6 suggested that the phenyl substituents on the α cabon of the ligands stabilize the coordination of amines to the rhodium center and

inhibit the smooth catalytic cycle for C−H amination, I envisioned that bulky substituents on the nitrogen inhibit coordination of **58** to rhodium center and the C(sp^2)−H amination of an aniline derivative could proceed via stabilization of the transition state for C(sp^2)−H amination. While the $Rh_2(oct)_4$ catalyzed reaction provided the desired *para*-C(sp^2)−H aminated product **59** in just 7% yield, the $Rh_2(tpa)_4$ catalyzed reaction afforded **59** in moderate yield (37%). Furthermore, in the presence of **56**, **59** was obtained in slightly improved yield of 40%. Although the stabilization effect or the proposed transition state for C(sp^2)−H amination by introduction of electron-donating groups on the ligands was not critical, the experimental results in this section have no contradictions with my expectations and proposal. In addition, to the best of my knowledge, this is the first example of dirhodium-catalyzed *para* selective C(sp^2)−H amination of aniline derivatives.

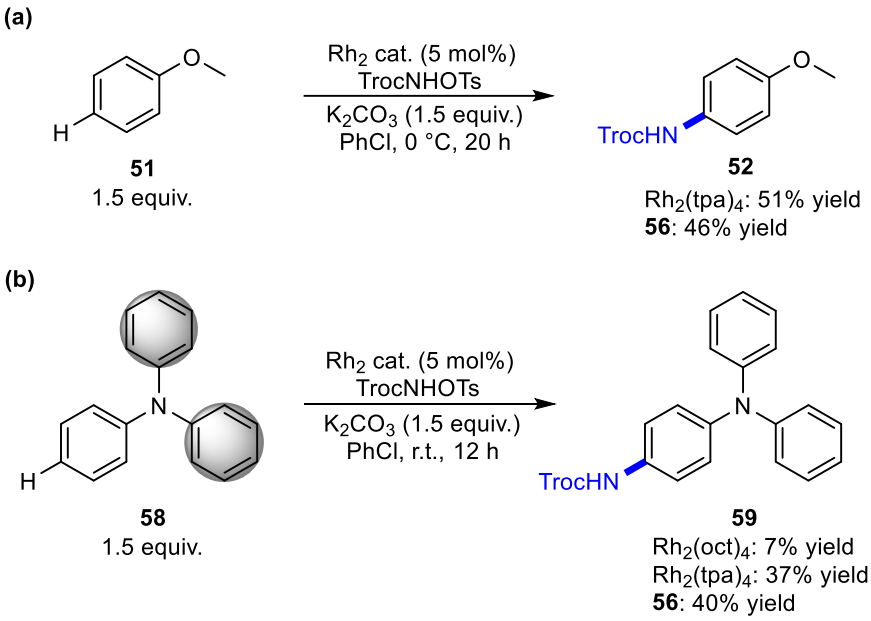

Scheme 3.5 Examination of C(sp^2)−H amination of anisole (**51**) and triphenylamine (**58**) with $Rh_2(tpa)_4$ and catalyst **56**.

Chapter 4 Catalytic asymmetric synthesis of inherently chiral calixarenes by enantioselective C(sp^2)−H amination

4.1 Background

Calixarenes are known to be representative molecules in host-guest chemistry. Because they have cavities surrounded by the electron rich aromatic rings and can encapsulate other molecules depending on the size and electronic nature, much efforts have been devoted to synthesis of functionalized calixarene derivatives and their application to host-guest chemistry.[30] Due to the bowl-shaped 3D structure, calixarenes have a non-classical chirality, inherent chirality, depending on the arrangement of achiral substituents.[31] For example, calix[4]arene derivative **60** with two different substituents on the upper rim (R^1, R^2) has the chirality: when (*cR*)-**60** or (*cS*)-**60** is viewed from the concave side, the array of the substituents (R^1, R^2) is assigned as clockwise or counterclockwise (CIP priority: R^1>R^2), respectively (Figure 4.1).

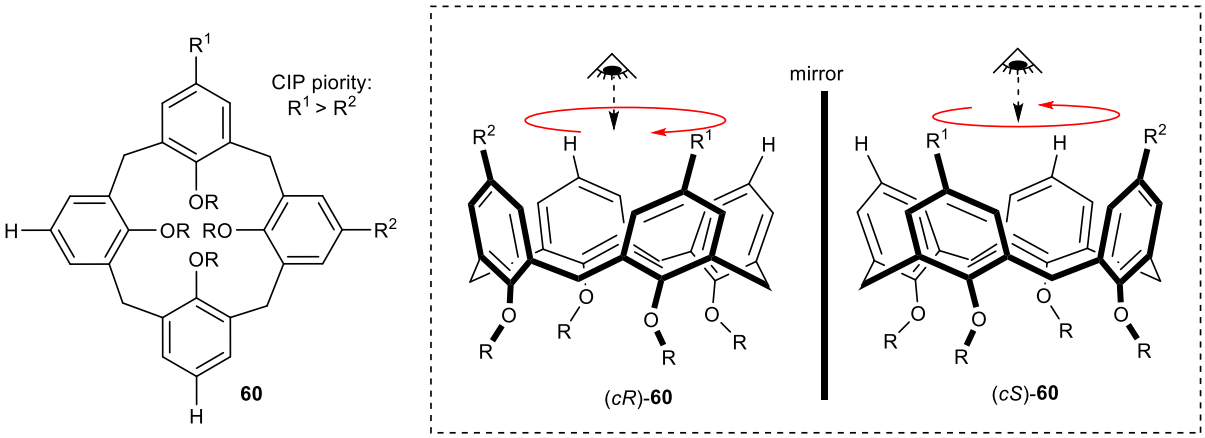

Figure 4.1 The concept of inherently chiral calix[4]arenes.

Since the concept of the non-classical chirality had been confirmed by optical resolution of the racemic inherently chiral calix[4]arenes (ICCs) in 1990,[32] various methods for preparation of ICCs including separation by chiral HPLC, separation of diastereomers by introduction of chiral fragments to racemic ICCs and asymmetric synthesis were reported.[33] Considering the application of the ICCs for development of functional molecules, asymmetric synthesis was required in terms of quantity.

Arnott *et al* reported the first successful asymmetric synthesis of ICCs by virtue of a chiral auxiliary (Scheme 4.1).[34] By treatment of calix[4]arene derivative **61** possessing a chiral oxazoline moiety, derived from L-valine, with cyclopentyllithium, *ortho*-lithiation took place diastereoselectively and following fluorination by *N*-fluorobenzenesulfonimide (NFSI) provided **62** in 73% yield and 93% de. After hydrolysis of the oxazoline moiety of **62**, the ICC **63** was obtained in high enantiomeric excess.

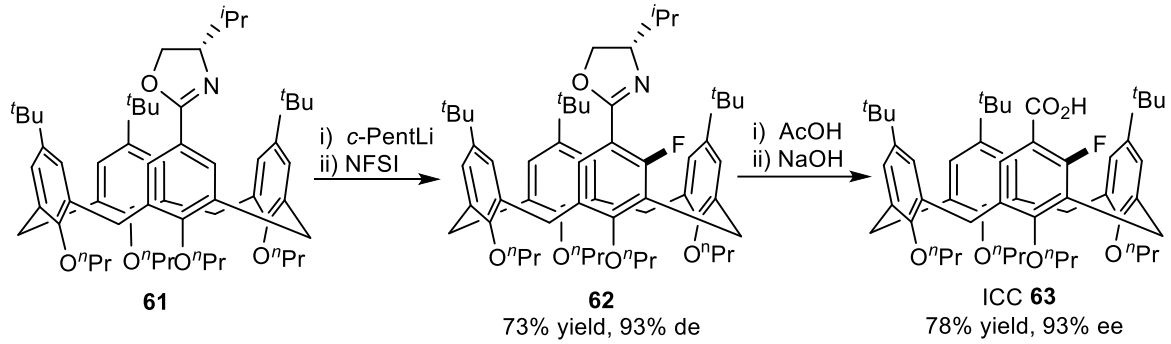

Scheme 4.1 The first diastereoselective synthesis of ICCs by virtue of chiral auxiliary.

Although there are many reports about synthesis of various types of ICCs, only one example of catalytic asymmetric synthesis of ICCs was reported[35] in spite of the widely known utility of catalytic asymmetric synthesis in preparation of chiral molecules. McKervey *et al* reported lipase-catalyzed acylative desymmetrization of C_s-symmetric calix[4]arene derivative **64** (Scheme 4.2). Although the method was able to provide enantiomerically pure ICC **65**, the yield of **65** was very low probably due to formation of other regioisomers and over-acylated products (diacylate or triacylate).

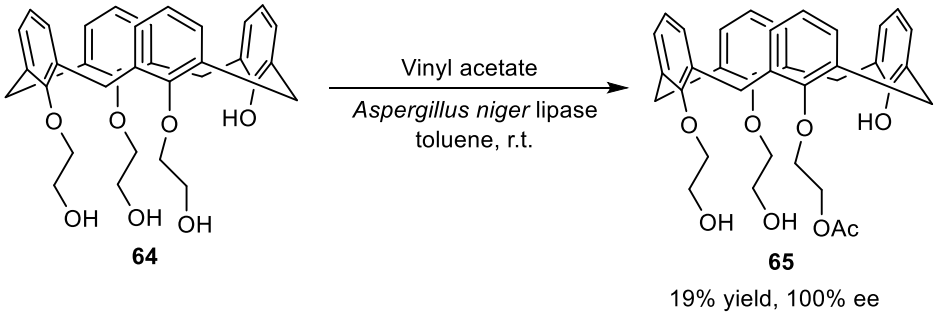

Scheme 4.2 The first catalytic asymmetric synthesis by enzymatic acylative desymmetrization.

During the study of dirhodim-catalyzed chemo- and site-selective C−H amination reaction, Ueda and Kawabata *et al* found that calix[4]arene derivative **66** underwent selective C−H amination at the *para* position of the phenolic hydroxy group by treatment with $Rh_2(tpa)_4$ and TrocNHOTs (Scheme 4.3a).[12] In this chapter, based on the discovery, I tried to develop the first efficient catalytic asymmetric synthesis of ICCs, using artificial catalysts. For the purpose, C−H aminative desymmetrization of C_s-symmetric calix[4]arene derivatives with two enantiotopic C(sp^2)−H bonds were designed and examined by use of chiral dirhodium complexes as catalysts (Scheme 4.3b).

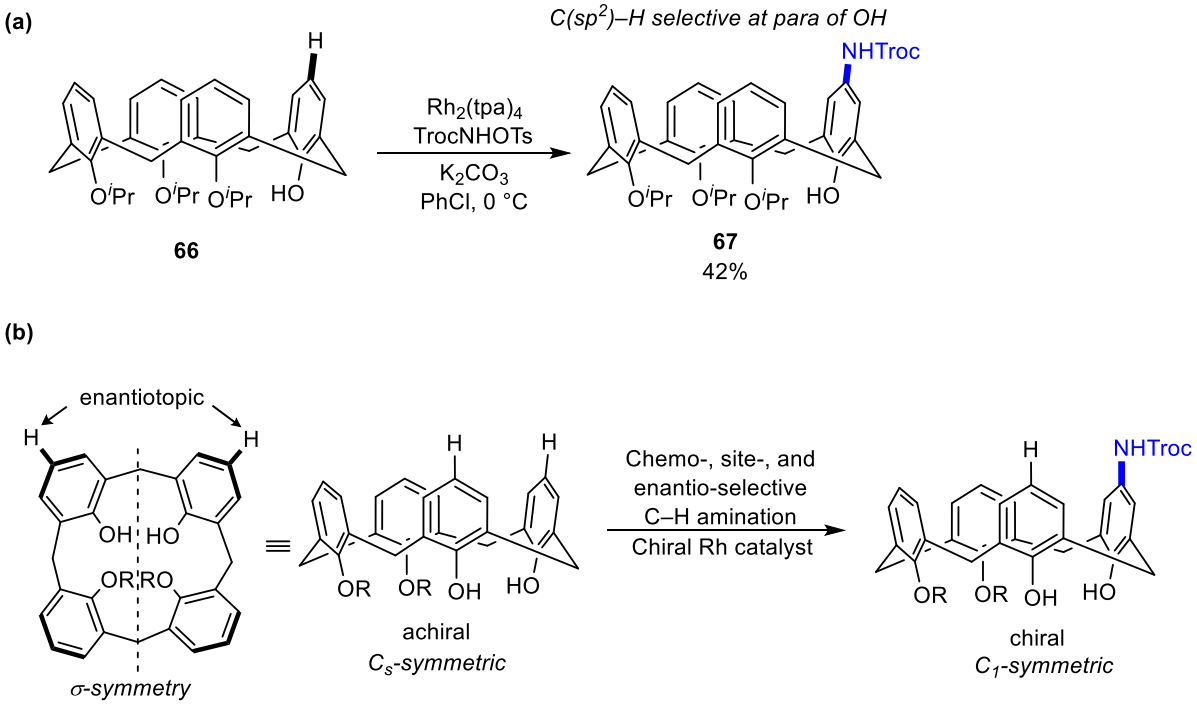

Scheme 4.3 (a) A previous example of dirhodium catalyzed chemo- and site-selective C(sp^2)–H amination of calix[4]arene derivative **66**. (b) The research aim and design of C–H aminative desymmetrization for catalytic asymmetric synthesis of ICCs.

4.2 Enantioselecitve C(sp^2)–H Amination of *O,O'*-di^{i}Pr-calix[4]arene

Firstly, 25,26-dihydroxy-27,28-diisopropoxycalix[4]arene (*O,O'*-di^{i}Pr-calix[4]arene) (**68**) was synthesized and enantioselective C(sp^2)−H amination was examined in the presence of various chiral dirhodium complexes (Table 4.1). In all experiment, the desired product was obtained just in trace amounts. Considering the color change of the reaction solutions from green to grey, decomposition of the dirhodium complexes was concerned probably due to the coordination of phenoxide derived from **68** and K_2CO_3 to the rhodium center.

Table 4.1 Trials for enantioselective C(sp^2)−H amination of *O,O'*-di^{i}Pr-calix[4]arene **68**.

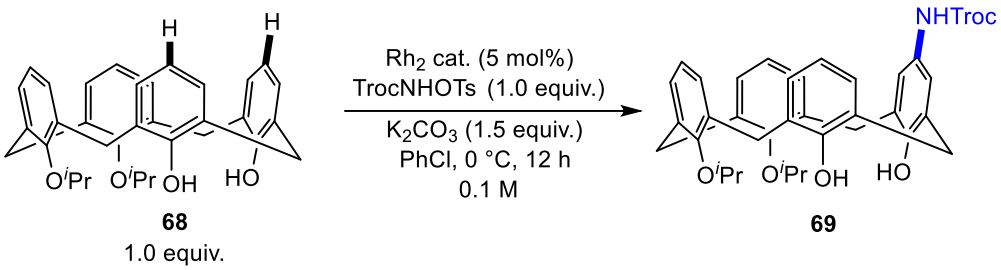

68
1.0 equiv.

69

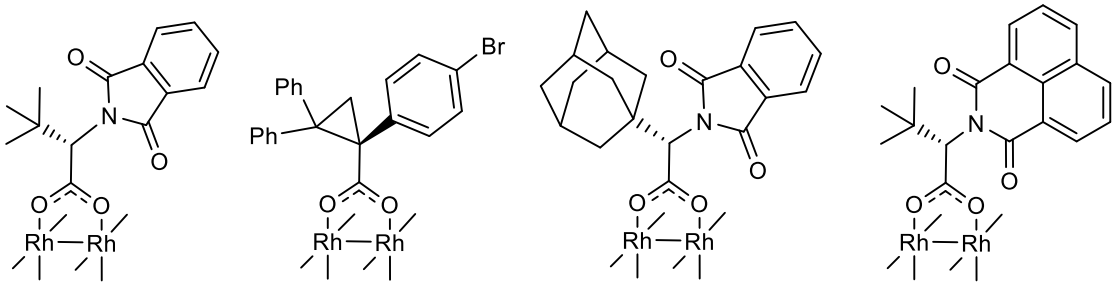

Rh$_2$(*S*-PTTL)$_4$
Trace

Rh$_2$(*R*-BTPCP)$_4$
Trace

Rh$_2$(*S*-PTAD)$_4$
Trace

Rh$_2$(*S*-NTTL)$_4$
Trace

4.3 Enantioselecitve C(sp^2)–H amination of silyl-protected calix[4]arene

To inhibit the coordination of phenoxide to the Rh center and decomposition of the catalysts, I planned to introduce bulky substituents on the lower rim instead of two isopropyl groups. In the literature, 1,1,3,3-tetraisopropyldisiloxane-1,3-diyl (TIPDS) group was reported as a useful protecting group for *O*,*O'*-difunctionalization of calix[4]arene. According to the literature,[36] TIPDS protected calix[4]arene **70** was synthesized in a similar way and catalytic desymmetrization of **70** was investigated (Table 4.2). While Rh_2(*S*-DOSP)$_4$ did not provide any C−H aminated products, Rh_2(*R*-BTPCP)$_4$ afforded the desired product **71** as a racemic mixture. Rh_2(*S*-PTTL)$_4$ catalyzed the enantioselective C(sp^2)−H amination of **70** with moderate enantioselectivity (26% yield, 50% ee). Further screening for catalysts, solvents, and bases did not improve the yield and enantioselectivity in the reaction of **70**.

Table 4.2 Catalyst screening for C−H aminative desymmetrization of TIPDS protected calix[4]arene.

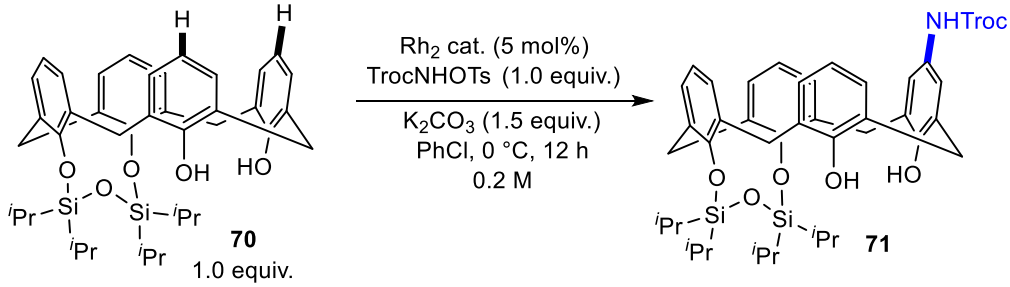

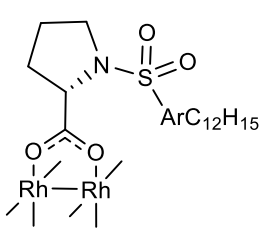

Rh_2(*S*-DOSP)$_4$
0% yield,[a] 0% ee[b]

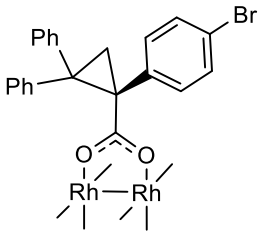

Rh_2(*R*-BTPCP)$_4$
8% yield,[a] 0% ee[b]

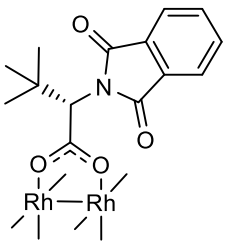

Rh_2(*S*-PTTL)$_4$
26% yield,[a] 50% ee[b]

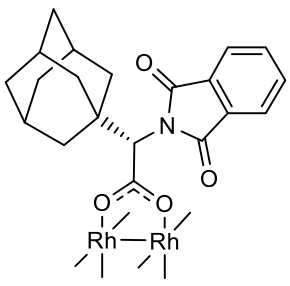

Rh_2(*S*-PTAD)$_4$
24% yield,[a] 50% ee[b]

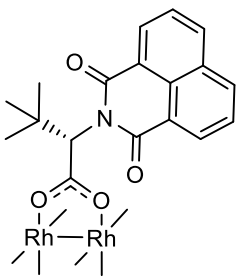

Rh_2(*S*-NTTL)$_4$
10% yield,[a] 37% ee[b]

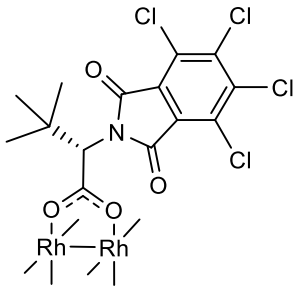

Rh_2(*S*-TCPTTL)$_4$
11% yield,[a] -21% ee[b]

[a] Isolated yields. [b] Determined by HPLC.

4.4 Design and synthesis of upper-rim-modified calix[4]arene

In the former sections, modification of the lower rim of the calix[4]arene was investigated to find that modification of lower rim was not enough for efficient asymmetric induction from the chiral dirhodium complexes in C(sp^2)−H amination of the upper rim. To improve enantioselectivity, a substrate **72** with substituents on the upper rim was designed (Scheme 4.4). Considering that substituents on the upper rim in close to the reacting site would interact or collide with substituents on the ligands of chiral dirhodium complexes, effective asymmetric induction was expected to be achieved. Phenyl groups were chosen as substituents because both attractive and repulsive interactions between a substrate and chiral dirhodium complex can be expected.

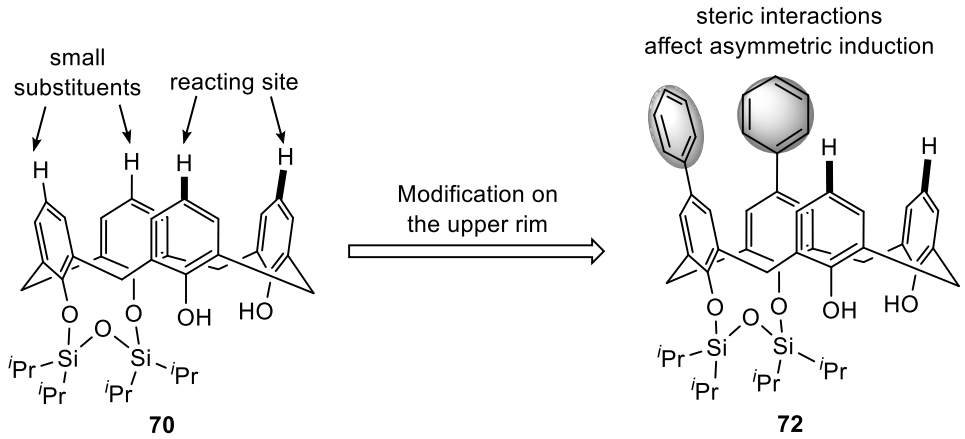

Scheme 4.4 Design of substrate for effective asymmetric induction.

A synthetic route of **72** was described in Scheme 4.5. Dibromide **73** was synthesized by 2 steps from calix[4]arene according to the reported procedure.[37] Treatment of **73** with TIPDSCl and ^{t}BuOK gave a mixture of conformational isomers of the desired product (**74a**:**74b** = 3.3:1), they can be separated by recycle HPLC. From the symmetry of the ^{1}H NMR spectra of **74a** and **74b**, the conformations of them could be assigned as cone or 1,2-alternate, not partial cone. The significant difference between the spectra was the chemical shift difference of methylene protons Ha and Hb (shown in structures of **74a** and **74b** in Scheme 4.5). Compared to the ^{1}H NMR spectra of the known 1,2-alternate compound,[38] the major product **74a** was assigned to 1,2-alternate and the minor product **74b** to cone. Suzuki-Miyaura coupling reaction of a mixture of **74a** and **74b** with phenylboronic acid and following deprotection of benzyl groups under hydrogenation condition afforded the desired compound **72** in 53% yield. Since the C−C bonds between the methylene groups and the aromatic rings of the calix[4]arene derivatives can freely rotate at r.t., when the phenols are not protected, both of 1,2-alternate **75a** and cone **75b** were converted to the desired compound **72**, whose conformation was assigned to cone by analysis of ^{1}H NMR spectrum of **72**.

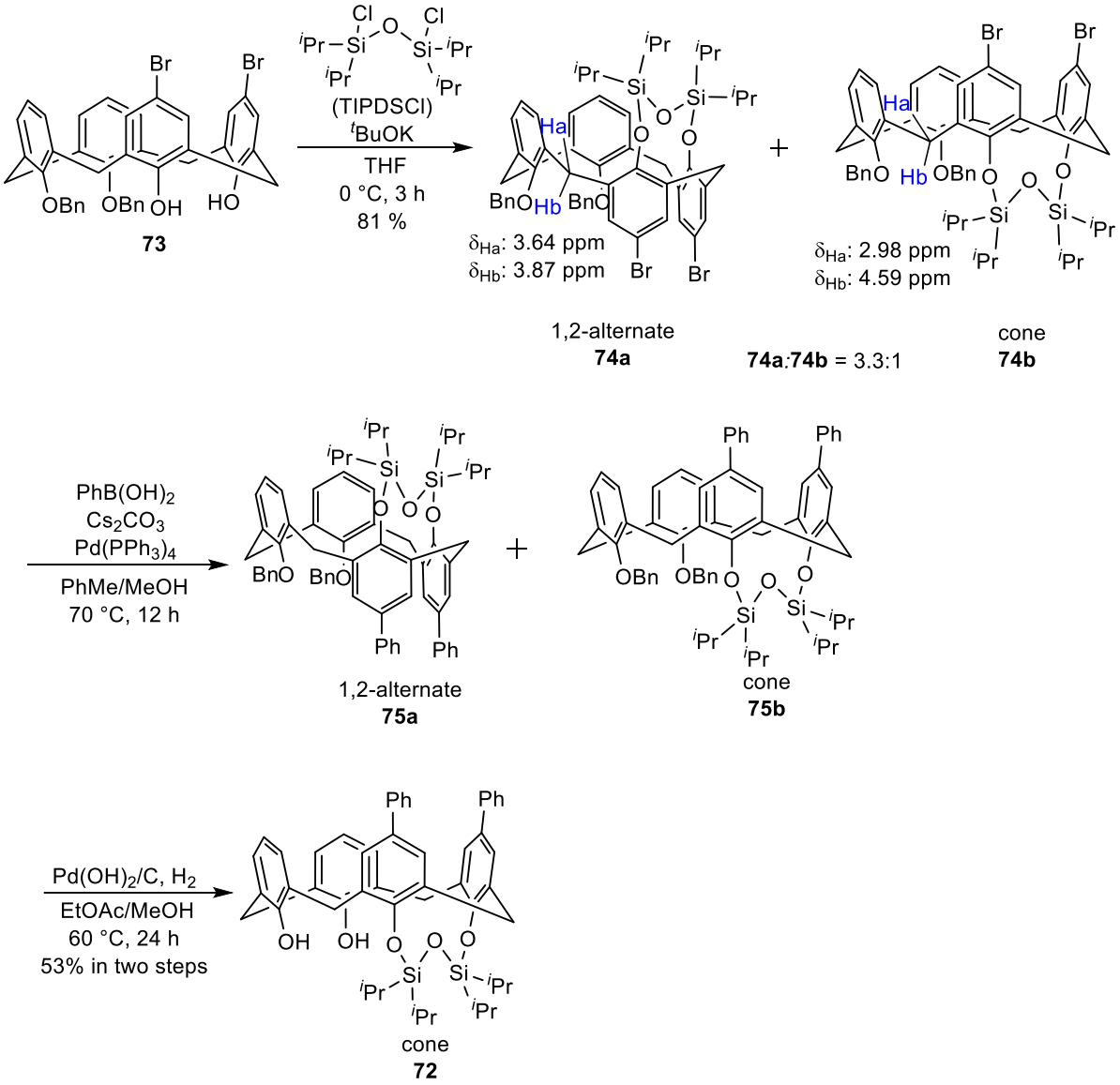

Scheme 4.5 A synthetic route of upper-rim-diPh-modified TIPDS-protected calix[4]arene.

4.5 Enantioselecitve C(sp^2)–H amination of upper-rim-modified calix[4]arene

With the newly designed substrate **72** in hand, catalyst screening was performed (Table 4.3). Rh_2(*S*-PTTL)$_4$, the most effective catalyst in C−H amination of **70**, gave only trace amount of the product **76**. On the other hand, another effective catalyst Rh_2(*S*-PTAD)$_4$ promoted the reaction to afford **76** with high enantioselectivity (87% ee). As expected, the introduction of substituents on the upper rim of the substrate affected the asymmetric induction significantly. Use of other analogues of Rh_2(*S*-PTTL)$_4$ and Rh_2(*S*-PTAD)$_4$ did not improve the yield and enantioselectivity.

Table **4.3** Catalyst screening for C−H aminative desymmetrization of upper-rim-modified substrate **72**.

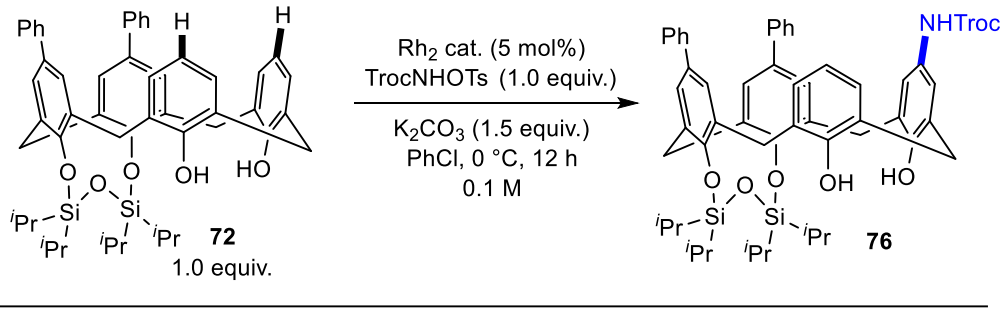

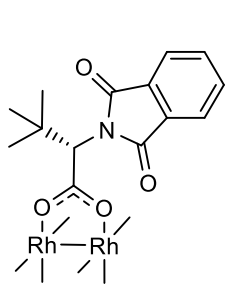

Rh_2(*S*-PTTL)$_4$
Trace[a]

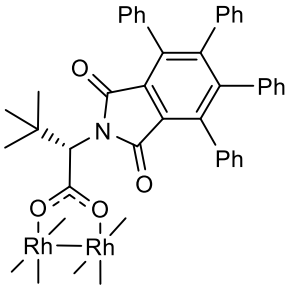

Rh_2(*S*-TPPTTL)$_4$
Trace[a]

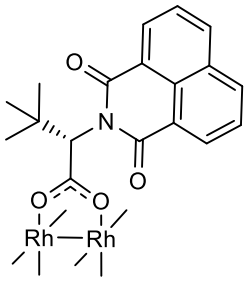

Rh_2(*S*-NTTL)$_4$
16% yield,[a] 82% ee[b]

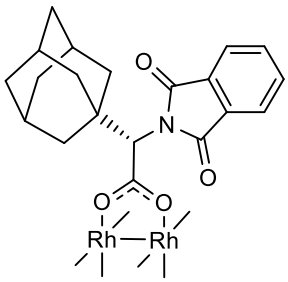

Rh_2(*S*-PTAD)$_4$
29% yield,[a] 87% ee[b]

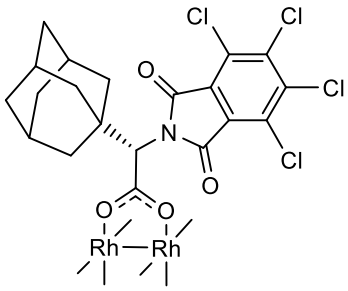

Rh_2(*S*-TCPTAD)$_4$
Trace[a]

[a] Isolated yields. [b] Determined by HPLC.

Then, screening of reaction parameters including solvents, bases, and temperature were conducted, using **72** as a substrate and Rh_2(*S*-PTAD)$_4$ as a catalyst (Table 4.4). Use of benzene or substituted benzene as solvent did not improve the reaction efficiency (entries 1−4). Screening of inorganic bases revealed that potassium salts were sufficient and relatively stronger bases such as K_3PO_4 and ^{t}BuOK increased the yield of **76** with slightly inferior enantioselectivity (entries 5−10). Investigation for the effects of temperature and addition of molecular sieves 4Å did not improve the enantioselectivity (entries 11−13).

Table 4.4 Screening of conditions for C−H aminative desymmetrization of **72**.

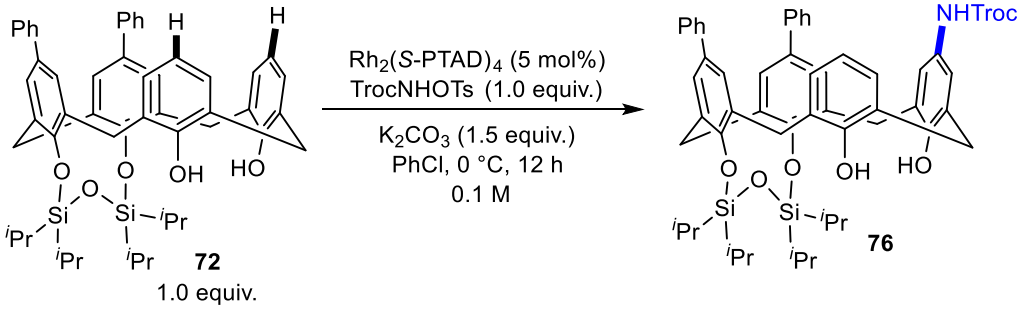

Entry	Solvent	Base	Temperature	Yield (%)[a]	ee (%)[b]
1	$PhCF_3$	K_2CO_3	0 °C	20	80
2	PhF	K_2CO_3	0 °C	Trace	-
3	PhH	K_2CO_3	20 °C	34	60
4	PhMe	K_2CO_3	0 °C	15	66
5	PhCl	Li_2CO_3	0 °C	10	78
6	PhCl	Na_2CO_3	0 °C	19	80
7	PhCl	Cs_2CO_3	0 °C	16	78
8	PhCl	KOAc	0 °C	20	80
9	PhCl	K_3PO_4	0 °C	34	84
10	PhCl	^{t}BuOK	0 °C	33	85
11	PhCl	K_2CO_3	20 °C	36	76
12	PhCl	K_2CO_3	-20 °C	22	76
13[c]	PhCl	K_2CO_3	0 °C	30	84

[a] Isolated yields. [b] Determined by HPLC. [c] Molecular Sieves 4Å as an additive.

The effects of aminating reagents were examined (Table 4.5). Use of trifluoroethyl derivative of TrocNHOTs provided C−H aminated product **77** in lower yield and enantioselectivity. On the other hand, treatment of **72** with tribromo derivative of TrocNHOTs gave the desired product **78** in slightly improved yield and enantioselectivity (31% yield, 88% ee). $TrocN_3$ was employed to the present C−H amination without base to find that high temperature was required for generation of the rhodium nitrene and N_2 gas, which resulted in decrease of enantioselectivity. Other aminating reagents did not provide the desired C−H aminated product.

Table 4.5 Effects of aminating reagents.

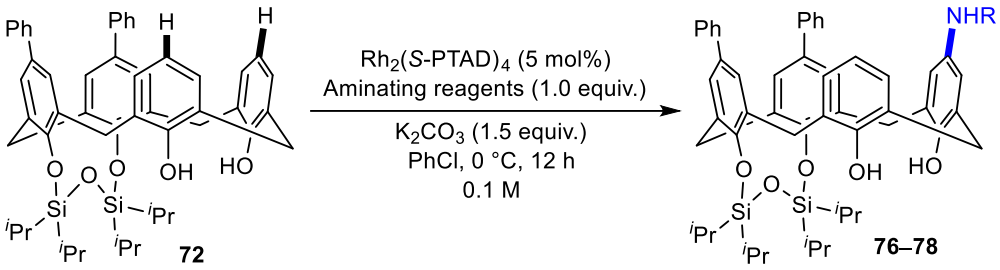

Aminating agent	Product	Aminating agent	Product
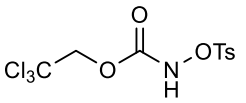	**76** (R = Troc) 29% yield,[a] 87% ee[b]	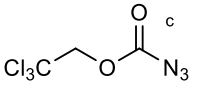	**76** (R = Troc) 31% yield,[a] 53% ee[b]
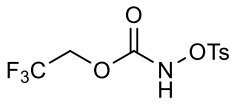	**77** (R = $CO_2CH_2CF_3$) 20% yield,[a] 68% ee[b]	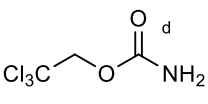	Trace
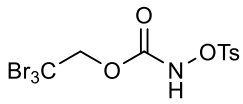	**78** (R = $CO_2CH_2CBr_3$) 31% yield,[a] 88% ee[b]	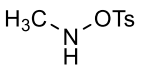	0% yield

[a] Isolated yields. [b] Determined by HPLC. [c] Without base, at 100 °C.
[d] $PhI(OAc)_2$ and MgO were used.

4.6 Discussion about stereochemistry

Based on the experimental results, the assumed asymmetric induction in the C−H amination was described in Figure 4.2. In the literature, single crystal X-ray analysis of Rh_2(*S*-PTAD)$_4$ revealed its C_4-symmetric structure.[39] The dirhodium nitrene structure was assumed from the crystal structure of Rh_2(*S*-PTAD)$_4$ (Figure 4.2a). To clarify the effects of the substituents on the chiral center, a Newman projection of the dirhodium nitrene complex from the viewpoint of a chiral center was drawn (Figure 4.2a). Possible molecular assemblies in the transition state of nucleophilic attack of the pro-(*cS*)- and pro-(*cR*)-aromatic rings to the nitrene were described in Figure 4.2b. In the model, while pro-(*cR*)-phenol seems to attack the nitrene without any significant steric repulsion between the substrate and the catalyst, steric repulsion between the phenyl group on the upper rim and phthalimide group on the chiral center could prevent attack of pro-(*cS*)-phenol to the nitrene. However, the absolute configuration of the obtained product **76** has not been determined yet due to the instability of the product in solution. To discuss the stereochemistry in the reaction, determination of the absolute configuration of the product and calculation of the transition state structure are necessary.

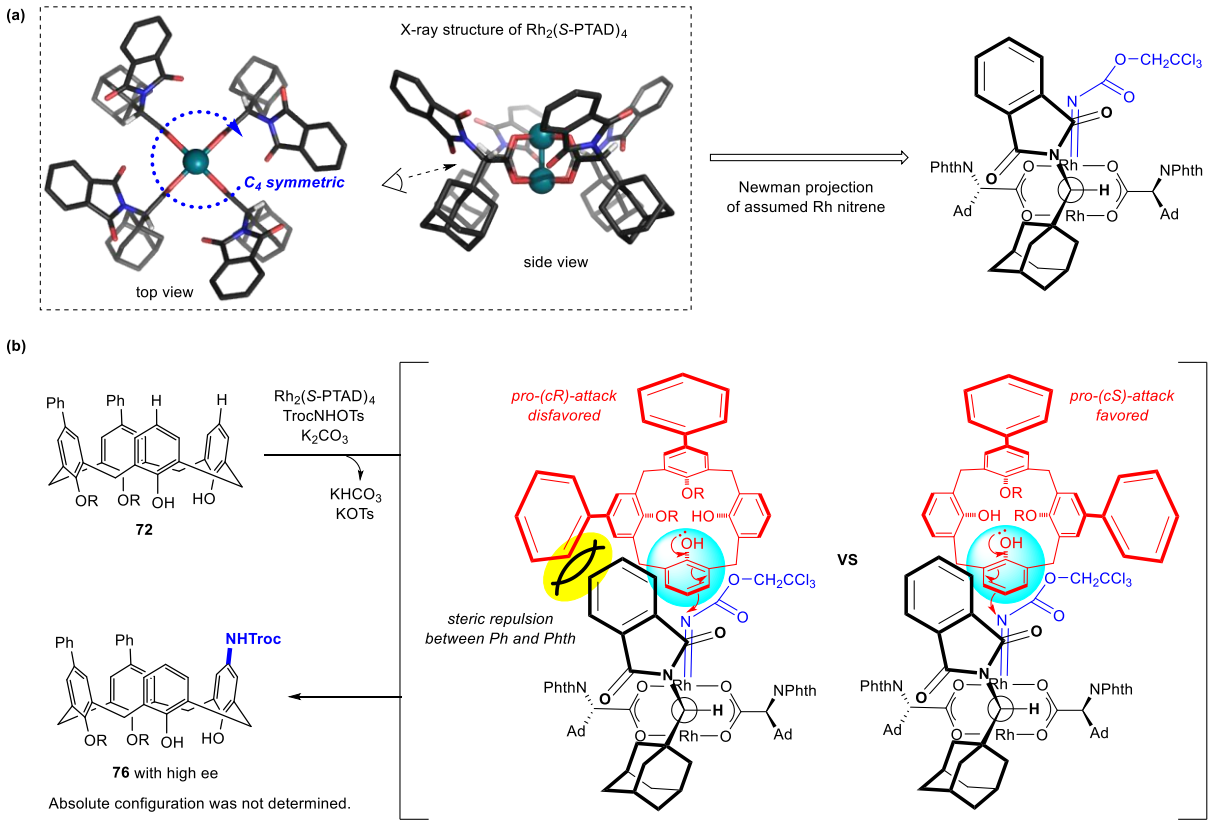

Figure 4.2 Discussion about stereochemistry. (a) Crystal structure of Rh_2(*S*-PTAD)$_4$ and Newman projection of assumed dirhodium nitrene complex. (b) Possible stereochemical paths.

Conclusion and outlook

By utilizing rhodium metal as catalyst and TrocNHOTs as nitrogen source, rhodium nitrene intermediated was generated, and the highly chemo and site- or stereo-selective C−H amination of different substrates were achieved. The results are summarized below.

Chapter 2. An optimal condition for dirhodium catalyzed C−H amination of aniline derivatives proceeded at C(sp^3)−H bonds α to the nitrogen atom was established, in a chemo and site-selective manner. Mechanistic study shows that the C−H bond cleavage was involved in the product-determining step in the concerted asynchronous C−H insertion process. The application of this amination to a two steps N-demethylation was demonstrated. This method provides an alternative way to the site-selective amination of *N*-methylaniline derivatives and will be possibly used in the N-demethylation of functional molecules.

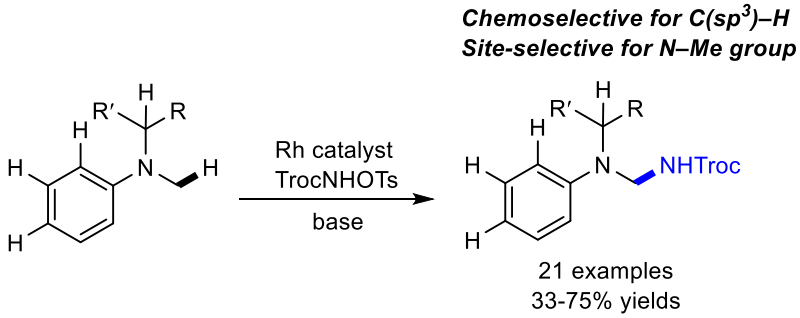

Chapter 3. The effects of ligands on dirhodium complexes on the chemoselective C−H amination reactions were studied. In the case of C(sp^3)−H amination of *N*,*N*-dimethylaniline, the numbers of phenyl substituents on the α carbon to the carboxyl group is negatively relate to the catalytic activity. Based on the relationship between the ligand structures and catalytic activities as well as NMR experiments and DFT calculation, it was proposed that the phenyl substituents stabilize the coordination state of substrates to the rhodium center by multiple C−H/π interactions to inhibit the smooth catalytic cycle. Oppositely, in the case of C(sp^2)−H amination of anisole, the numbers of phenyl substituents on the α carbon to the carboxyl group is positively relate to the catalytic activity. The relationship between the ligand structures and catalytic activities allowed me to propose the transition state structure for C(sp^2)−H amination, in which the generating δ+ on the reacting aromatic ring be stabilized by cation/π or C−H/π interactions. Based on the hypothesis, a newly designed catalyst was synthesized and examined to find it possessing comparable reactivity in C(sp^2)−H amination of anisole and triphenylamine.

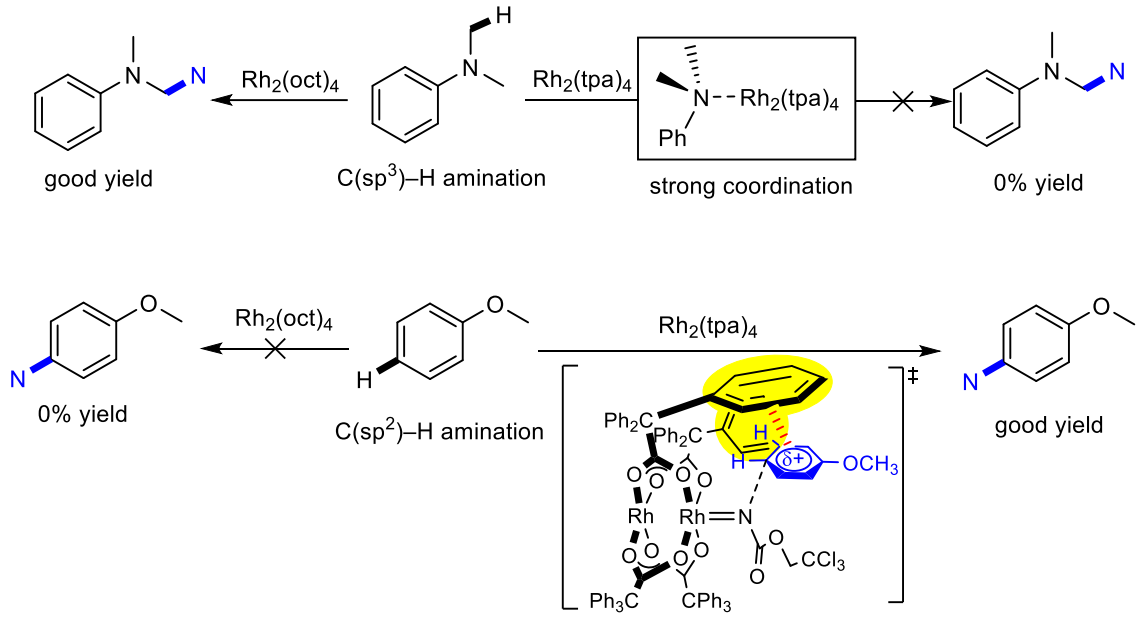

Chapter 4. Catalytic desymmetrization of C_s-symmetric calix[4]arene derivatives by enantioselective C(sp^2)–H amination was investigated. Various modification of lower and upper rim of the substrates to find one good condition for the purpose. The C(sp^2)–H amination of the calix[4]arene derivative with a TIPDS group on the lower rim and phenyl groups on the upper rim was achieved in high enantioselectivity (up to 88% ee), with a chiral dirhodium complex catalyst constituting of amino acid derivatives. To the best of my knowledge, this is the first example of catalytic asymmetric synthesis of inherently chiral calix[4]arene by rhodium catalyzed amination. Although highly selective amination was achieved about only one substrate and the absolute configuration of the product has not been determined yet, this achievement is expected to expand the methodology for catalytic asymmetric synthesis of ICCs and applications of ICCs for unique host-guest chemistry.

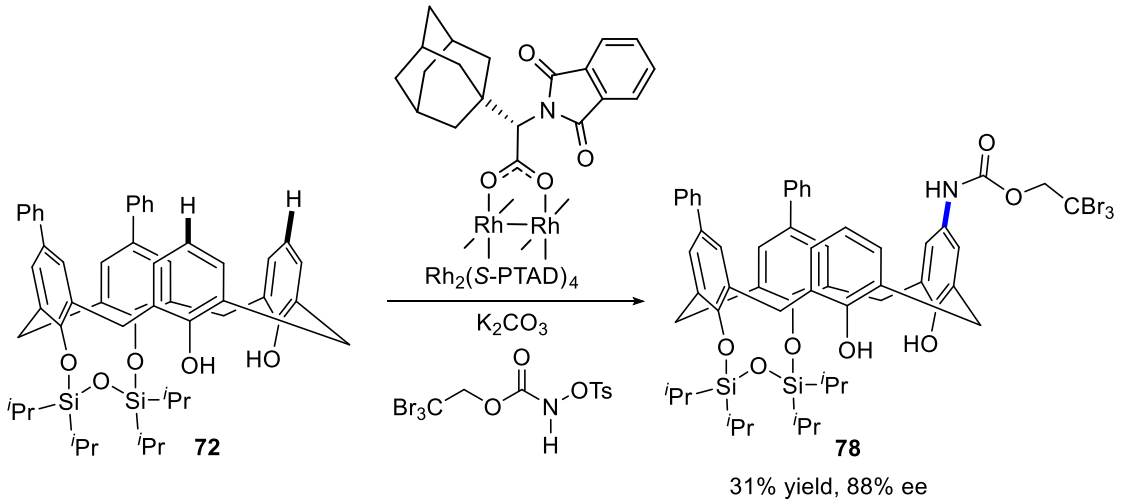

Experimental section

1. General information

^{1}H NMR spectra were recorded on JEOL ECX-400 (400 MHz) and are reported in ppm using solvent resonance as the internal standard ($CDCl_3$ at 7.26 ppm, acetone-d_6 at 2.05 ppm). When peak multiplicities are reported, the following abbreviations are used: s = singlet; d = doublet; dd = doublet doublet; t = triplet; q = quartet; sep = septet; m = multiplet; br = broad. ^{13}C NMR spectra were recorded on JEOL ECX-400 (100 MHz) or JEOL ECX-600 (150 MHz) and are reported in ppm using solvent resonance as the internal standard ($CDCl_3$ at 77.16 ppm, acetone-d_6 at 29.84 ppm). Unless otherwise noted, NMR spectra were recorded at 293 K. IR spectra were recorded with a JASCO FT/IR-4200 spectrometer. Mass spectra were obtained on Bruker Impact HD mass spectrometers or Bruker timsTOF mass spectrometer (IMS-QTOF) for ESI. Melting points were measured using a Yamagimoto micro point apparatus. Specific rotation was measured with JASCO P-2200 polarimeters. Analytic HPLC was run with a JASCO PU-2089 Plus instrument, equipped with Daicel CHIRAL PAK IB or COSMOSIL CHiRAL 5A columns, and a JASCO UV-2075 Plus UV/Vis detector at 254 nm. Recycle HPLC was run with a JASCO PU-2086 Plus instrument, equipped with a COSMOSIL 5SL column and a JASCO UV-2075 Plus UV/Vis detector at 254mn. Purification of reaction products was carried out by column chromatography on silica gel 60N (spherical, neutral, KANTO) or preparative thin layer chromatography on precoated plates (0.5 mm, Merck). Analytical thin layer chromatography was performed on precoated plates (0.25 mm, Merck). Visualization was accomplished with UV light.

TrocNHOTs,[13a] 2,2,2-trifluoroethyl-*N*-tosyloxycarbamate,[12] $Rh_2(tpa)_4$,[40] $Rh_2(Ph_2MeCCO_2)_4$,[40] $Rh_2(piv)_4$,[41] $Rh_2(PhMe_2CCO_2)_4$,[42] $Rh_2(PhCO_2)_4$,[43] Rh_2(*S*-PTTL)$_4$,[44] Rh_2(*S*-NTTL)$_4$,[45] Rh_2(*S*-DOSP)$_4$,[46] Rh_2(*S*-TPPTTL)$_4$[47] were prepared according to literature procedure. Rh_2(*R*-BPTCP)$_4$,[48] Rh_2(*S*-PTAD)$_4$,[49] Rh_2(*S*-TCPTTL)$_4$[4c] were purchased from Strem Chemicals, USA. $Rh_2(oct)_4$, $Rh_2(OAc)_4$ were purchased from TCI. $Rh_2(tfa)_4$, $Rh_2(esp)_2$ and Rh_2(*S*-TCPTAD)$_4$[4f] were purchased from Sigma-Aldrich. Li_2CO_3, K_2CO_3, Na_2CO_3, Cs_2CO_3, Rb_2CO_3, and KOAc were purchased from Wako Chemical. Anhydrous chlorobenzene, benzotrifluoride and 2,2,2-tribromoethanol were purchased from Sigma-Aldrich. Anhydrous toluene, chloroform, ethyl acetate and benzene were purchased from Wako Chemical. Anhydrous dichloromethane was purchased from Kanto Kagaku. Fluorobenzene was purchased from TCI. Anhydrous DMF and acetonitrile were purchased from Nacalai tesque. All chemical reagents were commercially purchased and used without further purification.

2. Chapter 2

General procedure for dirhodium-catalyzed intermolecular C−H amination of *N,N*-dialkylanilines

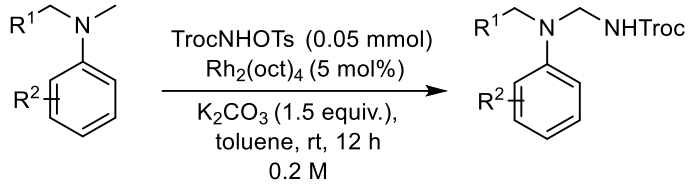

To a suspension of *N,N*-diakylanilines (0.5 mmol, 10 equiv. or 0.075 mmol, 1.5 equiv.), TrocNHOTs (18.1 mg, 0.05 mmol, 1.0 equiv.) and K_2CO_3 (10.4 mg, 0.075 mmol, 1.5 equiv.) in toluene (0.25 mL) were added $Rh_2(oct)_4$ (1.9 mg, 0.05 equiv.) at r.t.. After being stirred for 12 h, the reaction was quenched by addition of water and extracted with EtOAc. The organic layer was washed with brine, and dried over Na_2SO_4, filtered, and concentrated. The crude material was purified by preparative TLC or column chromatography to afford the aminated product. The product exists as a mixture of rotamers due to its carbamoyl moiety. For coalescence of the signals of the rotamers, ^{1}H NMR of product was measured at 323K.

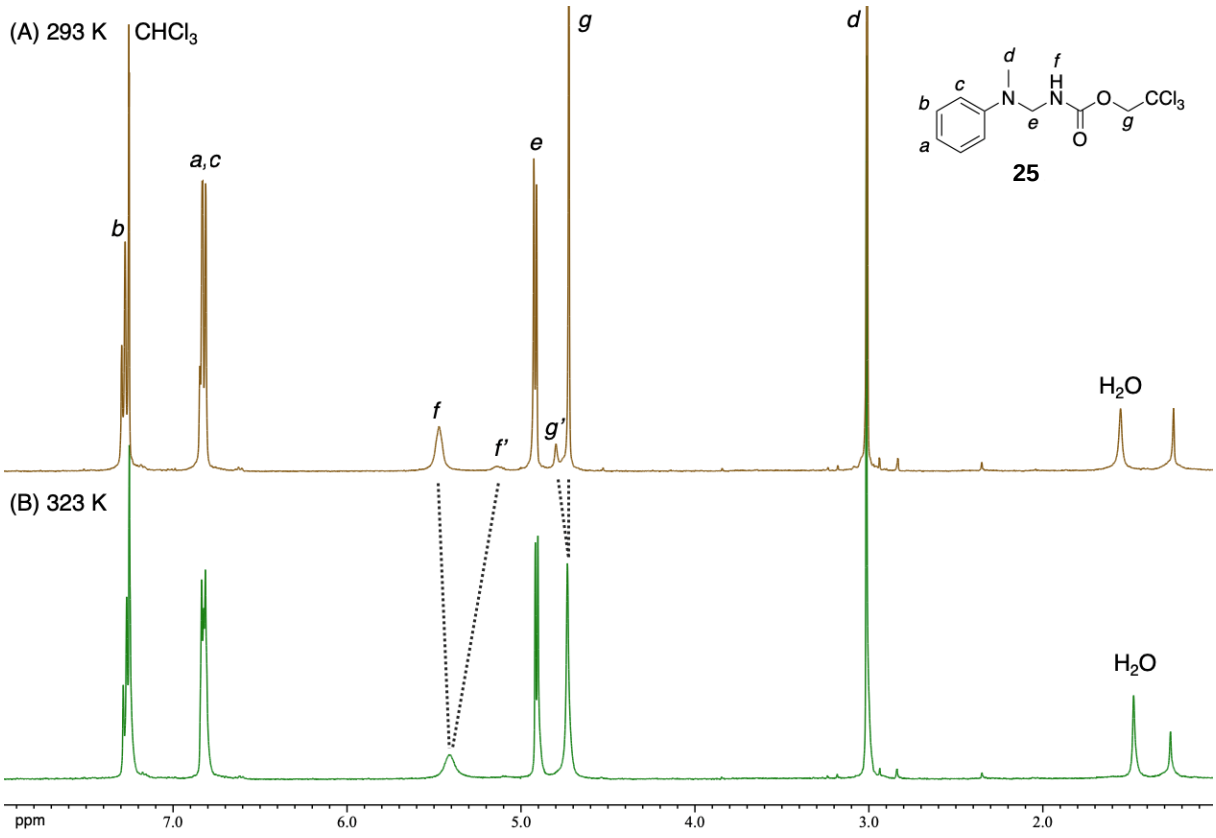

Figure S1. VT-^{1}H NMR spectra of **25** in $CDCl_3$ (A) at 293 K (B) at 323K.

Specific Procedures and Characterization Data

2,2,2-Trichloroethyl ((methyl(phenyl)amino)methyl)carbamate (25)

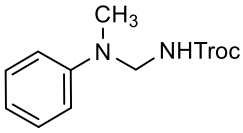

Following the general procedure, *N*,*N*-dimethylaniline (63 µL, 0.5 mmol, 10 equiv.), TrocNHOTs (18.1 mg, 0.05 mmol, 1.0 equiv.), K_2CO_3 (10.4 mg, 0.075 mmol, 1.5 equiv.), and $Rh_2(oct)_4$ (1.9 mg, 0.05 equiv.) were stirred at r.t. in toluene (0.25 mL) for 12 h. The crude material was purified by sequential preparative TLC (1st EtOAc/hexane = 1/9, 2nd $CHCl_3$/hexane = 1/1) to afford **25** as colorless oil (11.0 mg, 71%).

^{1}H NMR (400 M Hz, $CDCl_3$, 323 K) δ: 7.29−7.26 (m, 2H), 6.84−6.82(m, 3H), 5.42 (br s, 1H), 4.92 (d, *J* = 5.6 Hz, 2H), 4.74 (s, 2H), 3.02 (s, 3H); **^{13}C NMR** (100 M Hz, $CDCl_3$) δ: 154.9, 147.7 129.6, 118.7, 113.9, 95.6, 74.7, 59.7, 37.8; **IR** (neat, cm^{-1}): 3326, 2952, 1722, 1598, 1499, 1367, 1220, 1132, 1041, 993, 817, 750; **HRMS-ESI$^+$** (m/z): Calcd. for $C_{11}H_{14}Cl_3N_2O_2$ $[M+H]^+$ 311.0115; found, 311.0115.

2,2,2-Trifluoroethyl ((methyl(phenyl)amino)me9thyl)carbamate (26)

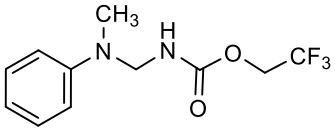

Following the general procedure, *N*,*N*-dimethylaniline (10 µL, 0.075 mmol, 1.5 equiv), 2,2,2-trifluoroethyl (tosyloxy)carbamate (15.6 mg, 0.05 mmol, 1.0 equiv.), K_2CO_3 (10.4 mg, 0.075 mmol, 1.5 equiv.), and $Rh_2(oct)_4$ (1.9 mg, 0.05 equiv.) were stirred at r.t. in chlorobenzene (0.25 mL) for 12 h. The crude material was purified by sequential preparative TLC (1st EtOAc/hexane = 1/9, 2nd $CHCl_3$/hexane = 1/1) to afford **26** as colorless oil (4.8 mg, 37%).

^{1}H NMR (400 M Hz, $CDCl_3$, 323 K) δ: 7.29−7.26 (m, 2H), 6.85−6.81 (m, 3H), 5.36 (br s, 1H), 4.88 (d, *J* = 5.6 Hz, 2H), 4.46 (q, *J* = 8.0 Hz, 2H), 3.01 (s, 3H); **^{13}C NMR** (100 M Hz, $CDCl_3$) δ: 154.8, 147.7 129.6, 123.1 (q, *J* = 276.5 Hz), 118.7, 113.9 and 113.6 (rotamers), 61.1 (q, *J* = 36.2 Hz), 59.7, 37.9; **IR** (neat, cm^{-1}): 3339, 2916, 1729, 1602, 1531, 1507, 1292, 1232, 1176, 973, 758, 694; **HRMS-ESI$^+$** (m/z): Calcd. for $C_{11}H_{14}F_3N_2O_2$ $[M+H]^+$ 263.1002; found, 263.1007.

2,2,2-Tribromoethyl ((methyl(phenyl)amino)methyl)carbamate (27)

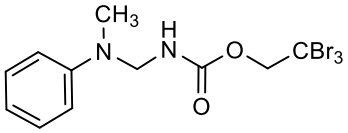

Following the general procedure, *N*,*N*-dimethylaniline (10 µL, 0.075 mmol, 1.5 equiv.), 2,2,2-tribromoethyl (tosyloxy)carbamate (24.8 mg, 0.05 mmol, 1.0 equiv.), K_2CO_3 (10.4 mg, 0.075 mmol, 1.5 equiv.), and $Rh_2(oct)_4$ (1.9 mg, 0.05 equiv.) were stirred at r.t. in chlorobenzene (0.25 mL) for 12 h. The crude material was purified by sequential preparative TLC (1st EtOAc/hexane = 1/9, 2nd $CHCl_3$/hexane

= 1/1) to afford **27** as colorless oil (8.0 mg, 36%).

^{1}H NMR (400 M Hz, $CDCl_3$, 323 K) δ: 7.30−7.26 (m, 2H), 6.85−6.81 (m, 3H), 5.46 (br s, 1H), 4.94−4.93 (m, 4H), 3.03 (s, 3H); **^{13}C NMR** (100 M Hz, $CDCl_3$) δ: 154.8, 147.8 129.6, 119.0 and 118.7 (rotamers), 113.9 and 113.7 (rotamers), 79.4, 60.4 and 59.7 (rotamers), 37.9, 37.2; **IR** (neat, cm^{-1}): 3318, 2920, 1725, 1598, 1495, 1359, 1216, 1129, 1041, 993, 750, 699, 635; **HRMS-ESI$^+$** (m/z): Calcd. for $C_{11}H_{14}{}^{79}Br_2{}^{81}BrN_2O_2$ $[M+H]^+$ 444.8580; found, 444.8583.

2,2,2-Trichloroethyl (((4-chlorophenyl)(methyl)amino)methyl)carbamate (28)

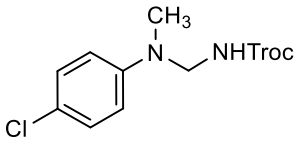

Following the general procedure, 4-chloro-*N*,*N*-dimethylaniline (78 mg, 0.5 mmol, 10 equiv.), TrocNHOTs (18.1 mg, 0.05 mmol, 1.0 equiv.), K_2CO_3 (10.4 mg, 0.075 mmol, 1.5 equiv.), and $Rh_2(oct)_4$ (1.9 mg, 0.05 equiv.) were stirred at r.t. in toluene (0.25 mL) for 12 h. The crude material was purified by sequential preparative TLC (1st EtOAc/hexane = 1/5, 2nd $CHCl_3$/hexane = 1/1) to afford **28** as colorless oil (13.0 mg, 75%).

^{1}H NMR (400 M Hz, $CDCl_3$, 323 K) δ: 7.21 (d, *J* = 8.4 Hz, 2H), 6.75 (d, *J* = 8.8 Hz, 2H), 5.42 (br s, 1H), 4.88 (d, *J* = 6.0 Hz, 2H), 4.74 (s, 2H), 3.00 (s, 3H); **^{13}C NMR** (100 M Hz, $CDCl_3$) δ: 154.9, 146.4, 129.4, 123.7, 115.1 and 114.9 (rotamers), 95.5, 74.7, 59.8, 38.0; **IR** (neat, cm^{-1}): 3331, 2920, 1725, 1499, 1363, 1216, 1140, 1005, 809, 722; **HRMS-ESI$^+$** (m/z): Calcd. for $C_{11}H_{13}Cl_4N_2O_2$ $[M+H]^+$ 344.9726; found, 344,9725.

2,2,2-Trichloroethyl (((4-bromophenyl)(methyl)amino)methyl)carbamate (29)

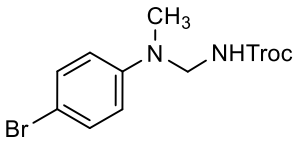

Following the general procedure, 4-bromo-*N*,*N*-dimethylaniline (100 mg, 0.5 mmol, 10 equiv.), TrocNHOTs (18.1 mg, 0.05 mmol, 1.0 equiv.), K_2CO_3 (10.4 mg, 0.075 mmol, 1.5 equiv.), and $Rh_2(oct)_4$ (1.9 mg, 0.05 equiv.) were stirred at r.t. in toluene (0.25 mL) for 12 h. The crude material was purified by sequential preparative TLC (1st EtOAc/hexane = 1/9, 2nd $CHCl_3$/hexane = 1/1) to afford **29** as colorless oil (13.8 mg, 71%).

^{1}H NMR (400 M Hz, $CDCl_3$, 323 K) δ: 7.35 (d, *J* = 9.2 Hz, 2H), 6.70 (d, *J* = 9.2 Hz, 2H), 5.43 (br s, 1H), 4.87 (d, *J* = 6.0 Hz, 2H), 4.74 (s, 2H), 2.99 (s, 3H); **^{13}C NMR** (100 M Hz, $CDCl_3$) δ: 154.9, 146.8, 132.3, 115.5 and 115.3 (rotamers), 110.9, 95.5, 74.7, 59.6, 38.0; **IR** (neat, cm^{-1}): 3326, 2948, 1725, 1598, 1495, 1363, 1208, 1132, 1052, 1000, 813, 722; **HRMS-ESI$^+$** (m/z): Calcd. for $C_{11}H_{13}BrCl_3N_2O_2$ $[M+H]^+$ 388.9220; found, 388.9218.

2,2,2-Trichloroethyl (((4-iodophenyl)(methyl)amino)methyl)carbamate (30)

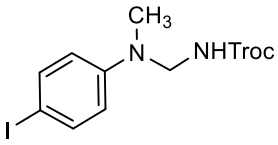

Following the general procedure, 4-iodo-*N*,*N*-dimethylaniline (124 mg, 0.5 mmol, 10 equiv.), TrocNHOTs (18.1 mg, 0.05 mmol, 1.0 equiv.), K_2CO_3 (10.4 mg, 0.075 mmol, 1.5 equiv.), and $Rh_2(oct)_4$ (1.9 mg, 0.05 equiv.) were stirred at r.t. in toluene (0.25 mL) for 12 h. The crude material was purified by sequential preparative TLC (1st EtOAc/hexane = 1/9, 2nd $CHCl_3$/hexane = 1/1) to afford **30** as colorless oil (15.0 mg, 69%).

^{1}H NMR (400 M Hz, $CDCl_3$, 323 K) δ: 7.52 (d, *J* = 8.8 Hz, 2H), 6.60 (d, *J* = 8.8 Hz, 2H), 5.45 (br s, 1H), 4.87 (d, *J* = 5.6 Hz, 2H), 4.74 (s, 2H), 2.99 (s, 3H); **^{13}C NMR** (100 M Hz, $CDCl_3$) δ: 154.9, 147.4, 138.2, 115.8, 95.5, 80.1, 74.7, 59.4, 37.9; **IR** (neat, cm^{-1}): 3335, 2948, 1722, 1590, 1490, 1359, 1224, 1140, 1052, 809, 727; **HRMS-ESI$^+$** (m/z): Calcd. for $C_{11}H_{13}Cl_3IN_2O_2$ $[M+H]^+$ 436.9082; found, 436.9079.

2,2,2-Trichloroethyl ((methyl(*p*-tolyl)amino)methyl)carbamate (31)

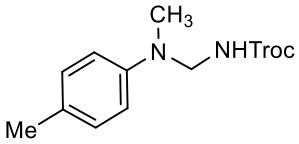

Following the general procedure, *N*,*N*,4-trimethylaniline (68 mg, 0.5 mmol, 10 equiv.), TrocNHOTs (18.1 mg, 0.05 mmol, 1.0 equiv.), K_2CO_3 (10.4 mg, 0.075 mmol, 1.5 equiv.), and $Rh_2(oct)_4$ (1.9 mg, 0.05 equiv.) were stirred at r.t. in toluene (0.25 mL) for 12 h. The crude material was purified by sequential preparative TLC (1st EtOAc/hexane = 1/9, 2nd $CHCl_3$/hexane = 1/1) to afford **31** as light yellow oil (6.7 mg, 41%).

^{1}H NMR (400 M Hz, $CDCl_3$, 323 K) δ: 7.09 (d, *J* = 7.2 Hz, 2H), 6.75 (d, *J* = 7.2 Hz, 2H), 5.39 (br s, 1H), 4.88 (d, *J* = 6.0 Hz, 2H), 4.74 (s, 2H), 2.98 (s, 3H), 2.28 (s, 3H); **^{13}C NMR** (100 M Hz, $CDCl_3$) δ: 155.0, 145.6, 130.1, 128.2, 114.4 and 114.2 (rotamers), 95.6, 74.9 and 74.6 (rotamers), 60.0, 37.8, 20.4; **IR** (neat, cm^{-1}): 3331, 2920, 1718, 1514, 1363, 1212, 1136, 1049, 957, 813, 730; **HRMS-ESI$^+$** (m/z): Calcd. for $C_{12}H_{16}Cl_3N_2O_2$ $[M+H]^+$ 325.0272; found, 325.0272.

Methyl 4-(methyl((((2,2,2-trichloroethoxy)carbonyl)amino)methyl)amino)benzoate (32)

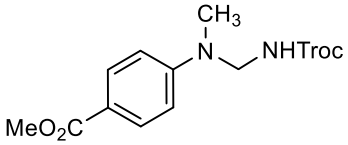

Following the general procedure, methyl 4-(dimethylamino)benzoate (90 mg, 0.5 mmol, 10 equiv.),

TrocNHOTs (18.1 mg, 0.05 mmol, 1.0 equiv.), K_2CO_3 (10.4 mg, 0.075 mmol, 1.5 equiv.), and $Rh_2(oct)_4$ (1.9 mg, 0.05 equiv.) were stirred at r.t. in toluene (0.25 mL) for 12 h. The crude material was purified by preparative TLC (EtOAc/hexane = 1/5) to afford **32** as a white solid (13.4 mg, 73%).

White solid: **m.p.** 152 ℃; **^{1}H NMR** (400 M Hz, $CDCl_3$, 323 K) δ: 7.95 (d, *J* = 8.8 Hz, 2H), 6.78 (d, *J* = 8.8 Hz, 2H), 5.51 (br s, 1H), 4.95 (d, *J* = 6.0 Hz, 2H), 4.75 (s, 2H), 3.87 (s, 3H), 3.11 (s, 3H); **^{13}C NMR** (100 M Hz, $CDCl_3$) δ: 167.3, 154.9, 151.2, 131.7, 119.5, 111.9, 95.4, 774.8, 58.9, 51.9, 38.2; **IR** (KBr, cm^{-1}): 3351, 2955, 1741, 1693, 1618, 1527, 1290, 1186, 1005, 831, 767; **HRMS-ESI$^+$** (m/z): Calcd. for $C_{13}H_{16}Cl_3N_2O_4$ $[M+H]^+$ 369.0170; found, 369.0171.

Ethyl 4-(methyl((((2,2,2-trichloroethoxy)carbonyl)amino)methyl)amino)benzoate (33)

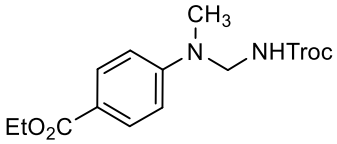

Following the general procedure, ethyl 4-(dimethylamino)benzoate (97 mg, 0.5 mmol, 10 equiv.), TrocNHOTs (18.1 mg, 0.05 mmol, 1.0 equiv.), K_2CO_3 (10.4 mg, 0.075 mmol, 1.5 equiv.), and $Rh_2(oct)_4$ (1.9 mg, 0.05 equiv.) were stirred at r.t. in toluene (0.25 mL) for 12 h. The crude material was purified by preparative TLC (EtOAc/hexane = 1/5) to afford **33** as a white solid (12.0 mg, 63%).

White solid: **m.p.** 120 ℃; **^{1}H NMR** (400 M Hz, $CDCl_3$, 323 K) δ: 7.95 (d, *J* = 9.2 Hz, 2H), 6.77 (d, *J* = 9.2 Hz, 2H) 5.53 (br s, 1H), 4.95 (d, *J* = 6.0 Hz, 2H), 4.75 (s, 2H), 4.34 (q, *J* = 7.2 Hz, 2H), 3.11 (s, 3H), 1.37 (t, *J* = 7.2 Hz, 3H); **^{13}C NMR** (100 M Hz, $CDCl_3$) δ: 166.8, 154.9, 151.1, 131.6, 119.8, 111.9, 95.4, 74.7, 60.6, 58.9, 38.1, 14.6; **IR** (KBr, cm^{-1}): 3343, 2965, 1729, 1682, 1518, 1295, 1184, 1106, 817, 722; **HRMS-ESI$^+$** (m/z): Calcd. for $C_{14}H_{18}Cl_3N_2O_4$ $[M+H]^+$ 383.0327; found, 383.0324.

2,2,2-Trichloroethyl (((4-methoxyphenyl)(methyl)amino)methyl)carbamate (34)

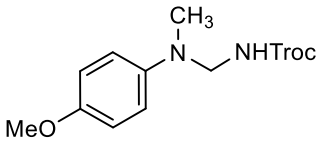

Following the general procedure, 4-methoxy-*N*,*N*-dimethylaniline (75 mg, 0.5 mmol, 10 equiv.), TrocNHOTs (18.1 mg, 0.05 mmol, 1.0 equiv.), K_2CO_3 (10.4 mg, 0.075 mmol, 1.5 equiv.), and $Rh_2(oct)_4$ (1.9 mg, 0.05 equiv.) were stirred at r.t. in toluene (0.25 mL) for 12 h. The crude material was purified by preparative TLC (EtOAc/hexane = 1/9) to afford **34** as colorless oil (8.9 mg, 53%).

^{1}H NMR (400 M Hz, $CDCl_3$, 323 K) δ: 6.87−6.81 (m, 4H), 5.36 (br s, 1H), 4.83 (d, *J* = 6.4 Hz, 2H), 4.73 (s, 2H), 3.77 (s, 3H), 2.93 (s, 3H); **^{13}C NMR** (100 M Hz, $CDCl_3$) δ: 155.0, 153.3, 142.1, 116.7 and 116.3 (rotamers), 115.0, 95.6, 74.6, 61.0, 55.8, 38.0; **IR** (neat, cm^{-1}): 3326, 2920, 1722, 1518, 1243, 1129, 1037, 822, 722; **HRMS-ESI$^+$** (m/z): Calcd. for $C_{12}H_{16}Cl_3N_2O_3$ $[M+H]^+$ 341.0221; found, 341.0220.

2,2,2-Trichloroethyl (((2-chlorophenyl)(methyl)amino)methyl)carbamate (35)

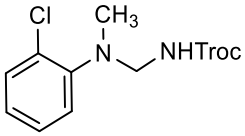

Following the general procedure, 2-chloro-*N*,*N*-dimethylaniline (77 mg, 0.5 mmol, 10 equiv.), TrocNHOTs (18.1 mg, 0.05 mmol, 1.0 equiv.), K_2CO_3 (10.4 mg, 0.075 mmol, 1.5 equiv.), and $Rh_2(oct)_4$ (1.9 mg, 0.05 equiv.) were stirred at r.t. in toluene (0.25 mL) for 12 h. The crude material was purified by preparative TLC (EtOAc/hexane = 1/9) to afford **35** as colorless oil (7.6 mg, 44%).

^{1}H NMR (400 M Hz, $CDCl_3$, 323 K) δ: 7.38 (d, *J* = 7.6 Hz, 1H), 7.22 (t, *J* = 7.1 Hz, 1H), 7.10 (d, *J* = 8.0 Hz, 1H), 7.00 (t, *J* = 8.0 Hz, 1H), 5.37 (br s, 1H), 4.74 (s, 2H), 4.68 (d, *J* = 6.8 Hz, 2H), 2.90 (s, 3H); **^{13}C NMR** (100 M Hz, $CDCl_3$) δ: 155.0, 146.5, 130.9, 128.5, 127.6 and 127.2 (rotamers), 124.6 and 124.4 (rotamers), 122.7 and 122.3 (rotamers), 95.7, 74.8 and 74.5 (rotamers), 61.9 and 61.6 (rotamers), 38.4; **IR** (neat, cm^{-1}): 3339, 2960, 1722, 1514, 1479, 1224, 1120, 1049, 718; **HRMS-ESI$^+$** (m/z): Calcd. for $C_{11}H_{13}Cl_4N_2O_2$ $[M+H]^+$ 344.9726; found, 344.9738.

2,2,2-Trichloroethyl (((2-bromophenyl)(methyl)amino)methyl)carbamate (36)

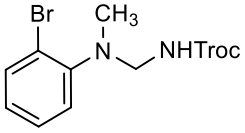

Following the general procedure, 2-bromo-*N*,*N*-dimethylaniline (100 mg, 0.5 mmol, 10 equiv.), TrocNHOTs (18.1 mg, 0.05 mmol, 1.0 equiv.), K_2CO_3 (10.4 mg, 0.075 mmol, 1.5 equiv.), and $Rh_2(oct)_4$ (1.9 mg, 0.05 equiv.) were stirred at r.t. in toluene (0.25 mL) for 12 h. The crude material was purified by preparative TLC (EtOAc/hexane = 1/9) to afford **36** as colorless oil (11.1 mg, 59%).

^{1}H NMR (400 M Hz, $CDCl_3$, 323 K) δ: 7.59 (d, *J* = 8.0 Hz, 1H), 7.27 (t, *J* = 7.6 Hz, 1H), 7.12 (d, *J* = 8.0 Hz, 1H), 6.95 (t, *J* = 7.6 Hz, 1H), 5.38 (br s, 1H), 4.74 (s, 2H), 4.65 (d, *J* = 6.4 Hz, 2H), 2.88 (s, 3H); **^{13}C NMR** (100 M Hz, $CDCl_3$) δ: 155.0 and 154.3 (rotamers), 147.9 and 147.6 (rotamers), 134.1, 128.6 and 128.3 (rotamers), 125.3 and 125.2 (rotamers), 123.3 and 123.0 (rotamers), 120.0 and 119.7 (rotamers), 95.7, 74.8 and 74.5 (rotamers), 62.4 and 62.0 (rotamers), 38.5; **IR** (neat, cm^{-1}): 3339, 2948, 1725, 1515, 1479, 1232, 1156, 722; **HRMS-ESI$^+$** (m/z): Calcd. for $C_{11}H_{13}BrCl_3N_2O_2$ $[M+H]^+$ 388.9220; found, 388.9219.

2,2,2-Trichloroethyl (((2-iodophenyl)(methyl)amino)methyl)carbamate (37)

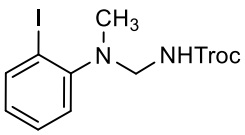

Following the general procedure, 2-iodo-*N*,*N*-dimethylaniline (124 mg, 0.5 mmol, 10 equiv.), TrocNHOTs (18.1 mg, 0.05 mmol, 1.0 equiv.), K_2CO_3 (10.4 mg, 0.075 mmol, 1.5 equiv.), and $Rh_2(oct)_4$ (1.9 mg, 0.05 equiv.) were stirred at r.t. in toluene (0.25 mL) for 12 h. The crude material was purified

by preparative TLC (EtOAc/hexane = 1/9) to afford **37** as colorless oil (11.4 mg, 52%).

^{1}H NMR (400 M Hz, $CDCl_3$, 323 K) δ: 7.87 (d, *J* = 8.4 Hz, 1H), 7.32 (t, *J* = 8.0 Hz, 1H), 7.12 (d, *J* = 8.4 Hz, 1H), 6.83 (t, *J* = 7.6 Hz, 1H), 5.37 (br s, 1H), 4.74 (s, 2H), 4.57 (d, *J* = 6.0 Hz, 2H), 2.84 (s, 3H); **^{13}C NMR** (100 M Hz, $CDCl_3$) δ: 155.0, 150.7, 140.4, 129.2, 126.3, 123,2, 98.2, 95.7, 74.5, 62.8, 39.0; **IR** (neat, cm^{-1}): 3339, 2920, 1729, 1510, 1463, 1236, 1125, 718; **HRMS-ESI$^+$** (m/z): Calcd. for $C_{11}H_{13}Cl_3IN_2O_2$ $[M+H]^+$ 436.9082; found, 436.9081.

2,2,2-Trichloroethyl ((methyl(*o*-tolyl)amino)methyl)carbamate (38)

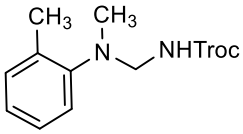

Following the general procedure, *N*,*N*,2-trimethylaniline (68 mg, 0.5 mmol, 10 equiv.), TrocNHOTs (18.1 mg, 0.05 mmol, 1.0 equiv.), K_2CO_3 (10.4 mg, 0.075 mmol, 1.5 equiv.), and $Rh_2(oct)_4$ (1.9 mg, 0.05 equiv.) were stirred at r.t. in toluene (0.25 mL) for 12 h. The crude material was purified by preparative TLC (EtOAc/hexane = 1/9) to afford **38** as light yellow oil (7.0 mg, 43%).

^{1}H NMR (400 M Hz, $CDCl_3$, 323 K) δ: 7.25−7.14 (m, 2H), 7.07 (d, *J* = 8.0 Hz, 1H), 7.02 (t, *J* = 7.2 Hz, 1H), 5.21 (br s, 1H), 4.73 (s, 2H), 4.51 (d, *J* = 6.4 Hz, 2H), 2.81 (s, 3H), 2.32 (s, 3H); **^{13}C NMR** (100 M Hz, $CDCl_3$) δ: 155.0, 148.4, 133.1, 131.5, 126.6, 124.1, 121,7 and 121,5 (rotamers), 95.7, 74.8 and 74.5 (rotamers), 61.9, 38.9, 18.4; **IR** (neat, cm^{-1}): 3335, 2952, 1738, 1594, 1503, 1316, 1224, 1049, 806, 727; **HRMS-ESI$^+$** (m/z): Calcd. for $C_{12}H_{16}Cl_3N_2O_2$ $[M+H]^+$ 325.0272; found, 325.0257.

2,2,2-Trichloroethyl (((2-methoxyphenyl)(methyl)amino)methyl)carbamate (39)

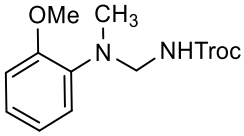

Following the general procedure, 2-methoxy-*N*,*N*-dimethylaniline (76 mg, 0.5 mmol, 10 equiv.), TrocNHOTs (18.1 mg, 0.05 mmol, 1.0 equiv.), K_2CO_3 (10.4 mg, 0.075 mmol, 1.5 equiv.), and $Rh_2(oct)_4$ (1.9 mg, 0.05 equiv.) were stirred at r.t. in toluene (0.25 mL) for 12 h. The crude material was purified by preparative TLC (EtOAc/hexane = 1/3) to afford **39** as colorless oil (9.1 mg, 54%).

^{1}H NMR (400 M Hz, $CDCl_3$, 323 K) δ: 7.02−6.88 (m, 4H), 5.38 (br s, 1H), 4.73 (s, 2H), 4.71 (d, *J* = 6.4 Hz, 2H), 3.89 (s, 3H), 2.91 (s, 3H); **^{13}C NMR** (100 M Hz, $CDCl_3$) δ: 155.2, 152.0, 138.4, 123.3, 121.1, 120.2 and 120.0 (rotamers), 111.4, 95.8, 74.5, 61.2, 55.7, 38.4; **IR** (neat, cm^{-1}): 3339, 2948, 1733, 1598, 1503, 1455, 1232, 1105, 809, 722; **HRMS-ESI$^+$** (m/z): Calcd. for $C_{12}H_{16}Cl_3N_2O_3$ $[M+H]^+$ 341.0221; found, 341.0219.

2,2,2-Trichloroethyl ((methyl(naphthalen-1-yl)amino)methyl)carbamate (40)

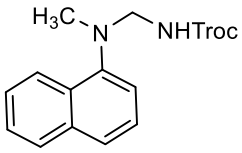

Following the general procedure, *N*,*N*-dimethylnaphthalen-1-amine (85 mg, 0.5 mmol, 10 equiv.), TrocNHOTs (18.1 mg, 0.05 mmol, 1.0 equiv.), K_2CO_3 (10.4 mg, 0.075 mmol, 1.5 equiv.), and $Rh_2(oct)_4$ (1.9 mg, 0.05 equiv.) were stirred at r.t. in toluene (0.25 mL) for 12 h. The crude material was purified by column chromatography (EtOAc/hexane = 1/9) to afford **40** as yellow oil (8.6 mg, 48%).

^{1}H NMR (400 M Hz, $CDCl_3$, 323 K) δ: 8.19 (d, *J* = 7.6 Hz, 1H), 7.84 (d, *J* = 8.8 Hz, 1H), 7.61 (d, *J* = 8.0 Hz, 1H), 7.51−7.47 (m, 2H), 7.41 (t, *J* = 8.0 Hz, 1H), 7.18 (d, *J* = 7.6 Hz, 1H), 5.22 (br s, 1H), 4.76−4.74 (m, 4H), 2.98 (s, 3H); **^{13}C NMR** (100 M Hz, $CDCl_3$) δ: 155.0, 146.3 and 145.9 (rotamers), 134.9, 129.1, 128.6, 126.2, 125.9, 125.6, 124.5, 123.5, 117.9 and 117.6 (rotamers), 95.7, 74.7 and 74.5 (rotamers), 63.2 and 62.7 (rotamers), 39.1 and 39.0 (rotamers); **IR** (neat, cm^{-1}): 3326, 3051, 2956, 2920, 1725, 1510, 1395, 1224, 1136, 1037, 933, 806, 781; **HRMS-ESI$^+$** (m/z): Calcd. for $C_{15}H_{16}Cl_3N_2O_2$ $[M+H]^+$ 361.0272; found, 361.0272.

Phenyl 5-(methyl((((2,2,2-trichloroethoxy)carbonyl)amino)methyl)amino)naphthalene-1-sulfonate (41)

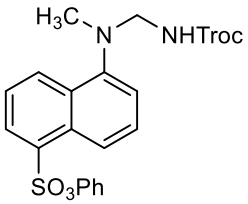

Following the general procedure, phenyl 5-(dimethylamino)naphthalene-1-sulfonate (164 mg, 0.5 mmol, 10 equiv.), TrocNHOTs (18.1 mg, 0.05 mmol, 1.0 equiv.), K_2CO_3 (10.4 mg, 0.075 mmol, 1.5 equiv.), and $Rh_2(oct)_4$ (1.9 mg, 0.05 equiv.) were stirred at r.t. in toluene (0.25 mL) for 12 h. The crude material was purified by column chromatography (EtOAc/hexane = 1/3) to afford **41** as light yellow oil (15.3 mg, 59%).

^{1}H NMR (400 M Hz, $CDCl_3$, 323 K) δ: 8.62 (d, *J* = 8.8 Hz, 1H), 8.60 (d, *J* = 6.4 Hz, 1H), 8.12 (d, *J* = 7.2 Hz, 1H), 7.70 (t, *J* = 8.0 Hz, 1H), 7.49 (t, *J* = 8.0 Hz, 1H), 7.36 (d, *J* = 7.6 Hz, 1H), 7.23−7.16 (m, 3H), 6.92 (d, *J* = 7.2 Hz, 2H), 5.30 (br s, 1H), 4.74−4.70 (m, 4H), 3.00 (s, 3H); **^{13}C NMR** (100 M Hz, $CDCl_3$) δ: 155.0, 149.8, 147.4, 131.6, 131.5, 131.3, 130.3, 130.2, 129.7, 128.8, 127.3, 123.9, 122.2, 121.5, 119.3, 95.6, 74.8 and 74.6 (rotamers), 63.2, 39.5; **IR** (neat, cm^{-1}): 3402, 2952, 1738, 1518, 1367, 1192, 1052, 862, 730; **HRMS-ESI$^+$** (m/z): Calcd. for $C_{21}H_{20}Cl_3N_2O_5S$ $[M+H]^+$ 517.0153; found, 517.0143.

2,2,2-Trichloroethyl ((ethyl(phenyl)amino)methyl)carbamate (42)

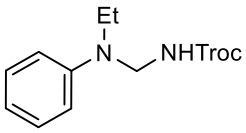

Following the general procedure, *N*-ethyl-*N*-methylaniline (68 mg, 0.5 mmol, 10 equiv.), TrocNHOTs (18.1 mg, 0.05 mmol, 1.0 equiv.), K_2CO_3 (10.4 mg, 0.075 mmol, 1.5 equiv.), and $Rh_2(oct)_4$ (1.9 mg, 0.05 equiv.) were stirred at r.t. in toluene (0.25 mL) for 12 h. The crude material was purified by preparative TLC (EtOAc/hexane = 1/9) to afford **42** as colorless oil (5.3 mg, 33%).

^{1}H NMR (400 M Hz, $CDCl_3$, 323 K) δ: 7.28−7.24 (m, 2H), 6.81−6.79 (m, 3H), 5.40 (br s, 1H), 4.90 (d, *J* = 5.2 Hz, 2H), 4.75 (s, 2H), 3.47 (q, *J* = 6.8 Hz, 2H), 1.23 (t, *J* = 7.2 Hz, 3H); **^{13}C NMR** (100 M Hz, $CDCl_3$) δ: 154.7, 146.6, 129.7, 118.1, 113.7 and 113.3 (rotamers), 95.6, 74.6, 58.0, 44.8, 13.2; **IR** (neat, cm^{-1}): 3318, 2965, 1725, 1503, 1372, 1200, 1140, 997, 822, 727; **HRMS-ESI$^+$** (m/z): Calcd. for $C_{12}H_{16}Cl_3N_2O_2$ $[M+H]^+$ 325.0272; found, 325.0274.

2,2,2-Trichloroethyl ((butyl(phenyl)amino)methyl)carbamate (43)

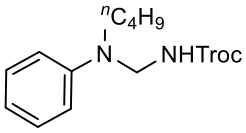

Following the general procedure, *N*-butyl-*N*-methylaniline (81 mg, 0.5 mmol, 10 equiv.), TrocNHOTs (18.1 mg, 0.05 mmol, 1.0 equiv.), K_2CO_3 (10.4 mg, 0.075 mmol, 1.5 equiv.), and $Rh_2(oct)_4$ (1.9 mg, 0.05 equiv.) were stirred at r.t. in toluene (0.25 mL) for 12 h. The crude material was purified by preparative TLC (EtOAc/hexane = 1/9) to afford **43** as colorless oil (7.6 mg, 43%).

^{1}H NMR (400 M Hz, $CDCl_3$, 323 K) δ: 7.27−7.24 (m, 2H), 6.81−6.78 (m, 3H), 5.37 (br s, 1H), 4.89 (d, *J* = 5.2 Hz, 2H), 4.75 (s, 2H), 3.38 (t, *J* = 7.2 Hz, 2H), 1.64−1.58 (m, 2H), 1.41−1.35 (m, 2H), 0.96 (t, *J* = 7.6 Hz, 3H); **^{13}C NMR** (100 M Hz, $CDCl_3$) δ: 154.7, 146.8, 129.7, 118.1, 113.6 and 113.2 (rotamers), 95.6, 74.6, 58.4, 50.4, 30.1, 20.4, 14.1; **IR** (neat, cm^{-1}): 3326, 2960, 2864, 1733, 1602, 1503, 1367, 1232, 1184, 817, 722; **HRMS-ESI$^+$** (m/z): Calcd. for $C_{14}H_{20}Cl_3N_2O_2$ $[M+H]^+$ 353.0585; found, 353.0586.

2,2,2-Trichloroethyl ((octyl(phenyl)amino)methyl)carbamate (44)

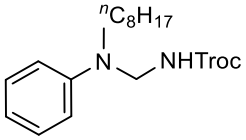

Following the general procedure, *N*-methyl-*N*-octylaniline (110 mg, 0.5 mmol, 10 equiv.), TrocNHOTs (18.1 mg, 0.05 mmol, 1.0 equiv.), K_2CO_3 (10.4 mg, 0.075 mmol, 1.5 equiv.), and $Rh_2(oct)_4$ (1.9 mg, 0.05 equiv.) were stirred at r.t. in toluene (0.25 mL) for 12 h. The crude material was purified by preparative TLC (EtOAc/hexane = 1/9) to afford **44** as colorless oil (8.2 mg, 40%).

^{1}H NMR (400 M Hz, $CDCl_3$, 323 K) δ: 7.27−7.23 (m, 2H), 6.81−6.77 (m, 3H), 5.37 (br s, 1H), 4.89 (d, *J* = 5.6 Hz, 2H), 4.75 (s, 2H), 3.36 (t, *J* = 7.2 Hz, 2H), 1.68−1.58 (m, 2H), 1.35−1.21 (m, 10H), 0.89 (t, *J* = 6.0 Hz, 3H); **^{13}C NMR** (100 M Hz, $CDCl_3$) δ: 154.7, 146.8, 129.7, 118.1, 113.5 and 113.2 (rotamers),

95.6, 74.6, 58.4, 50.7, 31.9, 29.6 and 29.4 (rotamers), 28.0, 27.3, 22.8, 14.3; **IR** (neat, cm^{-1}): 3335, 2956, 2857, 1729, 1602, 1503, 1367, 1224, 997, 817, 722; **HRMS-ESI**$^+$ (m/z): Calcd. for $C_{18}H_{28}Cl_3N_2O_2$ $[M+H]^+$ 409.1211; found, 409.1209.

2,2,2-Trichloroethyl ((isopropyl(phenyl)amino)methyl)carbamate (45)

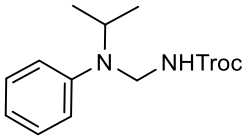

Following the general procedure, *N*-isopropyl-*N*-methylaniline (75 mg, 0.5 mmol, 10 equiv.), TrocNHOTs (18.1 mg, 0.05 mmol, 1.0 equiv.), K_2CO_3 (10.4 mg, 0.075 mmol, 1.5 equiv.), and $Rh_2(oct)_4$ (1.9 mg, 0.05 equiv.) were stirred at r.t. in toluene (0.25 mL) for 12 h. The crude material was purified by preparative TLC (EtOAc/hexane = 1/9) to afford **45** as colorless oil (7.1 mg, 42%).

^{1}H NMR (400 M Hz, $CDCl_3$, 323 K) δ: 7.28−7.24 (m, 2H), 6.87−6.80 (m, 3H), 5.19 (br s, 1H), 4.87 (d, *J* = 5.2 Hz, 2H), 4.75 (s, 2H), 4.06 (sep, 1H), 1.27 (d, *J* = 6.4 Hz, 6H); **^{13}C NMR** (100 M Hz, $CDCl_3$) δ: 153.9, 147.3, 129.8 and 129.5 (rotamers), 118.4, 114.0 and 113.7 (rotamers), 95.6, 74.8 and 74.5 (rotamers), 52.9, 48.0, 20.8; **IR** (neat, cm^{-1}): 3315, 2965, 1725, 1499, 1323, 1192, 1116, 1045, 822, 727; **HRMS-ESI**$^+$ (m/z): Calcd. for $C_{13}H_{18}Cl_3N_2O_2$ $[M+H]^+$ 339.0428; found, 339.0429.

2,2,2-Trichloroethyl ((benzyl(phenyl)amino)methyl)carbamate (46)

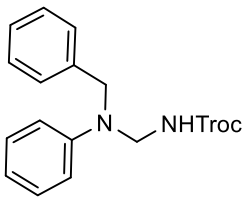

Following the general procedure, *N*-benzyl-*N*-methylaniline (100 mg, 0.5 mmol, 10 equiv.), TrocNHOTs (18.1 mg, 0.05 mmol, 1.0 equiv.), K_2CO_3 (10.4 mg, 0.075 mmol, 1.5 equiv.), and $Rh_2(oct)_4$ (1.9 mg, 0.05 equiv.) were stirred at r.t. in toluene (0.25 mL) for 12 h. The crude material was purified by preparative TLC (EtOAc/hexane = 1/9) to afford **46** as colorless oil (7.2 mg, 37%).

^{1}H NMR (400 M Hz, $CDCl_3$, 323 K) δ: 7.33−7.21 (m, 7H), 6.85−6.80 (m, 3H), 5.45 (br s, 1H), 4.98 (d, *J* = 6.0 Hz, 2H), 4.73 (s, 2H), 4.65 (s, 2H); **^{13}C NMR** (100 M Hz, $CDCl_3$) δ: 154.8, 147.2, 138.4, 129.7, 128.8, 127.2, 126.8, 118.7, 113.6, 95.5, 74.7, 58.4, 54.3; **IR** (neat, cm^{-1}): 3335, 3028, 1725, 1602, 1499, 1363, 1236, 1172, 809, 727; **HRMS-ESI**$^+$ (m/z): Calcd. for $C_{17}H_{18}Cl_3N_2O_2$ $[M+H]^+$ 387.0428; found, 387.0428.

2,2,2-trichloroethyl ((2-methylindolin-1-yl)methyl)carbamate (47)

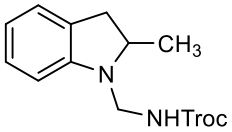

Following the general procedure, 1,2-dimethylindoline (75 mg, 0.5 mmol, 10 equiv.), TrocNHOTs (18.1 mg, 0.05 mmol, 1.0 equiv.), K_2CO_3 (10.4 mg, 0.075 mmol, 1.5 equiv.), and $Rh_2(oct)_4$ (1.9 mg, 0.05 equiv.) were stirred at r.t. in toluene (0.25 mL) for 12 h. The crude material was purified by preparative TLC (EtOAc/hexane = 1/9) to afford **47** as a white solid (5.6 mg, 33%).

White solid: **m.p.** 79 °C; **^{1}H NMR** (400 M Hz, $CDCl_3$, 323 K) δ: 7.10−7.06 (m, 2H), 6.73 (t, *J* = 7.6 Hz, 1H), 6.56 (d, *J* = 7.6 Hz, 1H), 5.38 (br s, 1H), 4.86−4.72 (m, 4H), 3.84−3.74 (m, 1H), 3.13 (dd, *J* = 8.8 Hz and 15.6 Hz, 1H), 2.64 (dd, *J* = 10.4 Hz and 15.2 Hz, 1H), 1.41 (d, *J* = 6.4 Hz, 3H); **^{13}C NMR** (100 M Hz, $CDCl_3$) δ: 155.2, 149.9, 129.7, 127.6, 124.9, 119.3, 107.3, 95.6, 74.7, 57.7, 52.0, 37.3, 19.2; **IR** (KBr, cm^{-1}): 3343, 2968, 1718, 1527, 1372, 1236, 1148, 989, 730; **HRMS-ESI$^+$** (m/z): Calcd. for $C_{13}H_{16}Cl_3N_2O_2$ $[M+H]^+$ 337.0272; found, 337.0253.

Procedure for Decomposition of Aminal 50

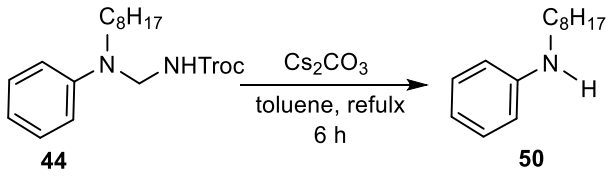

Cs_2CO_3 (78 mg, 0.24 mmol, 1.5 equiv.) was added to a solution of **44** (65 mg, 0.16 mmol, 1.0 equiv.) in toluene (1.6 mL) and the resulting mixture was allowed stirring under reflux condition. After being stirred for 6 h, the reaction was quenched by addition of 1N HCl and extracted with EtOAc. The organic layer was washed with brine, and dried over Na_2SO_4, filtered, and concentrated. The NMR yield of the product **50** (75%) was determined by ^{1}H NMR using 1,3-dinitrobenzene as an internal standard. The residue was purified by preparative TLC (EtOAc/hexane = 1/20) to afford the product **50** (19 mg, 58% yield) as colorless oil. The spectral data were identical to the reported data.[50]

KIE Measurements

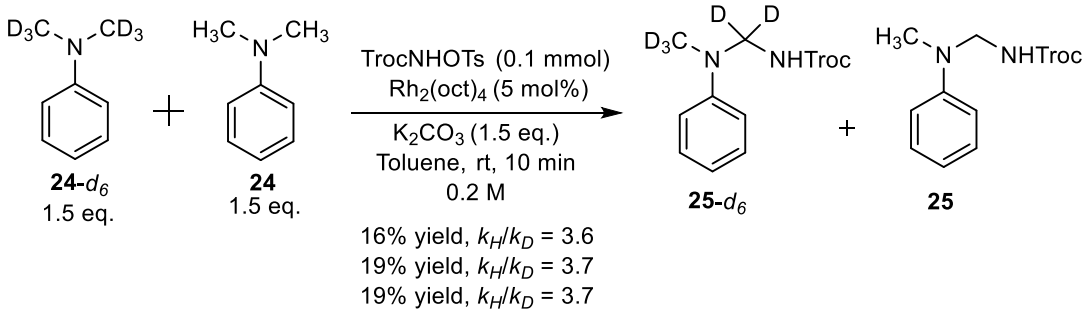

To a suspension of *N*,*N*-dimethylaniline (**24**; 18 mg, 0.15 mmol, 1.5 equiv.), *N*,*N*-bis(methyl-d_3)aniline (**24**-d_6; 19 mg, 0.15 mmol, 1.5 equiv.), TrocNHOTs (36.2 mg, 0.10 mmol, 1.0 equiv.) and K_2CO_3 (20.8 mg, 0.15 mmol, 1.5 equiv.) in toluene (0.5 mL) was added $Rh_2(oct)_4$ (4.0 mg, 0.005 mmol, 0.05 equiv.)

at r.t.. After being stirred for 10 min, the reaction was quenched by addition of water and extracted with EtOAc. The organic layer was washed with brine, and dried over Na_2SO_4, filtered, and concentrated in vacuo. The residue was purified by preparative TLC purification (EtOAc/hexane =1/9) to afford a mixture of **25** and **25**-d_6. KIE was calculated from the comparison of the integrals between an aromatic signal (δ 6.84−6.82 ppm, 3H of **25** and **25**-d_6) and a methylene (δ 4.92 ppm, 2H of **25**) in ^{1}H NMR of a solution of **25** and **25**-d_6 ($CDCl_3$). The experiments were performed three times and the determined KIE was the average of three runs.

Synthesis of reagents

2,2,2-tribromoethyl-*N*-tosyloxycarbamate (**S2**) was synthesized by the method described below.

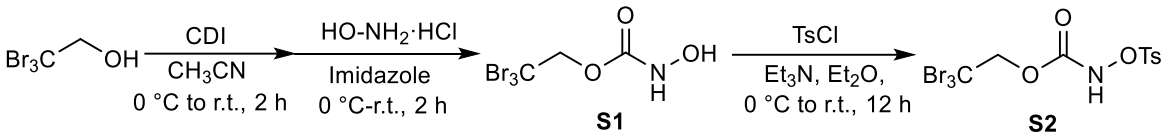

To a solution of 2,2,2-tribromoethanol (424 mg, 1.5 mmol, 1.0 equiv.) in CH_3CN (7.5 mL) was added CDI (267 mg, 1.6 mmol, 1.1 equiv.) at 0 °C. After being stirred for 2 h at r.t., the solution was cooled to 0 °C. Imidazole (306 mg, 4.5 mmol, 3.0 equiv.) and hydroxylamine hydrochloride (417 mg, 6 mmol, 4.0 equiv.) were added to the reaction mixture. The reaction mixture was stirred at r.t. for 2 h and acidified with 1 N HCl. The resulting mixture was extracted with diethylether, the organic layer was washed with brine, and dried over Na_2SO_4, filtered, and concentrated in vacuo. The yellow oil was solidified to a yellow solid. After recrystallization from $CHCl_3$/Hexane, the desired **S1** was obtained (220 mg, 43%) as a white solid.

To a solution of **S1** (170 mg, 0.5 mmol, 1.0 equiv.) in diethylether (10 mL) at 0 °C were added *p*-toluenesulfonyl chloride (105 mg, 0.55 mmol, 1.1 equiv.) and triethylamine (76 μL, 0.55 mmol, 1.1 equiv.). The resulting white suspension was stirred at r.t. for 2 h. The reaction was quenched by addition of water and extracted with diethylether. The organic layer was washed with brine, and dried over Na_2SO_4, filtered, and concentrated in vacuo. The desired product **S2** was obtained as a white solid (110 mg, 44% yield) after recrystallization from $CHCl_3$/Hexane.

White solid, **m.p.** 171 °C; **^{1}H NMR** (400 M Hz, acetone-d_6) δ: 11.1 (br s, 1H), 7.89 (d, J = 8.4 Hz, 2H), 7.50 (d, J = 8.4 Hz, 2H), 4.92 (s, 2H), 2.46 (s, 3H); **^{13}C NMR** (100 M Hz, acetone-d_6) δ: 155.1, 147.2, 131.6, 130.8, 130.4, 78.1, 36.3, 21.6; **IR** (KBr, cm^{-1}): 3247, 2948, 1765, 1594, 1447, 1383, 1280, 1232, 1180, 1101, 1052, 817, 730, 547; **HRMS-ESI$^+$** (m/z): Calcd. for $C_{10}H_{10}{}^{79}Br_2{}^{81}BrNO_5SNa$ $[M+Na]^+$ 517.7702; found, 517.7716.

3. Chapter 3

Synthesis of catalyst 56

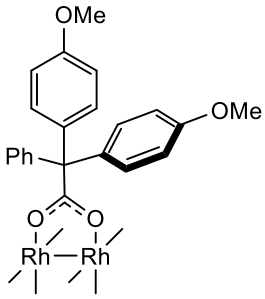

A mixture of $Rh_2(OAc)_4$ (40 mg, 0.09 mmol) and **57** (250 mg, 0.72 mmol) was heated at 150°C for 3 h. After allowing the mixture to cool to r.t., EtOAc was added and the dark green solution was washed with saturated aqueous $NaHCO_3$ and water. The solvent was removed and the residue was chromatographed on aluminium oxide (30% ethyl acetate/hexane) to give **56** (136 mg, 95%) as a green solid.

Green solid: **m.p.** >300 °C. ^{1}H NMR ($CDCl_3$, 400 M Hz, $CDCl_3$) δ: 7.05 (t, *J* = 6.8 Hz, 1H), 6.86 (t, *J* = 8.0 Hz, 2H), 6.66 (d, *J* = 7.6 Hz, 2H), 6.56 (d, *J* = 8.4 Hz, 4H), 6.40 (d, *J* = 8.8 Hz, 4H), 3.69 (s, 6H); ^{13}C NMR ($CDCl_3$, 100 MHz) δ: 193.2, 158.1, 144.2, 136.2, 131.5, 130.6, 127.3, 126.5, 113.0, 67.7, 55.8; **IR** (KBr, cm^{-1}): 3434, 2940, 2836, 1686, 1582, 1507, 1256, 1184, 1033, 802, 566; **HRMS-ESI**$^+$ (m/z): Calcd. for $(C_{88}H_{76}O_{16}Rh_2Na)_2$ $[M+Na]_2^{2+}$ 1617.8153 found, 1617.8162.

The procedure for amination of triphenylamine 58

To a suspension of triphenylamine **58** (18.4 mg, 0.075 mmol, 1.5 equiv.), TrocNHOTs (18.1 mg, 0.05 mmol, 1.0 equiv.) and K_2CO_3 (10.4 mg, 0.075 mmol, 1.5 equiv.) in chlorobenene (0.25 mL) were added $Rh_2(tpa)_4$ (3.4 mg, 0.05 equiv.) at r.t.. After being stirred for 12 h, the reaction was quenched by addition of water and extracted with EtOAc. The organic layer was washed with brine, dried over Na_2SO_4, filtered, and concentrated. The yield of the product **59** was determined by ^{1}H NMR using 1,3-dinitrobenzene as internal standard. The crude material was purified by preparative TLC (EtOAc/hexane =1/9) to afford the aminated product **59** (7.5 mg, 35%) as a white solid.

2,2,2-trichloroethyl (4-(diphenylamino)phenyl)carbamate (**59**)

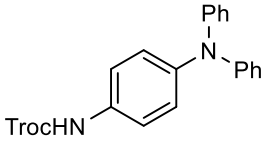

White solid: **m.p.** 204 °C; **^{1}H NMR** (400 M Hz, $CDCl_3$) δ: 7.31 (d, *J* = 8.4 Hz, 2H), 7.27−7.22 (m, 4H), 7.09−7.05 (m, 6H), 7.00 (t, *J* = 11.2 Hz, 2H), 6.81 (br s, 1H), 4.83 (s, 2H); **^{13}C NMR** (150 M Hz, $CDCl_3$) δ: 151.8, 147.9, 144.4, 132.1, 129.4, 125.4, 123.9, 122.8, 120.4, 95.4, 74.6; **IR** (KBr, cm^{-1}): 3291, 1718, 1546, 1487, 1275, 1243,1105, 742, 694; **HRMS-ESI**$^+$ (m/z): Calcd. for $C_{21}H_{17}Cl_3N_2O_2$ $[M]^+$ 434.0350

found, 434.0358.

NMR titration

N,*N*-dimethylaniline and $Rh_2(oct)_4$ mixture

$Rh_2(oct)_4$ (0.79 mg, 1.01 mmol) was dissolved in $CDCl_3$ (1.0 mL) to prepare a host solution (1.01mM). *N*,*N*-dimethylaniline **24** (4.77 mg, 0.0394 mmol) was dissolved in $CDCl_3$ (1.0 mL) to prepare a guest solution (39.4 mM). The titration was monitored by ^{1}H NMR spectroscopy with 0.6 mL of the host solution and $5 \times n\mu$L of the guest solution.

N,*N*-dimethylaniline and $Rh_2(tpa)_4$ mixture

$Rh_2(tpa)_4 \cdot 0.3EtOAc$ (1.34 mg, 0.97 mmol) was dissolved in $CDCl_3$ (1.0 mL) to prepare a host solution. *N*,*N*-dimethylaniline **24** (6.06 mg, 0.05 mmol) was dissolved in $CDCl_3$ (1.0 mL) to prepare a guest solution (50.0 mM). The titration was monitored by ^{1}H NMR spectroscopy with 0.6 mL of the host solution and $5 \times n\mu$L of the guest solution.

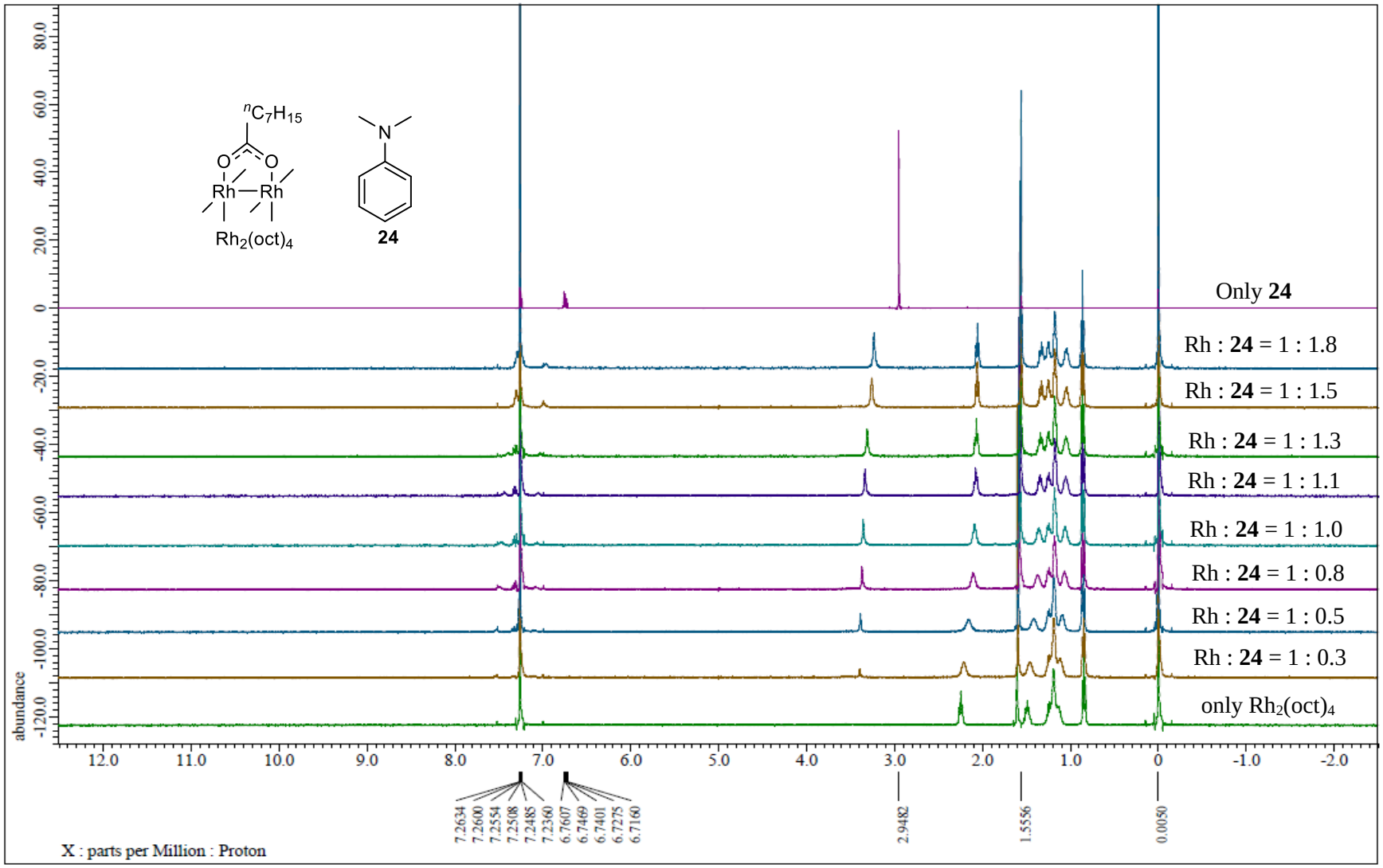

Figure S2 ^{1}H NMR spectra ($CDCl_3$, 293 K, 400 M Hz) of $Rh_2(oct)_4$ and mixtures with **24**.

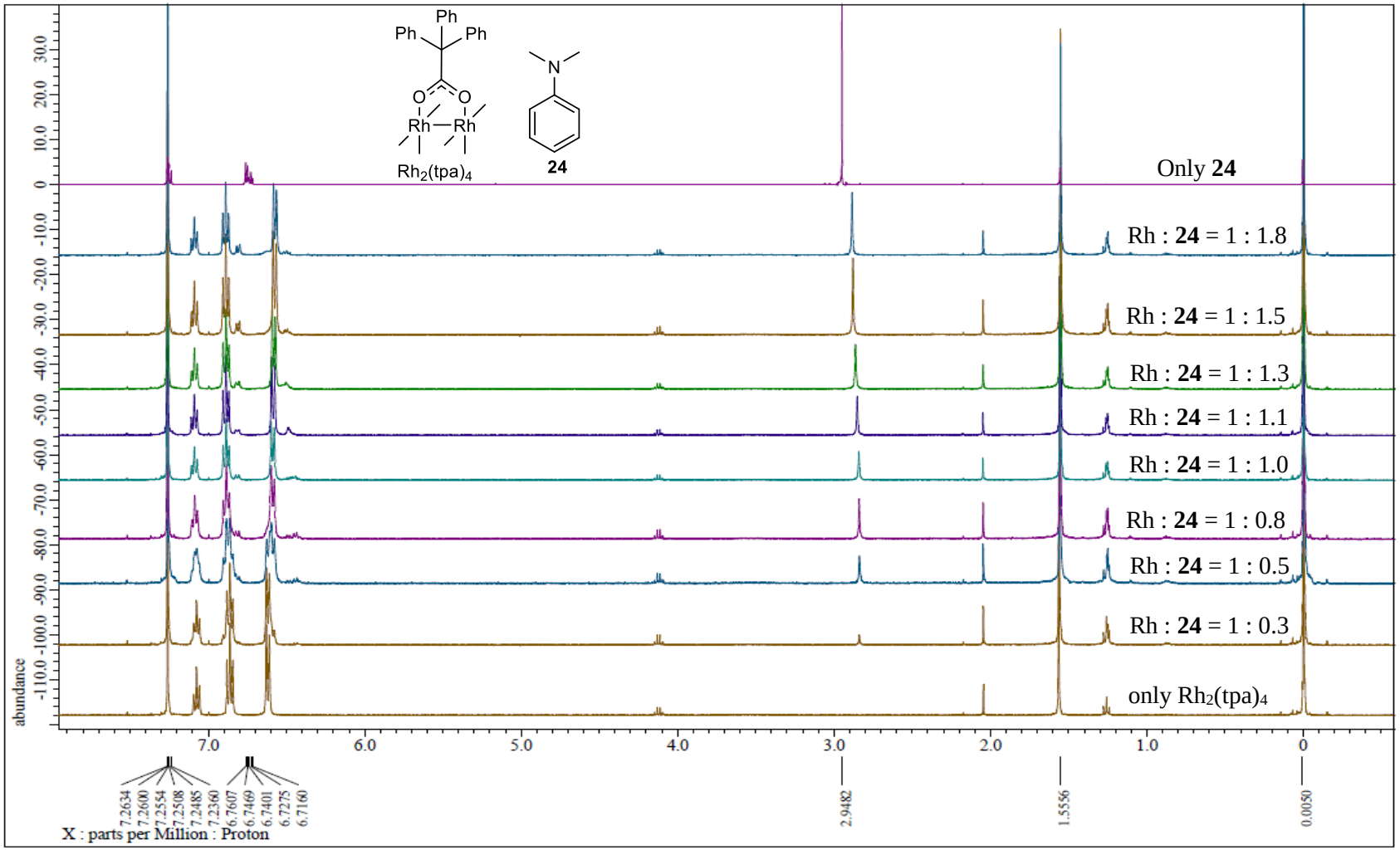

Figure S3 ^{1}H NMR spectra ($CDCl_3$, 293 K, 400 M Hz) of $Rh_2(tpa)_4$ and mixtures with **24**.

Computational details in this chapter

Geometry optimization and frequency calculation were performed by density functional theory (DFT) at the M06/LanL2DZ(Rh)/6-31G(d,p) level of theory, using Gaussian 16. XYZ coordinated and thermochemical data at 298.15K (energies in Hartree) of the calculated structures were described below.

N,*N*-dimethylaniline (**24**)

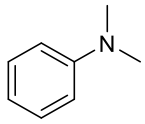

M06/6-31G(d,p)

Electronic Energy = –365.941659

Enthalpy = –365.759284

Free Energy = –365.802702

C 0.18209900 0.00001000 -0.05100700
C -0.54590500 -1.20431500 -0.02410700
C -1.93313200 -1.19426000 0.01142800
C -2.64460200 0.00000800 0.02833800
C -1.93313300 1.19428300 0.01179800
C -0.54590500 1.20433400 -0.02371300
H -0.02756600 -2.15839600 -0.03063900
H -2.46377600 -2.14414900 0.02986000
H -3.73077500 -0.00000100 0.05832100
H -2.46377400 2.14416700 0.03053500
H -0.02756500 2.15841500 -0.02988200
N 1.56592800 -0.00002300 -0.10691800
C 2.28021400 1.24399300 0.04276400
H 2.07836100 1.74007500 1.00642700
H 3.35421600 1.05420400 -0.02192200
H 2.02436400 1.95180600 -0.75756700
C 2.28010400 -1.24402000 0.04343900
H 2.02459100 -1.95212400 -0.75674200
H 3.35414100 -1.05428900 -0.02081400
H 2.07784600 -1.73974600 1.00720200

$Rh_2(OAc)_4$

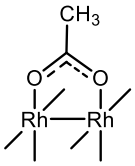

M06/LanL2DZ(Rh)/6-31G(d,p)

Electronic Energy = –1132.578552

Enthalpy = –1132.345459

Free Energy = –1132.42233

Rh -0.00342200 -0.00216800 1.19357700
Rh -0.00223400 -0.00358500 -1.19306000
O 1.44775700 1.45964300 -1.13048500
O 1.44164700 1.46575700 1.13009000
O 1.46257200 -1.44863300 1.13367500
O 1.45875000 -1.45505600 -1.12692000
O -1.46515000 1.44587900 -1.13176100
O -1.47088900 1.44275000 1.12884300
O -1.44780800 -1.46942100 1.13030700
O -1.45161800 -1.46595300 -1.13032700
C 1.85182400 1.86666400 -0.00034000
C 2.93839600 2.90019400 0.00268900
H 3.90565500 2.39309400 0.08565000
H 2.92604300 3.47007800 -0.92825000
H 2.82924800 3.55992400 0.86609800
C 1.86874100 -1.85482400 0.00427600
C 2.95237900 -2.89141200 -0.00383500
H 2.72653200 -3.65714300 -0.75017800
H 3.89483300 -2.41639400 -0.29546200
H 3.06699100 -3.33788700 0.98511900
C -1.85696700 -1.87158000 -0.00009400
C -2.94384700 -2.90457200 0.00287100
H -2.92808100 -3.47791900 -0.92588500
H -2.83816900 -3.56112600 0.86909800
H -3.91107600 -2.39648300 0.07984900
C -1.87149200 1.85196500 -0.00180400
C -2.90366000 2.93971300 -0.00518300
H -3.55150100 2.84325700 -0.87897500

H -2.39400500 3.90721900 -0.06686100
H -3.48627300 2.91562100 0.91766800

$Rh_2(OAc)_4$•**24**

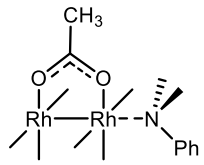

M06/LanL2DZ(Rh)/6-31G(d,p)
Electronic Energy = –1498.552900
Enthalpy = –1498.136609
Free Energy = –1498.228264

C -0.59242200 2.25654500 0.88719000
C 0.98676600 1.26779500 -2.33399600
C 2.55486200 -1.68735300 -0.65666600
C 0.94932500 -0.67009500 2.57770200
O 0.65019400 2.46113800 0.98869400
O -1.15587700 1.20397000 0.45793800
O 1.87874800 1.68762700 -1.54702000
O 0.08121800 0.41610300 -2.07014700
O 3.10907900 -0.63296900 -0.24523600
O 1.30412200 -1.90569100 -0.74168800
O 1.86326100 0.15219900 2.29491400
O 0.04168200 -1.09458500 1.79608000
Rh 1.94151700 0.96225500 0.39146800
Rh 0.00509400 -0.39368300 -0.15893200
N -1.77610900 -1.72915400 -0.69973600
C -1.63470400 -2.06551200 -2.12577700
H -1.50503900 -1.16490000 -2.72549900
H -0.72654400 -2.66132900 -2.24296400
H -2.50725100 -2.63638000 -2.47755900
C -1.63331500 -2.95507800 0.10161400
H -0.73444500 -3.47569800 -0.23588900
H -1.48708900 -2.71200900 1.15423700
H -2.51231300 -3.60556900 -0.02277400
C -2.93927600 -0.94303300 -0.38544600
C -3.46055900 -0.04204100 -1.31922900

C -3.51476800 -0.99754900 0.88721100
C -4.52452400 0.78372400 -0.98224400
H -3.01696300 0.04991300 -2.30510300
C -4.57884600 -0.16651800 1.21431300
H -3.12165900 -1.66710700 1.64480500
C -5.09304800 0.72967500 0.28517200
H -4.90965000 1.47887500 -1.72499900
H -5.00786200 -0.22606000 2.21213100
H -5.92747500 1.37644100 0.54449700
C 0.94740000 -1.21120100 3.97978600
H 1.82968200 -1.84417300 4.11860800
H 1.02777800 -0.38355600 4.68967300
H 0.04642500 -1.79433400 4.17687200
C 3.44816500 -2.81834800 -1.08331700
H 3.32450500 -3.65611300 -0.38955300
H 3.15102700 -3.17057200 -2.07518300
H 4.49252000 -2.50281700 -1.09068000
C 1.00930600 1.82737800 -3.72868300
H 1.04337800 2.91934700 -3.68153300
H 1.92392700 1.49673500 -4.23086800
H 0.13927300 1.50044600 -4.30030600
C -1.51959800 3.36216300 1.30473200
H -2.09834600 3.68977400 0.43535000
H -2.23457600 2.97851400 2.03871700
H -0.96206100 4.20323900 1.71962800

$Rh_2(tpa)_4$

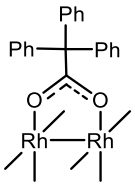

M06/LanL2DZ(Rh)/6-31G(d,p)
Electronic Energy = –3902.996024
Enthalpy = –3901.740677
Free Energy = –3901.929815

C -2.01708800 1.64366200 0.01937700
C -3.27171700 2.54365100 0.08786000

C -2.78302800 3.99769500 0.29323800
C -3.39519900 5.06321300 -0.37438800
H -4.18789900 4.86842900 -1.09224800
C -3.01546700 6.37932300 -0.12361300
H -3.51187800 7.18793600 -0.65581000
C -2.01354900 6.65931600 0.79813100
H -1.71194100 7.68689300 0.98736900
C -1.40733100 5.61001500 1.48006500
H -0.61926900 5.80472700 2.20529600
C -1.79295300 4.29587200 1.23819800
H -1.31332700 3.49295000 1.79317200
C -4.83869700 3.02617800 2.03920200
H -4.75621700 4.08690300 1.81111500
C -5.67962500 2.60963700 3.06820300
H -6.24036400 3.35055700 3.63391300
C -5.79860700 1.25982500 3.37422700
H -6.45005200 0.93569200 4.18268000
C -5.07463700 0.32454300 2.63930300
H -5.14935400 -0.73860300 2.86322900
C -4.24322000 0.74290000 1.60912800
H -3.68529500 -0.01316300 1.05586200
C -4.10613900 2.10015200 1.29830000
C -4.09206400 2.41813800 -1.20470200
C -5.43978100 2.05688400 -1.18626300
H -5.92436700 1.80891500 -0.24546100
C -6.18884700 2.01839200 -2.36264700
H -7.23959700 1.74050100 -2.31618900
C -5.60074900 2.33218700 -3.57986600
H -6.18389200 2.30350500 -4.49759900
C -4.25442100 2.69134800 -3.61285300
H -3.77929900 2.94540500 -4.55770000
C -3.51334400 2.74057400 -2.44116600
H -2.47141700 3.04952500 -2.48044500
C -1.63826100 -1.99708200 -0.02910500
C -2.63474200 -3.17584400 -0.09085900
C -3.56243500 -2.95630600 -1.29391400
C -4.06053800 -4.04104600 -2.01426700
H -3.72541100 -5.04791100 -1.77308800

C -4.98621700 -3.85230700 -3.03713800
H -5.36004500 -4.71364000 -3.58646600
C -5.42576000 -2.57393100 -3.35798000
H -6.14267400 -2.42594900 -4.16247200
C -4.93915300 -1.48285900 -2.64293200
H -5.26635300 -0.47129100 -2.87861100
C -4.02280700 -1.67568400 -1.61767400
H -3.65794700 -0.80058500 -1.07912500
C -3.45021600 -3.25785900 1.20803600
C -4.84553400 -3.23530300 1.19953200
H -5.38247700 -3.11545800 0.26217000
C -5.57372300 -3.37459000 2.38126500
H -6.66072700 -3.35975500 2.34190400
C -4.91904600 -3.53163300 3.59468400
H -5.48551400 -3.64156100 4.51671300
C -3.52560000 -3.55271100 3.61837200
H -2.99660000 -3.67961200 4.56022200
C -2.80231500 -3.42387300 2.44142300
H -1.71625000 -3.46818400 2.47473500
C -1.79164600 -4.45643100 -0.30792500
C -2.06247900 -5.63262600 0.39745500
H -2.84635800 -5.64486300 1.15023400
C -1.34865300 -6.80130700 0.14242000
H -1.58171700 -7.70173300 0.70686400
C -0.34952900 -6.81968200 -0.82320600
H 0.21322500 -7.73034200 -1.01561400
C -0.08527600 -5.66211900 -1.54751600
H 0.69135600 -5.65400300 -2.30980300
C -0.80083200 -4.49664600 -1.29810800
H -0.58491600 -3.60702400 -1.88408900
C 2.07907800 -1.67263600 0.01603500
C 3.26869400 -2.65314000 0.08822900
C 2.96644100 -3.65585100 1.21159400
C 3.93872000 -4.07705300 2.11490800
H 4.93604300 -3.64503100 2.08090000
C 3.64594300 -5.04623300 3.07354700
H 4.42031900 -5.35729600 3.77138900
C 2.37864500 -5.60896100 3.14234300

H 2.15301300 -6.36456200 3.89147400
C 1.39790000 -5.19549300 2.24297800
H 0.39799300 -5.62620600 2.26994100
C 1.69206600 -4.22959000 1.29169100
H 0.91355500 -3.92838400 0.58933200
C 3.44762400 -3.36745000 -1.26007900
C 3.36804400 -4.75368100 -1.38470200
H 3.14481800 -5.36722300 -0.51523700
C 3.57141100 -5.37489900 -2.61744600
H 3.50598800 -6.45923200 -2.68455700
C 3.85794400 -4.62057300 -3.74587600
H 4.01494700 -5.10456600 -4.70714600
C 3.95492100 -3.23484800 -3.63185100
H 4.18991400 -2.62953600 -4.50453700
C 3.75928300 -2.61989000 -2.40446600
H 3.85167700 -1.53882800 -2.32516900
C 4.53031000 -1.82977100 0.42167800
C 5.78348900 -2.30212200 0.01609900
H 5.84543100 -3.20941100 -0.58159500
C 6.95100700 -1.63955600 0.37767600
H 7.91210800 -2.03320300 0.05386100
C 6.89020800 -0.48200600 1.14658600
H 7.80049700 0.04764400 1.41878300
C 5.65221600 -0.00145300 1.55256800
H 5.58966000 0.91478600 2.13763400
C 4.48334400 -0.67010500 1.20121800
H 3.52894200 -0.27532800 1.54329800
C 1.71034500 2.06986600 -0.02931400
C 2.65644700 3.28670800 -0.09558900
C 2.10236300 4.22862000 -1.17446400
C 2.92276600 4.90202400 -2.07525900
H 3.99447200 4.71815900 -2.07749400
C 2.38171100 5.80928300 -2.98553600
H 3.04055100 6.32129000 -3.68353700
C 1.01592100 6.05885600 -3.00644000
H 0.59842200 6.76846700 -3.71720100
C 0.18504800 5.39071700 -2.10910500
H -0.88886600 5.57394400 -2.09671000

C 0.72718500 4.48515200 -1.20930500
H 0.06316200 3.98082100 -0.50683200
C 2.70250800 3.97963900 1.27511100
C 2.26138800 5.28765300 1.46843400
H 1.85382400 5.85494800 0.63515900
C 2.33623300 5.88956400 2.72514300
H 1.98934700 6.91406700 2.84649500
C 2.85353200 5.19426700 3.80836200
H 2.91133900 5.66368400 4.78773900
C 3.30819500 3.88951400 3.62566800
H 3.72377400 3.33274500 4.46261600
C 3.23715400 3.29516300 2.37500900
H 3.60320600 2.27917800 2.24096000
C 4.06015300 2.77869100 -0.48109200
C 5.18075400 3.53292700 -0.11499900
H 5.04676900 4.43245300 0.48299300
C 6.45887700 3.15870800 -0.51314200
H 7.31109600 3.76783100 -0.21955100
C 6.64612300 2.01339400 -1.28033700
H 7.64612200 1.70972900 -1.58221000
C 5.54277400 1.25386300 -1.64628400
H 5.67629400 0.34292500 -2.22731300
C 4.26150600 1.63367700 -1.25745700
H 3.41660500 1.02235100 -1.56696000
O -1.61257900 1.23229300 -1.10598300
O -1.46960900 1.38194700 1.13074900
O -1.17997000 -1.61035500 -1.14392000
O -1.33272300 -1.50439900 1.09498300
O 1.69886300 -1.24519600 -1.11245400
O 1.57888600 -1.34283000 1.13153800
O 1.29209600 1.64396900 -1.14568700
O 1.42520300 1.57360800 1.09911500
Rh 0.05992400 0.01298800 -1.19799800
Rh 0.06078600 0.02508700 1.18420700

$Rh_2(tpa)_4$•**24**

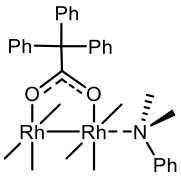

M06/LanL2DZ(Rh)/6-31G(d,p)

Electronic Energy = –4268.996250

Enthalpy = –4267.553745

Free Energy = –4267.756532

C -2.37653900 -0.73472700 -0.52771300
C -3.81386700 -1.31623400 -0.53887100
C -4.80973400 -0.15409600 -0.31402300
C -6.01370600 -0.09362200 -1.02462400
H -6.22687400 -0.83564300 -1.78998500
C -6.95695500 0.89601800 -0.76014800
H -7.88433500 0.91460500 -1.32862500
C -6.71788900 1.85056900 0.22166100
H -7.45124300 2.62781700 0.42406000
C -5.53297200 1.79053400 0.94674900
H -5.32345700 2.52061000 1.72796100
C -4.59323300 0.79762500 0.69066100
H -3.68537400 0.76623100 1.29016100
C -5.17211000 -2.54691800 1.22663900
H -6.03300500 -1.94804200 0.93601900
C -5.32185400 -3.53620900 2.19481900
H -6.29709600 -3.69745500 2.64944100
C -4.23299700 -4.30993800 2.58156400
H -4.34741500 -5.07974100 3.34164500
C -2.99382400 -4.09032300 1.98511500
H -2.12448000 -4.67927200 2.27595800
C -2.85248400 -3.11107600 1.00893900
H -1.86675900 -2.95965100 0.56888100
C -3.93708200 -2.31911600 0.61854400
C -4.07456100 -2.01574300 -1.88015700
C -4.41020400 -3.36686300 -1.96123600
H -4.46858000 -3.97036300 -1.05868100
C -4.68197300 -3.96560300 -3.19248100
H -4.94905600 -5.02011200 -3.22458100

C -4.61291000 -3.22512200 -4.36352900
H -4.82360400 -3.69111800 -5.32350700
C -4.27721500 -1.87374600 -4.29612500
H -4.22144200 -1.27810300 -5.20446700
C -4.01615600 -1.27806500 -3.07177400
H -3.76648500 -0.21972900 -3.03410400
C 0.86781500 -2.45389700 -0.32589100
C 1.37321600 -3.91761600 -0.32008900
C 0.74253400 -4.66654100 -1.50127200
C 1.41730900 -5.74134300 -2.08117700
H 2.42475200 -5.98453100 -1.74831800
C 0.81746000 -6.51039300 -3.07340900
H 1.36425200 -7.34275000 -3.51120400
C -0.46970600 -6.21341800 -3.50577800
H -0.93731600 -6.80839900 -4.28710100
C -1.15352100 -5.14481900 -2.93428900
H -2.15902500 -4.88822800 -3.26378100
C -0.55543600 -4.38285400 -1.93762600
H -1.11517400 -3.54511100 -1.52088100
C 1.00219800 -4.59935400 1.00352700
C 0.22310400 -5.75558800 1.04973400
H -0.15509900 -6.19331800 0.12936400
C -0.08311900 -6.36891300 2.26567200
H -0.68820900 -7.27302000 2.26792100
C 0.37260900 -5.82988900 3.46018200
H 0.13072700 -6.30493500 4.40823000
C 1.15467300 -4.67594500 3.42958800
H 1.53139800 -4.24375300 4.35521000
C 1.47218900 -4.07812200 2.21841000
H 2.10505400 -3.19230300 2.20866700
C 2.90852800 -3.84349200 -0.51648600
C 3.78679900 -4.60694000 0.25748800
H 3.39917200 -5.25052700 1.04338100
C 5.16196900 -4.56379500 0.03417200
H 5.82152100 -5.16601100 0.65572000
C 5.68730700 -3.75964500 -0.96931300
H 6.76189100 -3.71375200 -1.13458300
C 4.82157200 -3.01775900 -1.76704200

H 5.21344700 -2.38147900 -2.55893200
C 3.45035100 -3.06427400 -1.54890000
H 2.79143300 -2.48230100 -2.18689500
C 2.68303200 0.73932600 -0.23142000
C 4.16716400 1.12093400 -0.00447100
C 4.58632000 0.40674600 1.29143600
C 5.08706500 1.07939200 2.40190200
H 5.21645700 2.15906400 2.37246700
C 5.41664000 0.38299500 3.56664900
H 5.80419100 0.93020100 4.42337200
C 5.25458900 -0.99355200 3.63489900
H 5.51435300 -1.53341500 4.54278000
C 4.76062800 -1.67888600 2.52413600
H 4.63401000 -2.76099300 2.54682300
C 4.43009300 -0.98410700 1.37037900
H 4.03520500 -1.53041600 0.51175100
C 5.05269100 0.71893900 -1.19010600
C 6.23494800 -0.00210100 -1.01526700
H 6.51608100 -0.35310600 -0.02558200
C 7.06992400 -0.28502900 -2.09499000
H 7.98680300 -0.84693400 -1.92765800
C 6.73490800 0.14401800 -3.37215000
H 7.38250900 -0.08013600 -4.21683500
C 5.56659700 0.88044200 -3.55703900
H 5.29868600 1.23981300 -4.54815500
C 4.74539700 1.17733200 -2.47796300
H 3.85403200 1.77989800 -2.63034600
C 4.22368800 2.65021100 0.17884200
C 5.41931000 3.32725700 -0.08379200
H 6.26741400 2.77755700 -0.48712200
C 5.54431000 4.68736400 0.17482600
H 6.48700900 5.18796400 -0.03526700
C 4.47200400 5.40307400 0.69712700
H 4.56149200 6.46987900 0.88947400
C 3.27740300 4.74309200 0.95422300
H 2.42225400 5.30090000 1.33427400
C 3.15241800 3.38001900 0.70300200
H 2.20071800 2.89252800 0.91099800

C -0.64857400 2.59013400 -0.53084100
C -1.16084600 4.04440600 -0.61893400
C -2.28743900 4.05902100 -1.66326600
C -2.44869900 5.09344100 -2.58155100
H -1.72906900 5.90699300 -2.61836500
C -3.51943700 5.09272300 -3.47391700
H -3.62024000 5.90907200 -4.18590700
C -4.44772100 4.06053200 -3.46124100
H -5.28272800 4.06355200 -4.15824100
C -4.29759800 3.01853500 -2.54878000
H -5.01585700 2.19999900 -2.51022700
C -3.22566700 3.01966400 -1.66757300
H -3.13026500 2.19806600 -0.95581200
C -1.66806100 4.46383400 0.77268400
C -3.02205100 4.55656600 1.08891500
H -3.77509800 4.36851200 0.32744400
C -3.43556000 4.89026900 2.37963100
H -4.50042200 4.96467100 2.59480600
C -2.50443100 5.13800300 3.37849200
H -2.82841600 5.40095700 4.38310100
C -1.14582700 5.05275400 3.07473100
H -0.39896400 5.24491100 3.84289900
C -0.73956200 4.72244000 1.79001700
H 0.32418900 4.65483100 1.56466100
C 0.01211700 4.94256500 -1.05164000
C -0.06674500 6.32089900 -0.81294600
H -0.93895700 6.72328800 -0.29970300
C 0.94633000 7.18004100 -1.21999000
H 0.85506500 8.24667000 -1.02619400
C 2.07358800 6.67774800 -1.86517500
H 2.87613600 7.34554800 -2.17033700
C 2.16747900 5.31332800 -2.10087700
H 3.05553000 4.89627800 -2.57353400
C 1.14459700 4.45400500 -1.70741200
H 1.25382500 3.39063300 -1.90681000
O -1.74470200 -0.66174400 -1.61722500
O -1.94088800 -0.38149100 0.60640700
O 0.83257100 -1.89964700 -1.45732400

O 0.54856600 -1.91386200 0.77481200
O 2.19852300 0.67791200 -1.39005400
O 2.04431600 0.56088700 0.85057300
O -0.47831100 1.99184600 -1.62541800
O -0.42904000 2.11596400 0.62443200
Rh 0.20199100 0.04300800 -1.62001400
Rh 0.05829600 0.11752200 0.80287200
N 0.07559900 0.30941700 3.06655000
C 0.89149100 -0.80437800 3.58376200
H 0.51624700 -1.76265200 3.22489600
H 1.91347100 -0.68683300 3.20495700
H 0.89775200 -0.79192600 4.68428600
C 0.76002700 1.57605400 3.38423200
H 1.80155500 1.49249700 3.06103600
H 0.30102600 2.40685600 2.84499400
H 0.71869100 1.76744300 4.46726700
C -1.30877700 0.27080900 3.47037800
C -1.96561000 -0.95594100 3.60816000
C -2.03718200 1.45118000 3.65406400
C -3.31362200 -0.99837400 3.93745500
H -1.44767700 -1.89263400 3.41332000
C -3.38598400 1.39544800 3.98792600
H -1.57781700 2.42738700 3.52871000
C -4.03423000 0.17478500 4.13368600
H -3.80408300 -1.96681400 4.01447500
H -3.92669000 2.33092300 4.12604100
H -5.09276300 0.13640500 4.37987900

4. Chapter 4

A representative procedure for dirhodium-catalyzed intermolecular C−H amination of calixarene 70.

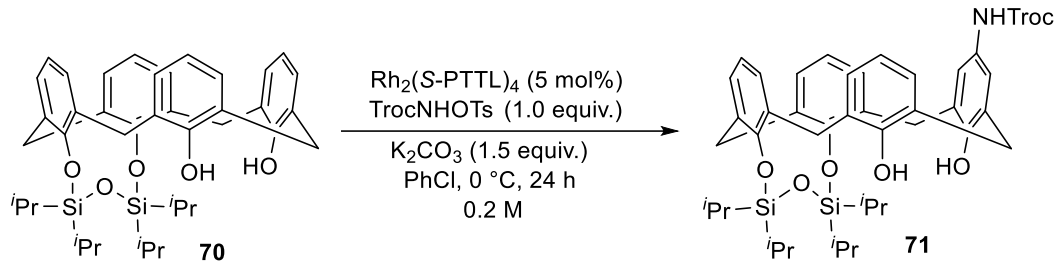

To a suspension of calixarene **70** (20.0 mg, 0.03 mmol, 1.0 equiv.), TrocNHOTs (10.9 mg, 0.03 mmol, 1.0 equiv.), K_2CO_3 (6.2 mg, 0.045 mmol, 1.5 equiv.) in PhCl (0.15 mL) was added Rh_2(*S*-PTTL)$_4$ (1.9 mg, 0.05 equiv.) at 0 °C. After being stirred for 24 h at 0 °C, the reaction was quenched by addition of water and extracted with EtOAc. The organic layer was washed with brine, dried over Na_2SO_4, filtered, and concentrated. The crude material was purified by preparative TLC (EtOAc/hexane = 1/9) to afford **71** (6.6 mg, 26%) as a white solid.

White solid: **m.p.** 145 °C; HPLC condition: CHIRALPAK IB column, eluent hexane: EtOAc = 97: 3, flow rate 1.0 ml/min, T = 20 ℃, retention time: t_{maj} = 11.7 min, t_{min} = 15.0 min. $[\alpha]_D{}^{20}$ = +13.0 (45% ee, *c* 1.0, $CHCl_3$). **^{1}H NMR** (400 M Hz, $CDCl_3$) δ: 8.71 (s, 1H), 8.38 (s, 1H), 7.13 (s, 1H), 7.07−6.98 (m, 7H), 6.74−6.67 (m, 3H), 6.57 (br s, 1H), 4.80−4.75 (m, 3H), 4.62 (d, *J* = 13.2 Hz, 1H), 4.52 (d, *J* = 13.6 Hz, 1H), 4.25 (d, *J* = 13.6 Hz, 1H), 3.46 (d, *J* = 13.6 Hz, 1H), 3.42 (d, *J* = 13.6 Hz, 1H), 3.37 (d, *J* = 13.2 Hz, 1H), 3.31 (d, *J* = 12.8 Hz, 1H), 1.64−1.50 (m, 2H), 1.45−1.39 (m, 12H), 1.23−1.13 (m, 2H), 1.13 (d, *J* = 6.4 Hz, 3H), 1.11 (d, *J* = 7.2 Hz, 3H), 0.80 (d, *J* = 7.6 Hz, 3H), 0.79 (d, *J* = 7.2 Hz, 3H); **^{13}C NMR** (100 M Hz, $CDCl_3$) δ: 151.7, 151.2 149.3, 148.4, 148.0, 132.5, 131.7, 131.6, 131.5, 131.1, 129.9, 129.5, 129.4, 129.3, 129.1, 129.0, 128.9, 128.8, 128.6, 128.3, 123,5, 122.8, 121.1, 119.8, 119.5, 95.5, 74.4, 34.5, 32.3, 31.7, 31.3, 21.2, 18.33, 18.25, 18.0, 17.5, 17.4, 17.0, 16.8, 15.2, 14.7, 13.7, 13.4; **IR** (KBr, cm^{-1}): 3335, 2951, 2865, 1733, 1469, 1258, 1214, 1032, 752, 700; **HRMS-ESI$^+$** (m/z): Calcd. for $C_{43}H_{52}Cl_3NO_7Si_2Na$ $[M+Na]^+$ 878.2240; found, 878.2224.

General Procedure for dirhodium-catalyzed intermolecular C−H amination of calixarene 72.

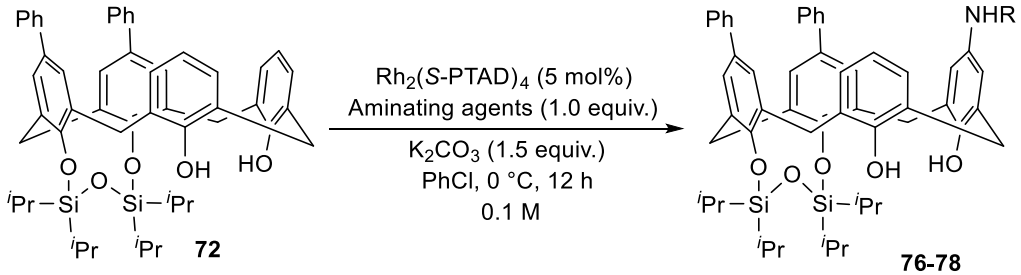

To a mixture of calixarene **72** (0.015 mmol, 1.0 equiv.), TrocNHOTs (5.4 mg, 0.015 mmol, 1.0 equiv.), Rh catalyst (0.05 equiv.) and K_2CO_3 (3.1 mg, 0.0225 mmol, 1.5 equiv.) was added PhCl (0.15 mL) at 0 °C under Argon atmosphere. After being stirred for 12 h at 0 °C, the reaction was quenched by addition

of water and extracted with EtOAc. The organic layer was washed with brine, dried over Na_2SO_4, filtered, and concentrated. The residue was purified by preparative TLC purification to afford the aminated product.

Trichloroethoxy carbamate **76**

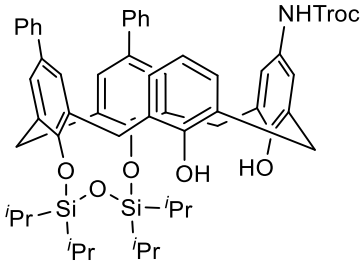

Following general method, calixarene **72** (12.3 mg, 0.015 mmol, 1.0 equiv.), TrocNHOTs (5.4 mg, 0.015 mmol, 1.0 equiv.), K_2CO_3 (3.1 mg, 0.0225 mmol, 1.5 equiv.), and Rh_2(*S*-PTAD)$_4$ (1.2 mg, 0.05 equiv.) were stirred at 0 °C in PhCl (0.15 mL) under Argon for 12 h. After raise up to r.t., water was added and the solution was extracted with EtOAc. The combined organic layer was washed with brine and dried with Na_2SO_4. The crude material was purified by preparative TLC (EtOAc/hexane = 1/9) to afford **76** (4.4 mg, 29%) as a white solid.

White solid: **m.p.** 147 °C; HPLC condition: CHIRALPAK IB column, eluent hexane: EtOAc = 97: 3, flow rate 1.0 ml/min, T = 20 °C, retention time: t_{maj} = 17.3 min, t_{min} = 15.2 min. $[\alpha]_D{}^{20}$ = +9.1 (85% ee, *c* 1.0, $CHCl_3$). **^{1}H NMR** (400 M Hz, $CDCl_3$) δ: 8.76 (s, 1H), 8.44 (s, 1H), 7.44−7.40 (m, 4H), 7.38−7.32 (m, 6H), 7.29−7.20 (m, 4H), 7.13−7.00 (m, 4H), 6.69 (t, *J* = 7.6 Hz, 1H), 6.54 (br s, 1H), 4.83 (d, *J* = 12.4 Hz, 1H), 4.75 (s, 2H), 4.70 (d, *J* = 13.2 Hz, 1H), 4.57 (d, *J* = 13.2 Hz, 1H), 4.28 (d, *J* = 13.2 Hz, 1H), 3.57 (d, *J* = 13.2 Hz, 1H), 3.50 (d, *J* = 13.2 Hz, 1H), 3.40 (d, *J* = 13.2 Hz, 1H), 3.38 (d, *J* = 12.8 Hz, 1H), 1.64−1.50 (m, 2H), 1.48−1.41 (m, 12H), 1.27−1.19 (m, 2H), 1.16 (d, *J* = 5.6 Hz, 3H), 1.14 (d, *J* = 6.0 Hz, 3H), 0.85 (d, *J* = 4.0 Hz, 3H), 0.83 (d, *J* = 4.0 Hz, 3H); **^{13}C NMR** (150 M Hz, $CDCl_3$) δ: 151.8, 151.3, 149.0, 148.23, 148.17, 140.9, 140.6, 136.2, 135.7, 132.8, 132.0, 131.7, 131.4, 131.2, 130.0, 129.5, 129.1, 128.8, 128.7, 128.35, 128.29, 128.26, 127.8, 127.5, 127.1, 127.0, 126.8, 121.3, 120.0, 119.7, 95.5, 74.4, 34.9, 32.4, 32.0, 31.5, 18.4, 18.3, 18.2, 18.0, 17.5, 17.4, 17.1, 16.9, 15.3, 14.8, 13.8, 13.5; **IR** (KBr, cm^{-1}): 3418, 2916, 2873, 1746, 1610, 1458, 1260, 1013, 802, 694; **HRMS-ESI$^+$** (m/z): Calcd. for $C_{55}H_{60}Cl_3NO_7Si_2Na$ $[M+Na]^+$ 1030.2866; found, 1030.2845.

Trifluoroethoxy carbamate **77**

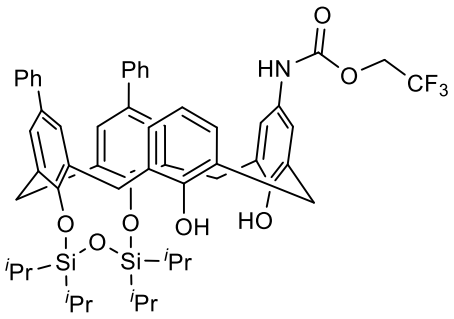

Following general method, calixarene **72** (12.3 mg, 0.015 mmol, 1.0 equiv.), 2,2,2-trifluoroethyl (tosyloxy)carbamate (4.7 mg, 0.015 mmol, 1.0 equiv.), K_2CO_3 (3.1 mg, 0.0225 mmol, 1.5 equiv.), and Rh_2(*S*-PTAD)$_4$ (1.2 mg, 0.05 equiv.) were stirred at 0 °C in PhCl (0.15 mL) under Argon for 12 h. After raise up to r.t., water was added and the solution was extracted with EtOAc. The combined organic layer was washed with brine and dried with Na_2SO_4. The crude material was purified by preparative TLC (EtOAc/hexane = 1/9) to afford **77** (2.9 mg, 20%) as a white solid.

White solid: **m.p.** 155 °C; HPLC condition: COSMOSIL CHiRAL 5A column, eluent hexane: EtOAc = 97: 3, flow rate 1.0 ml/min, T = 20 ℃, retention time: t_{maj} = 13.5 min, t_{min} = 11.5 min. $[\alpha]_D{}^{20}$ = +11.2 (64% ee, *c* 1.0, $CHCl_3$). **^{1}H NMR** (400 M Hz, $CDCl_3$) δ: 8.75 (s, 1H), 8.46 (s, 1H), 7.49−7.22 (m, 13H), 7.11−7.02 (m, 4H), 6.69 (t, *J* = 7.2 Hz, 1H), 6.46 (br s, 1H), 4.83 (d, *J* = 12.4 Hz, 1H), 4.71 (d, *J* = 13.2 Hz, 1H), 4.59 (d, *J* = 12.8 Hz, 1H), 4.47 (q, *J* = 8.4 Hz, 2H), 4.29 (d, *J* = 13.2 Hz, 1H), 3.58 (d, *J* = 13.2 Hz, 1H), 3.51 (d, *J* = 13.2 Hz, 1H), 3.40 (d, *J* = 13.6 Hz, 1H), 3.39 (d, *J* = 12.8 Hz, 1H), 1.69−1.56 (m, 2H), 1.48−1.42 (m, 12H), 1.27−1.19 (m, 2H), 1.17 (d, *J* = 6.4 Hz, 3H), 1.15 (d, *J* = 6.0 Hz, 3H), 0.86 (d, *J* = 4.4 Hz, 3H), 0.84 (d, *J* = 4.0 Hz, 3H); **^{13}C NMR** (150 M Hz, $CDCl_3$) δ: 151.7, 151.3, 149.0, 148.3, 148.2, 140.9, 140.6, 136.2, 135.8, 132.8, 132.0, 131.7, 131.4, 131.2, 129.8, 129.5, 129.1, 128.8, 128.7, 128.34, 128.29, 128.24, 127.8, 127.5, 127.1, 127.0, 126.8, 123.2 (q, *J* = 276 Hz), 121.3, 120.2, 119.9, 60.9 (q, *J* = 37.5 Hz), 34.9, 32.4, 32.0, 31.5, 18.34, 18.29, 18.22, 18.0, 17.5, 17.4, 17.1, 16.9, 15.2, 14.8, 13.8, 13.5; **IR** (KBr, cm^{-1}): 3335, 2944, 2864, 1742, 1463, 1264, 1172, 1013, 758, 694; **HRMS-ESI**$^+$ (m/z): Calcd. for $C_{55}H_{60}F_3NO_7Si_2Na$ $[M+Na]^+$ 982.3753; found, 982.3737.

Tribromoethoxy carbamate **78**

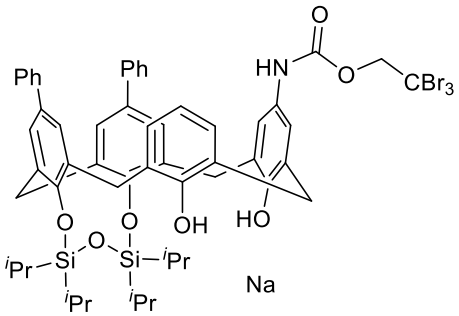

Following general method, calixarene **72** (12.3 mg, 0.015 mmol, 1.0 equiv.), 2,2,2-tribromoethyl (tosyloxy)carbamate (7.4 mg, 0.015 mmol, 1.0 equiv.), K_2CO_3 (3.1 mg, 0.0225 mmol, 1.5 equiv.), and

Rh_2(*S*-PTAD)$_4$ (1.2 mg, 0.05 equiv.) were stirred at 0 °C in PhCl (0.15 mL) under Argon for 12 h. After raise up to r.t., water was added and the solution was extracted with EtOAc. The combined organic layer was washed with brine and dried with Na_2SO_4. The crude material was purified by preparative TLC (EtOAc/hexane = 1/9) to afford **78** (5.3 mg, 31%) as a white solid.

White solid: **m.p.** 159 °C; HPLC condition: COSMOSIL CHiRAL 5A column, eluent hexane: EtOAc = 97: 3, flow rate 1.0 ml/min, T = 20 °C, retention time: t_{maj} = 22.4 min, t_{min} = 17.9 min. $[\alpha]_D^{20}$ = +16.6 (86% ee, *c* 1.0, $CHCl_3$). **^{1}H NMR** (400 M Hz, $CDCl_3$) δ: 8.77 (s, 1H), 8.44 (s, 1H), 7.45−7.22 (m, 13H), 7.15−7.03 (m, 4H), 6.69 (t, *J* = 7.6 Hz, 1H), 6.58 (br s, 1H), 4.93 (d, *J* = 2.4 Hz, 2H), 4.84 (d, *J* = 12.4 Hz, 1H), 4.71 (d, *J* = 13.2 Hz, 1H), 4.57 (d, *J* = 13.2 Hz, 1H), 4.29 (d, *J* = 13.6 Hz, 1H), 3.57 (d, *J* = 12.8 Hz, 1H), 3.50 (d, *J* = 12.8 Hz, 1H), 3.41 (d, *J* = 13.6 Hz, 1H), 3.39 (d, *J* = 12.4 Hz, 1H), 1.67−1.50 (m, 2H), 1.48−1.41 (m, 12H), 1.31−1.19 (m, 2H), 1.16 (d, *J* = 5.6 Hz, 3H), 1.15 (d, *J* = 6.0 Hz, 3H), 0.85 (d, *J* = 4.0 Hz, 3H), 0.83(d, *J* = 4.4 Hz, 3H), **^{13}C NMR** (150 M Hz, $CDCl_3$) δ: 151.6, 151.3, 149.0, 148.2, 148.1, 140.9, 140.6, 136.2, 135.7, 132.8, 132.0, 131.7, 131.4, 131,2, 130.1, 129.9, 129.5, 129.1, 128.75, 128.69, 128.4, 128.30, 128.27, 127.8, 127.5, 127.1, 127.0, 126.9, 121.3, 119.9, 119.6, 68.1, 37.2, 34.9, 32.4, 32.0, 31.5, 18.4, 18.29, 18.25, 18.0, 17.5, 17.4, 17.1, 16.9, 15.3, 14.8, 13.8, 13.4; **IR** (KBr, cm^{-1}): 3386, 2940, 2864, 1738, 1467, 1256, 1024, 750, 699, 523; **HRMS-ESI$^+$** (m/z): Calcd. for $C_{55}H_{60}{}^{79}Br^{81}Br_2NO_7Si_2Na$ $[M+Na]^+$ 1164.1336; found, 1164.1344.

HPLC chart

Racemic **71**

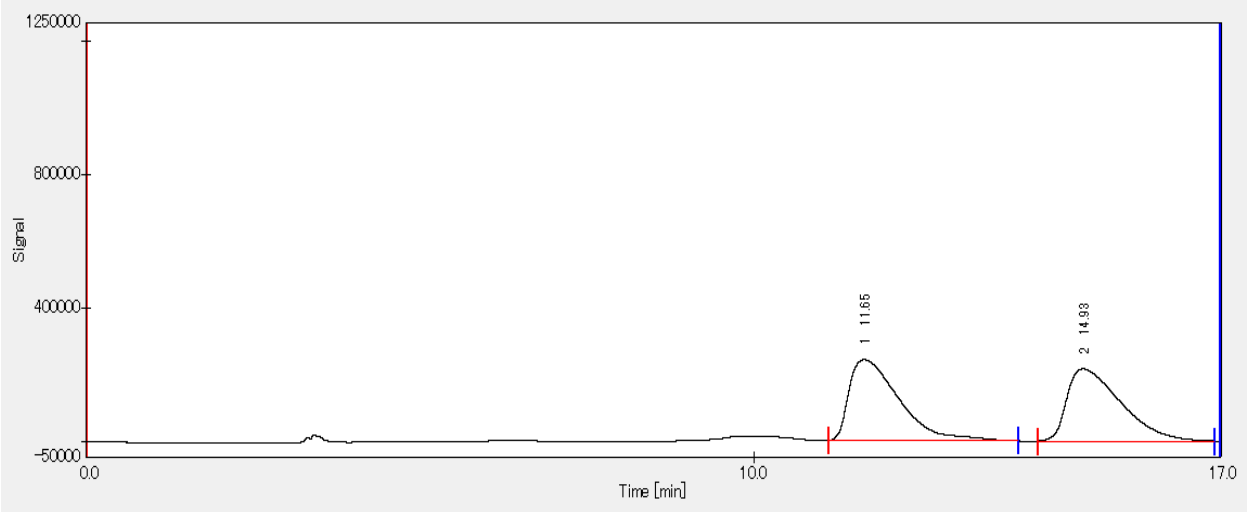

No	Rt (min)	Area	Area (%)
1	11.65	12251221	50.2
2	14.93	12132207	49.7

Chiral **71**

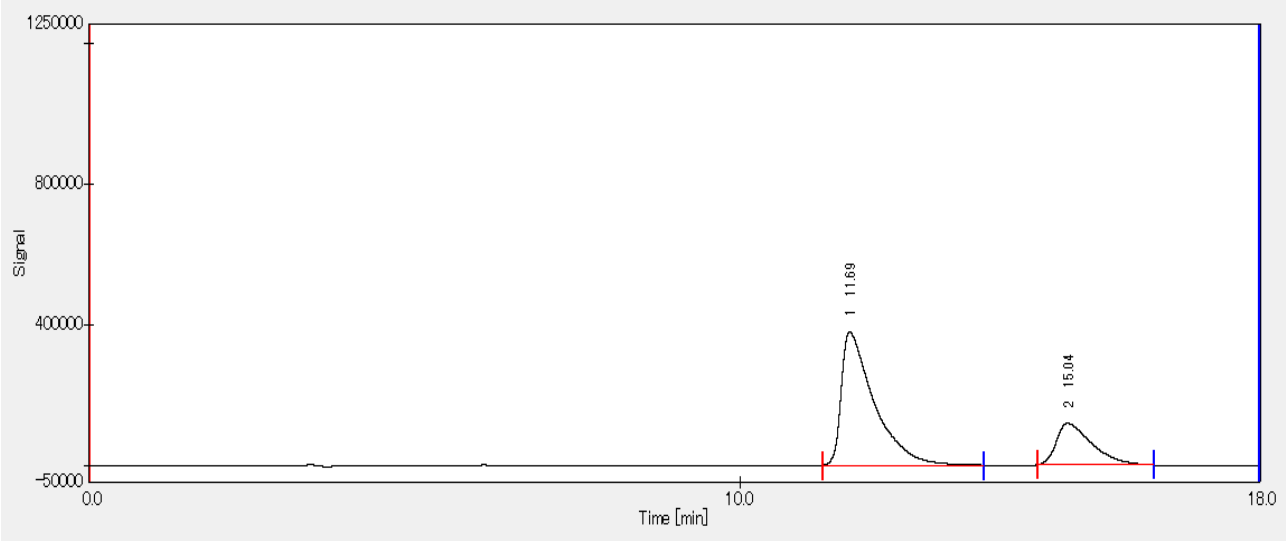

No	Rt (min)	Area	Area (%)
1	11.69	13241622	74.9
2	15.04	4443984	25.1

Racemic **76**

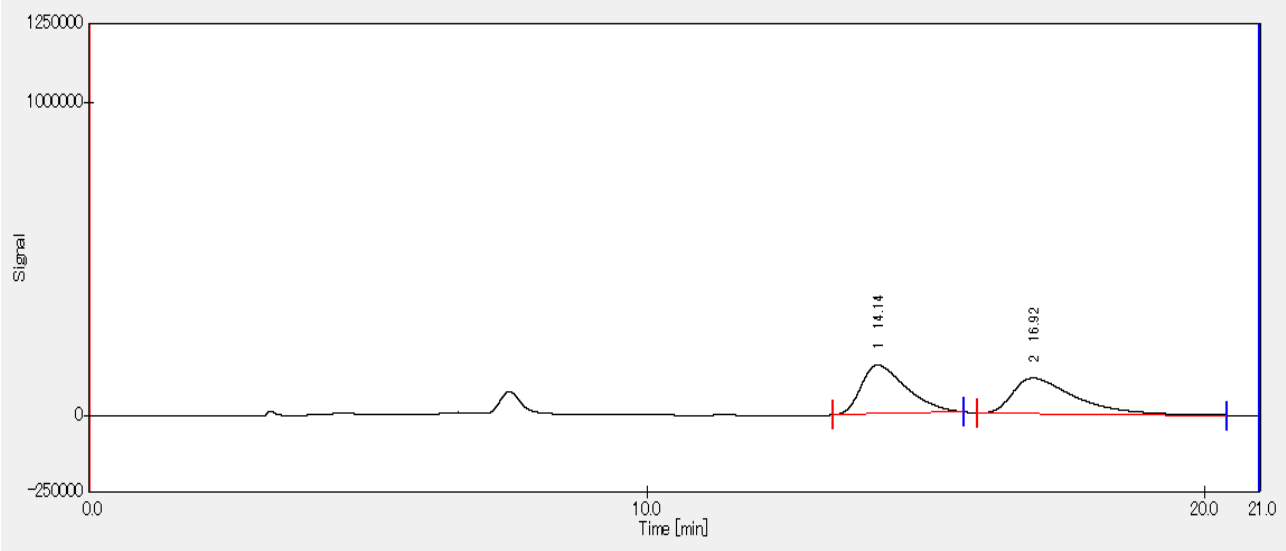

No	Rt (min)	Area	Area (%)
1	14.14	8845905	50.3
2	16.92	8716296	49.6

Chiral **76**

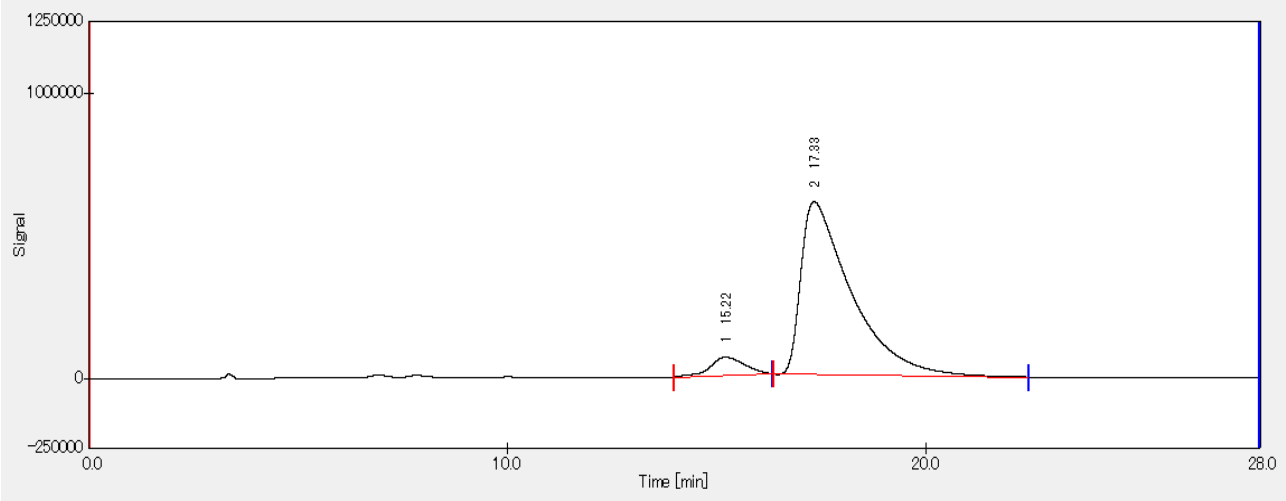

No	Rt (min)	Area	Area (%)
1	15.22	3631699	6.6
2	17.33	51024399	93.4

Racemic **77**

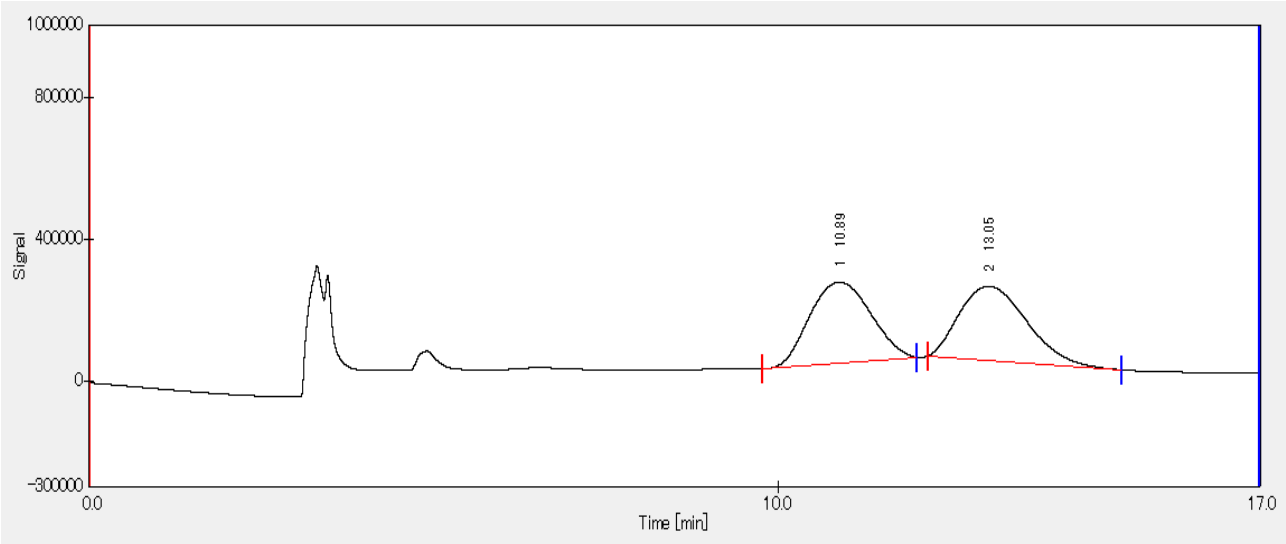

No	Rt (min)	Area	Area (%)
1	10.89	14053809	49.7
2	13.05	14202414	50.3

Chiral **77**

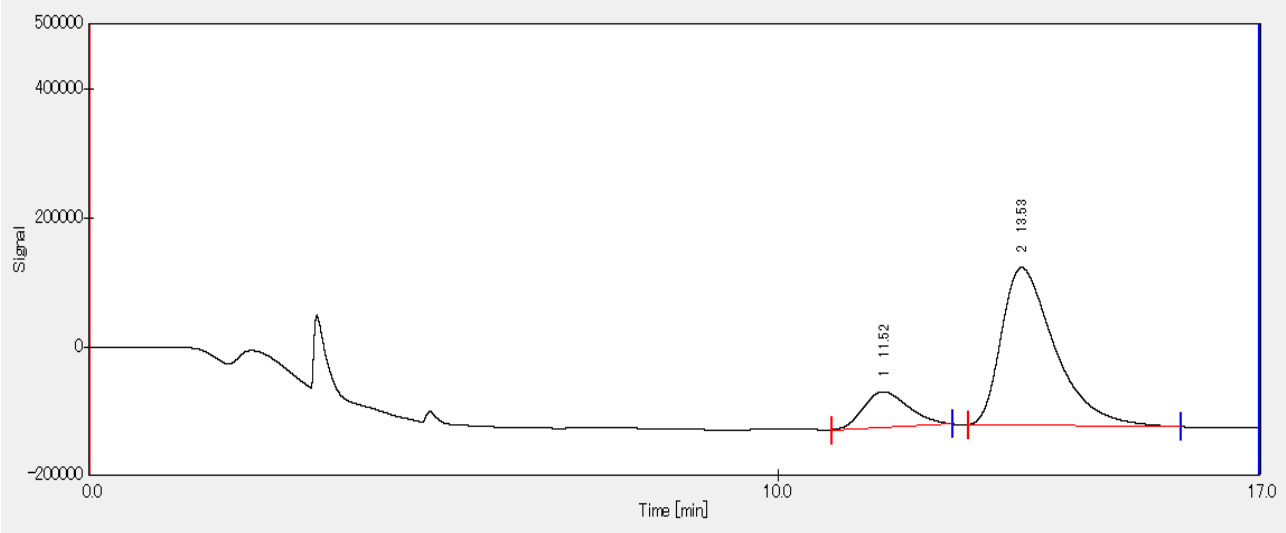

No	Rt (min)	Area	Area (%)
1	11.52	2514013	16.0
2	13.53	13183281	84.0

Racemic **78**

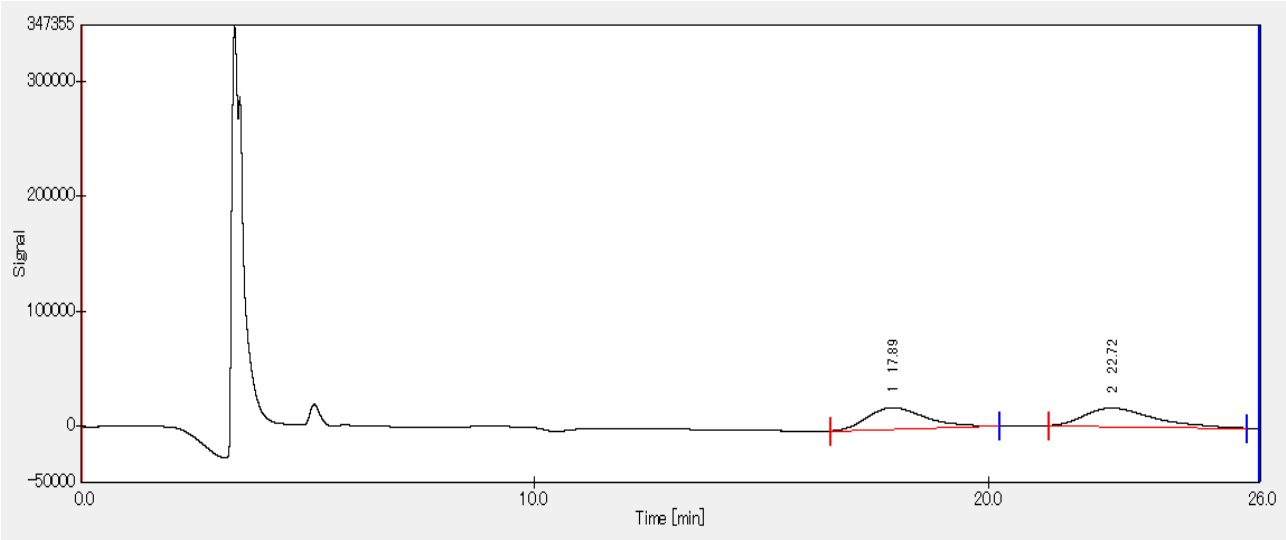

No	Rt (min)	Area	Area (%)
1	17.89	1662654	50.0
2	22.72	1664165	50.0

Chiral **78**

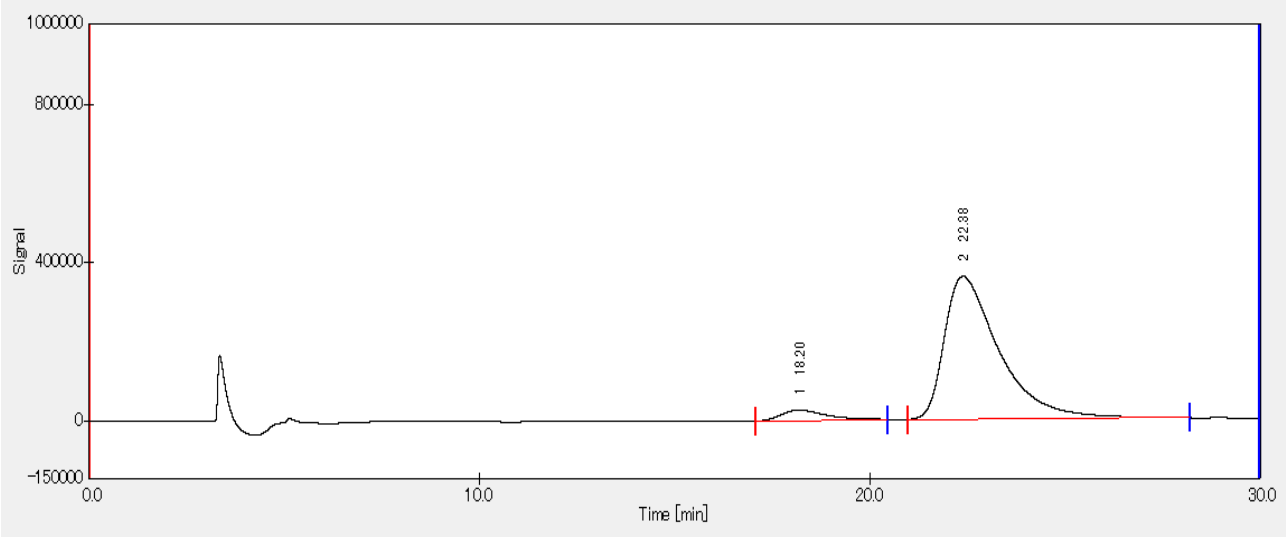

No	Rt (min)	Area	Area (%)
1	18.20	2168413	5.8
2	22.38	35302888	94.2

Synthesis of 68

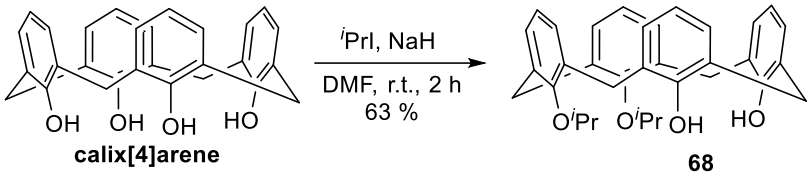

25,26-dihydroxy-27,28-diisopropoxycalix[4]arene (**68**).

To a solution of calix[4]arene (1.06 g, 2.5 mmol, 1.0 equiv.) in DMF (10 mL) was added NaH (60% in mineral oil, 0.36 g, 9.0 mmol, 3.6 equiv.) at r.t.. After stirring for 15 min, ^{i}PrI (0.53 mL, 5.38 mmol, 2.15 equiv.) was added to the mixture slowly. 2 h later, the reaction was quenched with 1M HCl, and extracted with EtOAc. The combined organic layer was washed with brine, dried over Na_2SO_4, filtered, and concentrated to get the crude product. Recrystallization of the crude product by dichloromethane and methanol gave the product **68** as a white solid (650 mg, 51%).

White solid: **m.p.** 244 °C; **^{1}H NMR** (400 M Hz, $CDCl_3$) δ: 9.11 (s, 2H), 7.04−6.94 (m, 8H), 6.75 (t, *J* = 7.6 Hz, 2H), 6.62 (t, *J* = 7.2 Hz, 2H), 4.69 (d, *J* = 12.4 Hz, 1H), 4.39−4.30 (sep, 2H), 4.33 (d, *J* = 13.6 Hz, 2H), 4.31 (d, *J* = 14.0 Hz, 1H), 3.39 (d, *J* = 13.2 Hz, 2H), 3.38 (d, *J* = 12.4 Hz, 1H), 3.36 (d, *J* = 13.2 Hz, 1H), 1.59 (d, *J* = 5.6 Hz, 6H), 1.53 (d, *J* = 6.0 Hz, 6H); **^{13}C NMR** (100 M Hz, $CDCl_3$) δ: 151.7, 151.4, 135.2, 134.9, 129.6, 129.1, 128.82, 128.78, 128.7, 128.1, 124.3, 120.5, 78.3, 32.5, 31.8, 30.7, 22.4, 22.2; **IR** (KBr, cm^{-1}): 3328, 2971, 2932, 1590, 1448, 1373, 1096, 917, 750; **HRMS-ESI^{+}** (m/z): Calcd. for $C_{34}H_{36}O_4Na$ $[M+Na]^+$ 531.2506; found, 531.2499.

Synthesis of 70

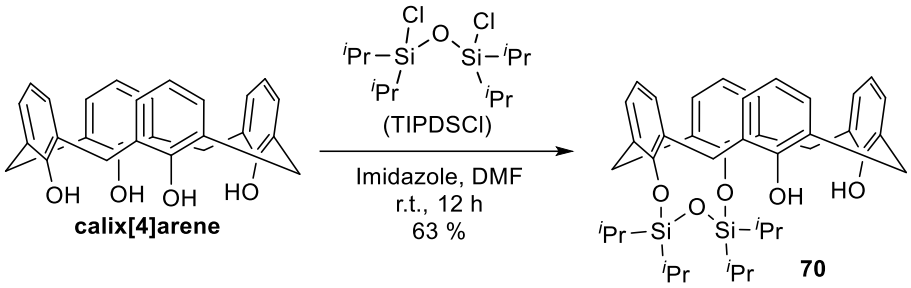

To a solution of calix[4]arene (212 mg, 0.5 mmol, 1.0 equiv.) in anhydrous DMF (5 mL) was added imidazole (102 mg, 1.5 mmol, 3.0 equiv.) and stirred for 30 min at r.t.. Then a solution of 1,3-dichloro-1,1,3,3-tetraisopropyldisiloxane (TIPDSCl) (187 μL, 0.6 mmol, 1.2 equiv.) in DMF (2.5 mL) was added dropwise to the solution. After stirred overnight, the mixture was cooled to 0°C and added 2M HCl. The precipitate was filtered and washed with water. The product was recrystallized from dichloromethane and methanol and dried to get **70** as a white powder (210 mg, 63%).

25,26-dihodroxy-27,28-(1,1,3,3-tetraisopropyldisiloxane-1,3-diyl)-calix[4]arene (**70**).

White solid: **m.p.** 258 °C; **^{1}H NMR** (400 M Hz, $CDCl_3$) δ: 8.70 (s, 2H), 7.10−7.02 (m, 8H), 6.76 (t, *J* = 7.2 Hz, 2H), 6.71 (t, *J* = 7.2 Hz, 2H), 4.70 (d, *J* = 12.8 Hz, 2H), 4.67 (d, *J* = 13.2 Hz, 1H), 4.30 (d, *J* = 14.0 Hz, 1H), 3.51 (d, *J* = 13.2 Hz, 1H), 3.46 (d, *J* = 12.8 Hz, 1H), 3.42 (d, *J* = 12.8 Hz, 2H), 1.63 (sep, 2H), 1.47 (t, *J* = 7.6 Hz, 12H), 1.25 (sep, 2H), 1.17 (d, *J* = 7.2 Hz, 6H), 0.85 (d, *J* = 7.6 Hz, 6H); **^{13}C NMR** (100 M Hz, $CDCl_3$) δ: 151.2, 148.8, 132.3, 131.2, 129.9, 129.4, 128.9, 128.8, 128.7, 128.3, 123.1, 121.2, 34.5, 32.3, 31.5, 18.3, 18.1, 17.4, 16.9, 15.0, 13.6; **IR** (KBr, cm^{-1}): 3322, 2952, 2864, 1463, 1260, 1021, 893, 754; **HRMS-ESI$^+$** (m/z): Calcd. for $C_{40}H_{50}O_5Si_2Na$ $[M+Na]^+$ 689.3089; found, 689.3096.

Synthesis of 72

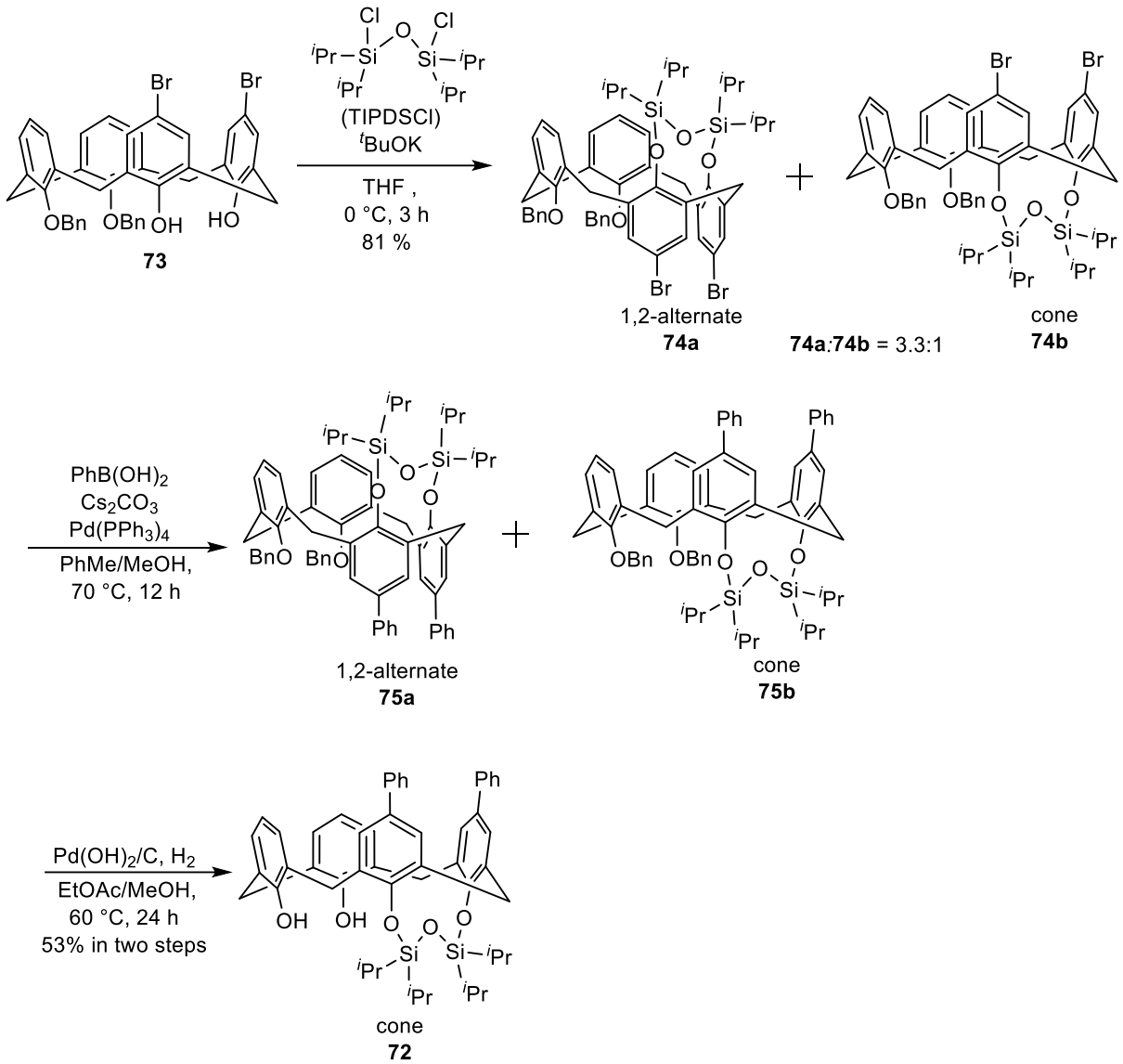

To a solution of **73** (800 mg, 1.05 mmol, 1.0 equiv.) in THF (21 mL) was added *t*-BuOK (354 mg, 3.15 mmol, 3.0 equiv.) under an atmosphere of Argon at 0 ℃. 20 min later, 1,3-dichloro-1,1,3,3-tetraisopropyldisiloxane (TIPDSCl) (657 μL, 2.1 mmol, 2.0 equiv.) was added dropwise to the solution. After being stirring at 0 °C for 2 h, the reaction was quenched by addition of water and extracted with EtOAc. The organic layer was washed with brine, dried over Na_2SO_4, filtered, and concentrated to get the crude product. The combined NMR yield was 81% (with 1,1,2,2-tetrachloroethane as an internal standard). The ratio of **74a**:**74b** is 3.3:1. The crude product was purified by flash column (DCM/hexane = 1/6) to get a mixture of **74a** and **74b** (730 mg, 70% yield) as a white solid. To analyze the conformation, **74a** and **74b** were separated by recycle HPLC (EtOAc/hexane = 1/9).

1,2-alternate-5,11-Dibromo-25,26-dibenzyloxy-27,28-(1,1,3,3-tetraisopropyldisiloxane-1,3-diyl) calix[4]arene (**74a**).

White solid: **m.p.** 235 °C; **^{1}H NMR** (400 M Hz, $CDCl_3$) δ: 7.25−7.23 (m, 2H), 7.19−7.09 (m, 8H), 7.01 (d, *J* = 7.2 Hz, 2H), 6.89−6.84 (m, 4H), 6.49 (d, *J* = 8.0 Hz, 4H), 4.35 (d, *J* = 13.6 Hz, 1H), 4.28 (s, 4H), 3.88 (d, *J* = 12.8 Hz, 2H), 3.78 (d, *J* = 12.4 Hz, 1H), 3.67 (d, *J* = 12.4 Hz, 1H), 3.24 (d, *J* = 13.2 Hz, 1H), 2.78 (d, *J* = 12.8 Hz, 1H), 1.06−0.93 (m, 14H), 0.82−0.73 (m, 2H), 0.73 (d, *J* = 6.0 Hz, 6H), 0.34 (d, *J* = 7.6 Hz, 6H); **^{13}C NMR** (100 M Hz, $CDCl_3$) δ: 155.6, 151.4, 137.1, 135.5, 133.7, 132.5, 131.9, 131.5, 131.1, 129.2, 129.0, 128.0, 127.3, 127.2, 123.2, 113.1, 75.1, 38.5, 32.8, 28.9, 17.8, 17.3, 16.9, 16.8, 14.0, 13.9; **IR** (KBr, cm^{-1}): 2994, 2864, 1458, 1264, 1221, 1034, 936, 828, 760, 696; **HRMS-ESI^{+}** (m/z): Calcd. for $C_{54}H_{64}{}^{79}Br^{81}BrNO_5Si_2$ $[M+NH_4]^+$ 1022.2672; found, 1022.2672.

cone-5,11-Dibromo-25,26-dibenzyloxy-27,28-(1,1,3,3-tetraisopropyldisiloxane-1,3-diyl) calix[4]arene (**74b**).

White solid: **m.p.** 254 °C; **^{1}H NMR** (400 M Hz, $CDCl_3$) δ: 7.33−7.23 (m, 6H), 7.15−7.12 (m, 4H), 6.79−6.75 (m, 4H), 6.67−6.59 (m, 4H), 6.52 (dd, *J* = 6.8 Hz and 2.0 Hz, 2H), 4.95 (d, *J* = 11.6 Hz, 2H), 4.82 (d, *J* = 11.6 Hz, 2H), 4.32 (d, *J* = 13.6 Hz, 1H), 3.65 (d, *J* = 13.2 Hz, 1H), 3.12 (d, *J* = 13.6 Hz, 1H), 2.98 (d, *J* = 13.2 Hz, 2H), 2.56 (d, *J* = 13.2 Hz, 1H), 1.53−1.45 (m, 2H), 1.32 (d, *J* = 7.2 Hz, 6H), 1.25 (d, *J* = 8.0 Hz, 6H), 1.13−1.03 (m, 2H), 1.04 (d, *J* = 6.0 Hz, 6H), 0.83 (d, *J* = 6.8 Hz, 6H); **^{13}C NMR** (100 M Hz, $CDCl_3$) δ: 154.3, 150.2 137.0, 136.2, 135.3, 134.0, 132.0, 131.6, 130.5, 130.4, 128.5, 128.3, 128.2, 128.0, 122.9, 112.6, 76.6, 34.0, 31.3, 29.9, 18.2, 18.1, 17.8, 17.4, 16.0, 14.4; **IR** (KBr, cm^{-1}): 2944, 2866, 1458, 1300, 1239, 1211, 1083, 943, 821, 761, 698; **HRMS-ESI^{+}** (m/z): Calcd. for $C_{54}H_{64}{}^{79}Br^{81}BrNO_5Si_2$ $[M+NH_4]^+$ 1022.2672; found, 1022.2694.

The ratios of **74a** and **74b** were determined by comparison of the integration of the both signals in crude ^{1}H NMR spectra as shown below.

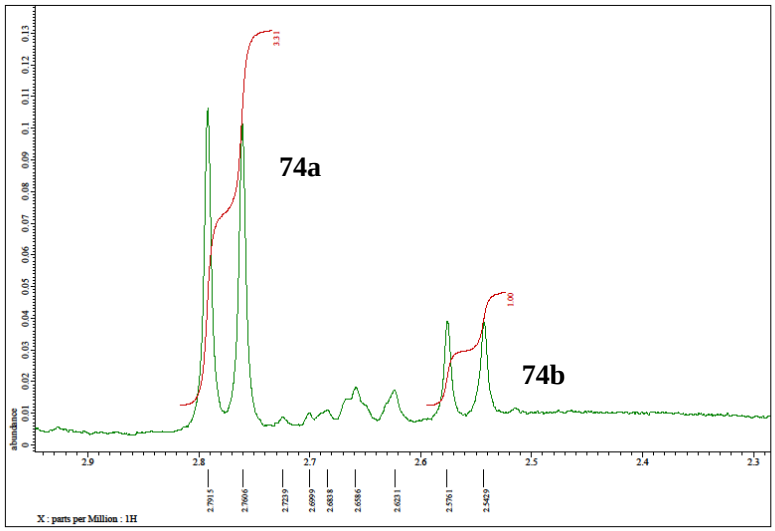

cone-5,11-Diphenyl-25,26-dihydroxy-27,28-(1,1,3,3-tetraisopropyldisiloxane-1,3-diyl)-calix[4]arene (**72**)

To a mixture of **74a** and **74b** (300 mg, 0.3 mmol, 1.0 equiv.), phenylboronic acid (183 mg, 1.5 mmol, 5.0 equiv.), Cs_2CO_3 (543 mg, 1.5 mmol, 5.0 equiv.) was added toluene (3 mL) and MeOH (3 mL), then Argon blowing for 30 minutes. After that, $Pd(PPh_3)_4$ (63 mg, 0.06 mmol, 0.2 equiv.) was added to the solution. The yellow solution was stirring at 70 ℃ for 12 h. After cooling to r.t., the solution was filtrated by Celite, add water and extracted with EtOAc. The combined organic layer was washed with brine and dried with Na_2SO_4. After removal of solvent, the crude material was purified by flash column (EtOAc/hexane = 1/15) to afford a mixture of **75a** and **75b** and their mono phenyl ring byproducts. To a solution of the mixture in EtOAc/MeOH (15 mL) was added 10 % palladium hydroxyl on carbon (150 mg). The mixture was stirred at 60 ℃ under a hydrogen atmosphere (1 atm) for 24 h. After filtration and evaporation of the solvent, the residue was first purified by flash column (EtOAc/hexane = 1/9) to get a mixture of the desired product and its mono phenyl ring side-product. They were further separated by recycle HPLC (EtOAc/hexane = 1/9) to get pure **72** (130 mg, 53% yield in 2 steps) as a white powder. White solid: m.p. 146 °C; **^{1}H NMR** (400 M Hz, $CDCl_3$) δ: 8.69 (s, 2H), 7.43−7.40 (m, 4H), 7.34 (t, *J* = 7.6 Hz, 4H), 7.29−7.22 (m, 6H), 7.08 (d, *J* = 7.6 Hz, 2H), 6.99 (d, *J* = 6.4 Hz, 2H), 6.66 (t, *J* = 7.2 Hz, 2H), 4.71 (d, *J* = 13.2 Hz, 3H), 4.28 (d, *J* = 13.6 Hz, 1H), 3.57 (d, *J* = 13.6 Hz ,1H), 3.45 (d, *J* = 12.8 Hz, 2H), 3.43 (d, *J* = 13.6 Hz, 1H), 1.65−1.53 (m, 2H), 1.49−1.42 (m, 12H), 1.27−1.22 (m, 2H), 1.15 (d, *J* = 7.6 Hz, 6H), 0.84 (d, *J* = 7.2 Hz, 6H); **^{13}C NMR** (100 M Hz, $CDCl_3$) δ: 151.3, 148.6, 140.8, 135.9, 132.6, 131.4, 129.8, 129.7, 129.0, 128.7, 128.6, 128.4, 128.3, 127.6, 127.0, 126.8, 126.6, 121.2, 34.9, 32.3, 31.8, 18.3, 18.1, 17.5, 17.0, 15.0, 13.6; **IR** (KBr, cm^{-1}): 3358, 2948, 2873, 1471, 1256, 1079, 1021, 942, 860, 837; **HRMS-ESI$^+$** (m/z): Calcd. for $C_{52}H_{58}O_5Si_2Na$ $[M+Na]^+$ 841.3715; found, 841.3715.

References

1. (a) Henkel, T.; Brunne, R. M.; Müller, H.; Reichel, F. *Angew. Chem., Int. Ed.* **1999**, *38*, 643. (b) Feher, M.; Schmidt, J. M. *J. Chem. Inf. Comput. Sci.* **2003**, *43*, 218. (c) Hili, R.; Yudin, A. K. *Nat. Chem. Biol.* **2006**, *6*, 284.
2. (a) Hartwig, J. F. *Acc. Chem. Res.* **2008**, *41*, 1534. (b) Surry, D. S.; Buchwald, S. L. *Angew. Chem., Int. Ed.* **2008**, *47*, 6338. (c) Bariwal, J.; Van der Eycken, E. *Chem. Soc. Rev.* **2013**, *42*, 9283. (d) Ricci, A. *Amino Group Chemistry: From Synthesis to the Life Sciences*; Wiley-VCH: Weinheim, 2008.
3. (a) Godula, K.; Sames, D. *Science* **2006**, *312*, 67. (b) Zalatan, D. N.; Du Bois, J. *Top. Curr. Chem.* **2010**, *292*, 347. (c) Dequirez, G.; Pons, V.; Dauban, P. *Angew. Chem., Int. Ed.* **2012**, *51*, 7384. (d) Jiao, J.; Murakami, K.; Itami, K. *ACS Catal.* **2016**, *6*, 610. (e) Hazelard, D.; Nocquet, P. A.; Campain, P. *Org. Chem. Front.* **2017**, *4*, 2500. (f) Park, Y.; Kim, Y.; Chang, S. *Chem. Rev.* **2017**, *117*, 9247.
4. For selected pioneering examples, see: (a) Breslow, R.; Gellman, S. H. *J. Am. Chem. Soc.* **1983**, *105*, 6728. (b) Espino, C. G.; Du Bois, J. *Angew. Chem., Int. Ed.* **2001**, *40*, 598. (c) Yamawaki, M.; Tsutsui, H.; Kitagaki, S.; Anada, M.; Hashimoto, S. *Tetrahedron Lett.* **2002**, *43*, 9561. (d) Espino, C. G.; Fiori, K. W.; Kim, M.; Du Bois, J. *J. Am. Chem. Soc.* **2004**, *126*, 15378. (e) Lebel, H.; Huard, K.; Lectard, S. *J. Am. Chem. Soc.* **2005**, *127*, 14198. (f) Reddy, R. P.; Davies, H. M. L. *Org. Lett.* **2006**, *8*, 5013.
5. For reviews, see: (a) Davies, H. M. L.; Manning, J. R. *Nature* **2008**, *451*, 417. (b) Du Bois, J. *Org. Process Res. Dev.* **2011**, *15*, 758. (c) Collet, F.; Lescot, C.; Dauban, P. *Chem. Soc. Rev*. **2011**, *40*, 1926.
6. Hartwig, J. F.; Larsen, M. A. *ACS Cent. Sci.* **2016**, *2*, 281.
7. Nägeli, I.; Baud, C.; Bernardinelli, G.; Jacquier, Y.; Moran, M.; Müller, P. *Helv. Chim. Acta*, **1997**, *80*, 1087.
8. Ninomiya, R.; Arai, K.; Chen, G.; Morisaki, K.; Kawabata, T.; Ueda, Y. *Chem. Commun.* **2020**, *56*, 5759.
9. (a) Stokes, B. J.; Dong, H.-J; Leslie, B. E.; Pumphrey, A. L.; Driver, T. G. *J. Am. Chem. Soc.* **2007**, *129*, 7500. (b) Kong, C.; Jana, N.; Jones, C.; Driver, T. G. *J. Am. Chem. Soc.* **2016**, *138*, 13271. (c) Singh, R.; Nagesh, K.; Parameshwar, M. *ACS Catal.* **2016**, *6*, 6520.
10. Tanaka, M.; Kurosaki, Y.; Washio, T.; Anada, M.; Hashimoto, S. *Tetrahedron Lett.* **2007**, *48*, 8799.
11. Paudyal, M. P.; Adebesin, A. M.; Burt, S. R.; Ess, D. H.; Ma, Z.; Kürti, L.; Falck, J. R. *Science* **2016**, *353*, 6304.
12. Arai, K.; Ueda, Y.; Morisaki, K.; Furuta, T.; Sasamori, T.; Tokitoh, N.; Kawabata, T. *Chem. Commun*. **2018**, *54*, 2264.
13. (a) Lebel, H.; Huard, K. *Org. Lett.* **2007**, *9*, 639. (b) Huard, K.; Lebel, H. *Chem. Eur. J.* **2008**, *14*, 6222.

14. Chen, G.; Arai, K.; Morisaki, K.; Kawabata, T.; Ueda, Y. *Synlett.* DOI: 10.1055/a-1334-6450.
15. (a) Quintas-Cardama, A.; Kantarjian, H.; Cortes, J. *Nat. Rev. Drug Discov.* **2007**, *6*, 834. (b) Shirota, Y.; Kageyama, H. *Chem. Rev.* **2007**, *107*, 953.
16. (a) Li, C.-J. *Acc. Chem. Res.* **2009**, *42*, 335. (b) Girard, S. A.; Knauber, T.; Li, C.-J. *Angew. Chem., Int. Ed.* **2014**, *53*, 74.
17. C(sp^3)-H amidation by Cu catalysis: (a) Zhang, Y.; Fu, H.; Jiang, Y.; Zhao, Y. *Org. Lett.* **2007**, *9*, 3813. (b) Sengoden, M.; Bhowmick, A.; Punniyamurthy, T. *Org. Lett*. **2017**, *19*, 158. (c) Singh, S. K.; Chandna, N.; Jain, N. *Org. Lett.* **2017**, *19*, 1322. (d) Lin, B.; Shi, S.; Cui, Y.; Liu, Y.; Tang, G.; Zhao, Y. *Org. Chem. Front.* **2018**, *5*, 2860.
18. C(sp^3)–H amidation by Fe catalysis: (a) Rao Volla, C. M.; Vogel, P. *Org. Lett.* **2009**, *11*, 1701. (b) Zhu, F.; Lu, B.; Sun, H.-M.; Shen, Q. *Tetrahedron Lett.* **2016**, *57*, 4152. (c) Wusiman, A.; Hudabaierdi, R. *Tetrahedron Lett.* **2019**, *60*, 681.
19. C(sp^3)–H amidation under transition-metal-free conditions: (a) Lao, Z.-Q.; Zhong, W.-H.; Lou, Q.-H.; Li, Z.-J.; Meng, X.-B. *Org. Biomol. Chem.* **2012**, *10*, 7869. (b) Zheng, Y.; Mao, J.; Chen, J.; Rong, G.; Liu, D.; Yan, H.; Chi, Y.; Xu, X. *RSC Adv.* **2015**, *5*, 50113. (c) Satheesh, V.; Sengoden, M.; Punniyamurthy, T. *J. Org. Chem.* **2016**, *81*, 9792.
20. C(sp^3)–H amidation with hypervalent iodine reagents or *N*–haloimide reagents: (a) Kiyokawa, K.; Kosaka, T.; Kojima, T.; Minakata, S. *Angew. Chem., Int. Ed.* **2015**, *54*, 13719. (b) Xu, X.-J.; Amuti, A.; Wuisman, A. *Adv. Synth. Catal.* **2020**, *362*, 5002.
21. Cu-nitrene-mediated C(sp^3)–H amidation of *N*-methylaniline derivatives has been reported, see: (a) Liu, X.-W.; Zhang, Y.-M.; Wang, L.; Fu, H.; Jiang, Y.-Y.; Zhao, Y.-F. *J. Org. Chem.* **2008**, *73*, 6207. (b) Bagchi, V.; Paraskevopoulou, P.; Das, P.; Chi, L.-Y.; Wang, Q.-W.; Choudhury, A.; Mathieson, J. S.; Cronin, L.; Pardue, D. B.; Cundari, T. R.; Mitrikas, G.; Sanakis, Y.; Stavropoulos, P. *J. Am. Chem. Soc.* **2014**, *136*, 11362.
22. Ito, M.; Nakagawa, T.; Higuchi, K.; Sugiyama, S. *Org. Biomol. Chem.* **2018**, *16*, 6876.
23. Tamura, Y.; Ikeda, H.; Morita, I.; Tsubouchi, H.; Ikeda, M. *Chem. Pharm. Bull.* **1982**, *30*, 1221.
24. Lwowski, W.; Maricich, T. J. *J. Am. Chem. Soc.* **1965**, *87*, 3630.
25. Azek, E.; Khalifa, M.; Bartholoméüs, J.; Ernzerhof, M.; Lebel, H. *Chem. Sci.* **2019**, *10*, 718.
26. (a) Lebel, H.; Trudel, C.; Spitz, C. *Chem. Commun.* **2012**, *48*, 7799. (b) Lebel, H.; Laparra, L. M.; Khalifa, M.; Trudel, C.; Audubert, C.; Szponarski, M.; Leduc, C. D.; Azek, E.; Ernzerhof, M. *Org. Biomol. Chem.* **2017**, *15*, 4144.
27. Thavaneswaran, S.; McCamley, K.; Scammells, P. J. *Nat. Prod. Commun.* **2006**, *1*, 885.
28. Jung, H.; Schrader, M.; Kim, D.; Baik, M.-Y.; Park, Y.; Chang, S. *J. Am. Chem. Soc.* **2019**, *141*, 15356.
29. Yonezawa, N.; Hino, T.; Matsuda, K.; Matsuki, T.; Narushima, D.; Kobayashi, M.; Ikeda, T. *J. Org. Chem.* **2000**, *65*, 94.
30. (a) Ikeda, A.; Shinkai, S. *Chem. Rev.* **1997**, *97*, 1713. (b) Dondoni, A.; Marra, A. *Chem. Rev.* **2010**, *110*, 4949. (c) Szumna, A. *Chem. Soc. Rev.* **2010**, *39*, 4274. (d) Nimse, S. B.; Kim, T. *Chem. Soc.*

Rev. **2013**, *42*, 366. (e) Lavendomme, R.; Zahim, S.; Leener, D. G.; Inthasot, A.; Mattiuzzi, A.; Luhmer, M.; Reinaud, O.; Jabin, I. *Asian J. Org. Chem.* **2015**, *4*, 710.

31. (a) Böhmer, V.; Kraft, D.; Tabatabai, *J. Incl. Phenom. Macro. Chem.* **1994**, *19*, 17. (b) Cort, A. D.; Mandolini, L.; Pasquini, C.; Schiaffino, L. *New J. Chem.* **2004**, *28*, 1198.
32. Iwamoto, K.; Yanagi, A.; Arimura, T.; Matsuda, T.; Shinkai, S. *Chem. Lett.* **1990**, *19*, 1901.
33. (a) Li, S.-Y.; Xu, Y.-W.; Liu, J.-M.; Su, C.-Y. *Int. J. Mol. Sci.* **2011**, *12*, 429. (b) Arnott, G. E. *Chem. Eur. J.* **2018**, *24*, 1744.
34. Herbert, S. A.; Arnott, G. E. *Org. Lett*. **2009**, *11*, 4986.
35. Browne, J. K.; McKervey, M. A.; Pitarch, M.; Russell, J. A. *Tetrahedron Lett.* **1998**, *39*, 1787.
36. Narumi, F.; Morohashi, N.; Matsumura, N.; Iki, N.; Kameyama, H.; Miyano, S. *Tetrahedron Lett.* **2002**, *43*, 621.
37. Shimizu, S.; Moriyama, A.; Kito, K.; Sasaki, Y. *J. Org. Chem.* **2003**, *68*, 2187.
38. Narumi, F.; Hattori, T.; Morohashi, N.; Matsumura, N.; Yamabuki, W.; Kameyama, H.; Miyano, S. *Org. Biomol. Chem.* **2004**, *2*, 890.
39. Adly, F. G.; Gardiner, M. G.; Ghanem, A. *Chem. Eur. J.* **2016**, *22*, 3447.
40. Hashimoto, S.; Watanabe, N.; Ikegami, S. *Tetrahedron Lett.* **1992**, *33*, 2709.
41. Kwok, S. W.; Zhang, L.; Grimster, N. P.; Fokin, V. V. *Angew. Chem., Int. Ed*. **2014**, *53*, 3452.
42. Panne, P.; Fox, J. M. *J. Am. Chem. Soc*. **2007**, *129*, 1, 22.
43. Legxdins, P.; Mitchell, R. W.; Rempel, G. L.; Ruddick, I. D.; Wilkinson, G. *J. Chem. Sot. (A)* **1970**, 3322.
44. Hashimoto, S.; Watanabe, N.; Satoa, T.; Shiroa, T.; Ikegami, S. *Tetrahedron Lett*. **1993**, *34*, 5109.
45. Müller, P.; Allenbach, Y.; Robert, E. *Tetrahedron: Asymmetry* **2003**, *14*, 779.
46. Hodgson, D. M.; Stupple, P. A.; Pierard, F. Y. T. M.; Labande, A. H.; Johnstone, C. *Chem. Eur. J.* **2001**, *7*, 4465.
47. Fu, J.-T.; Ren, Z.; Bacsa, J.; Musave, D. J.; Davies, H. M. L. *Nature* **2018**, *564*, 395.
48. Negretti, S.; Cohen, M. C.; Chang, J. J.; Guptill, D. M.; Davies, H. M. L. *Tetrahedron* **2015**, *71*, 7415.
49. Reddy, R. P.; Lee, G. H.; Davies, H. M. L. *Org. Lett.* **2006**, *8*, 3437.
50. Bismuto, A.; Delcaillau, T.; Müller, P.; Morandi, B. *ACS Catal.* **2020**, *10*, 4630.

Acknowledgements

First and foremost, I would like to convey my sincere gratitude to Professor Takeo Kawabata (Kyoto University) for his continuous guidance and encouragement. His innovative research philosophy and the spirit of challenging difficulties benefited me a lot. This has made me to develop critical thinking and problem solving skill, which will be with my future career.

I also would like to express my appreciation to Assistant Professor Yoshihiro Ueda (Kyoto University) for his useful help during these four years. Whenever I have any problems, he is willing to help me with great patience. He always shares his knowledge and experimental skills to me, and respects my opinions. I also would like to thank to Assistant Professor Kazuhiro Morisaki (Kyoto University) for his warm help and useful suggestions to my study and life.

I am grateful to Professor Takumi Furuta (Kyoto Pharmaceutical University) and Kazunori Tsubaki (Kyoto Prefectural University) for their useful discussions.

I appreciate Professor Kiyosei Takasu (Kyoto University) and Professor Hiroaki Ohno (Kyoto University) for reviewing my thesis and providing valuable comments.

I wish to thank Dr. Kenta Arai (Otsuka Pharmaceutical Co., Ltd.), Dr. Naruhiro Gondo (Ono Pharmaceutical Co., Ltd.), and Dr. Hiromitsu Shibayama (Shionogi & Co., Ltd.) for their valuable discussions and suggestions. I greatly thank all past and present members of Kawabata Group for active discussions and sharing various experiences. I am thankful to Secretary Ms. Kaori Hashimoto for her support to my daily life.

I would like to express my thanks to China Scholarship Council for the financial support during my PhD course.

I am thankful to Dr. Wenjie Lu (Kuraray Co., Ltd.) and Shuo Wang for their kind help and encouragement during my stay in Japan.

At last, I would like to show my deepest thanks to my parents and my brother's family for their understanding and constant encouragement. And I also would like to express my great appreciation to my friend Peng Lin for her kind support and encouragement through these years, she was always on my side to share my happiness and help me to overcome difficulties.

Thank you, all.